Scuola di Medicina
Dipartimento di Medicina Traslazionale

Corso di Dottorato di Ricerca in Medical Sciences and Biotechnologies
ciclo XXXIII

Sex differences in hepatitis C virus infection: characterisation of 17,β-estradiol-modulated antiviral defences in an HCV cell culture system

SSD (Settore Scientifico Disciplinare) MED/09

Coordinatrice

Professoressa Marisa GARIGLIO

Tutor

Professor Mario PIRISI

Dottorando

Matteo Nazzareno BARBAGLIA

INDEX

INTRODUCTION

Hepatitis C virus

Morphology and composition

The hepatitis C virus (HCV) infection is the leading cause of several liver diseases such as chronic hepatitis, cirrhosis and hepatocellular carcinoma (HCC) [1,2]. The HCV belongs to the family of *Flaviviridae* genus *Hepacivirus*, and phylogenetic analysis discovered the presence of 6 major genotypes divided into further subtypes [1]. In the last few years new HCV genotypes (7a/b and 8) were discovered in central Africa and India, respectively [3–5]. Overall, genotypes 1 and 2 are ubiquitously distributed over the world. The most common genotype in Europe and America is genotype 1, while 3 and 6 are mainly distributed in Asia. In Africa, there is a greater distribution of genotypes 2 in the West, compared to the Centre and the South, where genotypes 4 and 5 are more prevalent, respectively [1].

The morphology and composition of the viral particles is characterised by a lipid bilayer obtained by the interaction between the HCV virion assembly-release process and the host lipoprotein formation [6]. The so-called Lipo-Viro-Particles (LVPs) are characterised by a diameter ranging 30-80 nm and the presence of lipid bilayers means that HCV is a hybrid particle, composed by viral factors and lipoproteins derived by a host cell including several apolipoproteins (ApoB-100, ApoC and ApoE) [7]. The two viral glycoproteins (E1 and E2) are anchored to a lipid membrane envelope, which surrounds the icosahedral structure of capsid formed by Core proteins (C) containing the viral genome (HCV RNA) (**Figure 1A**). However, the exact LVP structure is still debated; according to the main two hypotheses, the viral particles can interact transiently with lipoproteins (**Figure 1B**) or they form fully integrated particles (**Figure 1C**) [8].

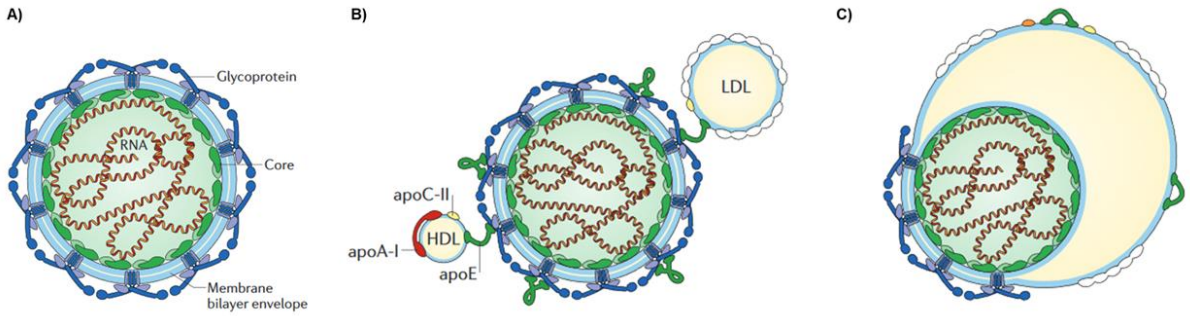

Figure 1. HCV Lipo-Viro-Particles (LVPs). A) HCV viral structure. **B)** and **C)** different LVP conformation and interaction with host lipoproteins. The image was taken and adapted from Lindenbach & Rice 2013 [8].

The viral genome is a single-strand positive RNA (ssRNA+) approximately 9.6 kb-long, bordered by two untranslated regions at 5' and 3' (5'-NTR and 3'-NTR, respectively). ssRNA+ translation starts from the internal ribosome entry site (IRES) located in the 5'-NTR. The presence of a single open reading frame (ORF) leads to the formation of a single polyprotein of approximately 3000 amino acids (aa), which is processed by viral and host proteases, obtaining ten mature viral proteins classified as three structural (C, E1 and E2) and seven non-structural proteins (p7, NS2, NS3, NS4A, NS4B, NS5A and NS5B) [9] (**Figure 2**).

As mentioned above, the structural proteins include:

- Core (21 kDa): a dimeric alpha helix (α-helix) protein, generated at the endoplasmic reticulum lumen by the cleavage of the viral polyprotein by the signal peptidase (SP) and signal peptide peptidase (SPP). The mature protein shows two different domains; the D1, located at the N-terminal, has hydrophilic properties and is mainly involved in the RNA binding process, whereas the D2 domain in the C-terminus has hydrophobic properties and is essential for an efficient lipid droplet (LD) localization [10]. It has been demonstrated that mutations occurring in the D2 domain can compromise the normal assembly process, showing its essential role in virion production [11].
- Glycoproteins E1 and E2 (33-35 and 70-72 kDa, respectively): transmembrane proteins essential for the entry viral step. They present an extracellular ectodomain N-terminal of 164 and 334 aa for E1 and E2, while a 30-aa-long hydrophobic domain is located at the C-terminus. The N-terminal ectodomain is divided into two highly glycosylated regions, highly conserved within HCV genotypes. Respectively, such regions constitute a receptor binding domain and, at its C-terminal, a sequence essential for the anchorage to endoplasmic reticulum and cytoplasmic membranes [12]. Moreover, the N-terminal portion of glycoprotein E2 is characterised by a 27-aa-long hypervariable region (HVR1) and is involved in the interaction with cellular receptors that are essential for the viral entry step. Indeed, it has been demonstrated that the deletion of this region leads to loss of viral infectivity [13,14].

The non-structural proteins include:

- p7 (7 kDa): member of the viroporin family, it is a small 27-aa-long ion-channel protein formed by two hydrophobic transmembrane regions. The functions of this protein are still an object of debate and they would seem to interact with different steps of the viral cycle [15]. As proposed by Gentzsch *et al.*, its ability to interact and modulate cytoplasmic membrane structures may influence the incorporation of ssRNA+ into the HCV viral capsid, during the assembly process

[16]. Furthermore, the ability of p7 to regulate pH levels makes this protein important during the secretion step as it protects HCV particles from pH-dependent uncoating [17].

- NS2 (21-23 kDa): a non-glycosylated membrane cysteine protease with an N-terminal transmembrane domain and a C-terminal domain, which, in combination with the N-terminal of NS3 forms the NS2-NS3 protease. This enzyme is responsible for the cleavage of the NS2-NS3 junction, crucial for viral genome replication. Additionally, NS2 is able to interact with E1, E2 and p7, promoting the primary phases of viral assembly [18].
- NS3-NS4A complex (69 and 6 kDa): NS3 is a multifunctional protein with a N-terminal serine protease domain, and a C-terminal domain containing a NTPase/RNA helicase catalytic site [19]. The protease activity requires the interaction with the NS4A cofactor, and it catalyzes the cleavage of viral polyprotein between non-structural protein junctions (NS3/4A, NS4A/4B, NS4B/5A e NS5A/5B). The helicase site allows the interaction between viral RNA replication and the packaging process, during virion production [20].
- NS4B (27 kDa): a hydrophobic protein with four transmembrane domains and a nucleotide-binding motif, mediating HCV viral replication and replication-related focus formation. Indeed, NS4B induces alterations in the endoplasmic reticulum leading to the formation of membranous structures that are important for viral replication [21]. Focusing on the possible role of HCV infection in hepatocarcinogenesis, it is interesting to mention that NS4B is able to induce epithelial mesenchymal transition (EMT), upregulating the Snail host protein in infected *in vitro* cell lines [22].
- NS5A (56-58 kDa): a 447-aa-long zinc metalloprotein. At the N-terminal, there are a highly conserved amphipathic α-helix (which allows the association between NS5A and the endoplasmic reticulum membranes), and three domains (D1-3) that are separated by low complexity sequences [23,24]. Studies have identified two differentially phosphorylated forms of NS5A, called p58 and p56. The interaction between NS5A, NS4A and the host kinase family members (such as the casein kinase II (CKII), the mitogen-activated protein kinases (MAPKs) and the glycogen synthase kinase 3 (GSK-3)) induces a center-and-C-terminal NS5A phosphorylation, generating the p58 form. Similarly, the p56 form is hyperphosphorylated within a serine-rich sequence in the center of the protein [25,26]. NS5A's interaction with viral RNA, NS5B, Core protein, and lipid droplets is essential for the formation of the viral replicative complex and for the virion assembly step. Moreover, it is involved in interferon resistance mechanisms [27–29].
- NS5B (68 kDa): a RNA-dependent RNA polymerase (RdRp), key enzyme for viral genome synthesis. The C-terminal is an alpha-helical transmembrane insertion sequence, while the other

part of the enzyme can be subdivided in three domains called “palm”, “finger” and “thumb”; the first of which is the highly conserved active site [30]. The lack of proofreading activity is the main cause of viral quasispecies generation [31].

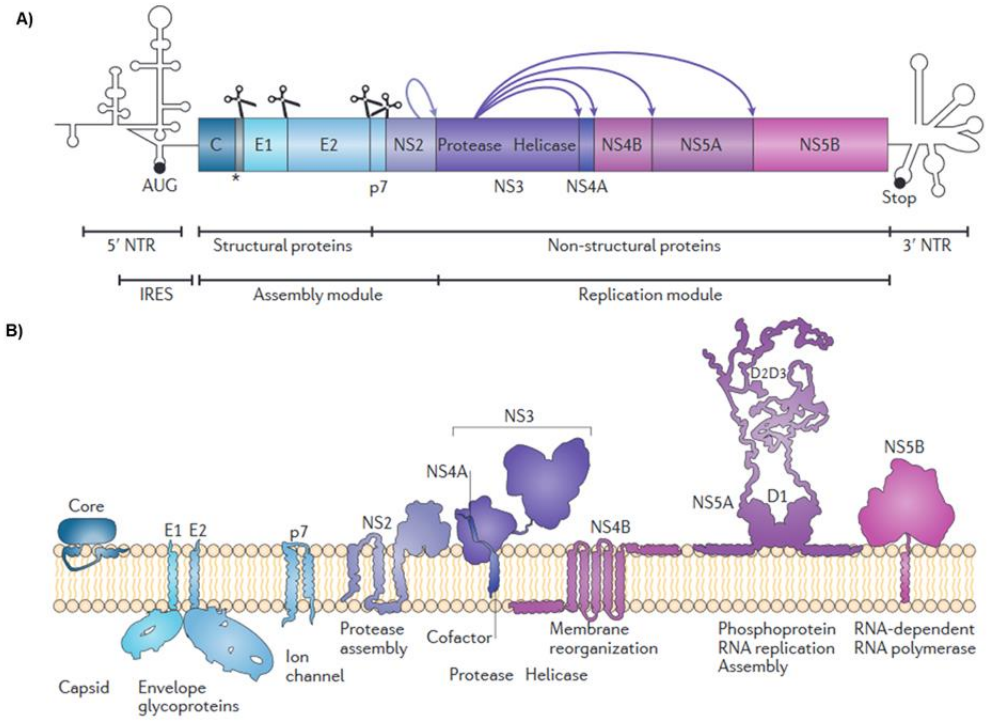

Figure 2. HCV genome organization (A) and HCV proteins (B). Image taken and adapted from Bartenschlager *et al.* 2013 [9].

HCV replication cycle

The peculiar conformation of the HCV particles reflects the complexity of its viral replication cycle, which occurs in hepatocytes. This process is strictly connected with the host cell factors and can be divided into the following steps: binding to cell membrane surface, disruption of viral capsid and release of viral genome in cellular cytoplasm, ssRNA+ translation and polyprotein maturation, viral RNA replication, nucleocapsid assembly and budding of the viral particles, and finally, transport to cell surface and release of the new viral particles (**Figure 3**).

The LVP chimeric nature allows the binding and endocytosis into hepatocytes via several receptors. Due to the presence of apolipoproteins on the envelope surface, the LDL receptor (LDLR) and the glycosaminoglycans (GAG) mediate the initial attachment step [32]. The bond with the cell surface is strengthened by the interaction of envelope proteins E1 and the E2 HVR1 with Scavenger receptor class B type 1 (SR-B1). It has been demonstrated that E2 HVR1 deletion or mutation, which alters the glycoprotein E2/SR-B1 binding, prevents the viral entry process; highlighting the great importance of SR-B1 in the viral entry step [33]. It has been proposed that the interaction between

the glycoprotein E2 and the SR-B1 induces a conformational change, which leads to the unmasking of the tetraspanin (CD81) binding site of E2. The CD81 protein is able to interact with the tight-junction protein claudin-1 (CLDN1). It has been observed that the activation of the epidermal growth factor receptor (EGFR) and the ephrin receptor type A2 (EphA2) pathways can promote the interaction between CD81 and CLDN1, favouring HCV entry step [34]. The receptors CD81, CLDN1 and OCLN are the key players of the viral endocytosis step. Furthermore, the cholesterol molecules present on the viral particle surface allow the interaction with the cholesterol transporter Niemann-Pick C1-like 1 (NPC1L1), leading to the clathrin-mediated and dynamin-dependent endocytosis [35]. The CLDN1, OCLN and NPC1L1 proteins are located in the hepatocytes' tight junctions; it has been hypothesized that they may play an important role not only during viral entry step but also during the virus cell-to-cell transmission. The late stage of fusion and viral uncoating mechanisms are poorly understood. Using an *in vitro* model, Coller *et al.* showed that HCV virion is transported to Ras-related protein Rab-5A positive early endosomes along actin stress fibers [36]. Subsequently, endocytotic vesicles mature into acidic endosomes, thus promoting low pH-dependent HCV fusion [37].

The HCV positive-strand RNA genome is released in cytoplasm, and it is translated in a single polyprotein at the level of the endoplasmic reticulum. As previously reported, the HCV polyprotein is processed by cellular and viral proteases, inducing the formation of the individual viral proteins. These proteins localize on the host endoplasmic reticulum and LD membranes, generating the viral replication complex and inducing profound changes in cytoplasmic membrane organization. R. Bartenschlager *et al.* widely studied the “membranous web” formation by the electron microscopy and 3D reconstructions methods, however the entire process has not been completely clarified [38]. Interacting with endoplasmic reticulum membranes, the HCV proteins NS4A and NS5B induce the formation of double-membrane vesicles (DMVs). The DMVs are the ideal place for HCV RNA replication; on one hand they offer physical protection from hepatocyte antiviral proteins, on the other hand, the close proximity to LD surrounded by the Core protein and NS5A, can promote the virion assembly process [39]. The HCV infection is able to alter the expression of the host proteins Rubicon and UV radiation resistance-associated gene protein (UVRAG), thus interacting with the autophagosome formation and promoting DMV production [40].

Several studies showed that hepatocyte metabolism changes profoundly during the HCV infection. Principally, the virus induces an up-regulation of glycolysis and fatty acid synthesis [41,42]. The Core protein is able to interact host proteins (such as the sterol regulatory element-binding protein 1c (SREBP-1c) and the peroxisome proliferator-activated receptors alpha and gamma (PPAR-α/γ))

promoting the expression of genes involved in lipogenesis and inducing LD cytoplasmic accumulation [43–45]. In addition the host protein tail-interacting protein 47 (TIP47) can interact with the NS5A inducing LD proximity to the viral replication complex [39]. The promotion of autophagosome formation and the LD accumulation favour the membranous web formation and consequently viral replication.

At the DMVs levels, the first step of viral ssRNA+ replication is the production of an intermediate RNA negative-strand. In combination with the NS3 helicase, the NS5B protein uses the negative strand as the template to obtain a new ssRNA+. The most important host factor that influences viral RNA replication is the miRNA-122. Through the bond to ssRNA+ 5'-NTR portion, the miRNA-122 stimulate the RNA translation and protects the viral genome against degradation operated by the 5'-3' exoribonuclease 1 (Xrn1) [46,47]. The miRNA-122 is strictly expressed in hepatocytes compared to other cell types, partially explaining the hepatic tropism of HCV infection. As mentioned above, the proximity of the DMVs with the LDs promote the new HCV RNA positive-strands assembling into the viral nucleocapsid. This process is mainly orchestrated by the NS2, NS5A and Core viral proteins. On one side, the NS5A, in combination with NS2 and NS3 and p7, traffics the viral genome out of DMVs near LDs [48,49]. Moreover, the E1 and E2 heterodimers are located on the endoplasmic reticulum surface, and they migrate on the luminal LD (luLDs) surface near the cytosolic LD (cLDs). This shift occurs by the interaction of E1-E2 heterodimer with the other viral proteins NS2, NS3-4A and p7 [48,50]. On the other side, the cLDs are coated by the Core protein; a process mediated by the viral proteins NS2 and NS3-4A [51]. The cLD Core coating is also allowed by the presence of the Core amphipathic regions and by its interaction with the host proteins phospholipase A2 G4A (PLA2GA4) and diacylglycerol acyltransferase 1 (DGAT-1) [52,53]. Due to the proximity of DMVs to Core-coated LDs, it has been proposed that HCV particles might be formed through budding into ER [54].

During the final stage of the assembly/release step, the nascent HCV particles interact with the VLDL production pathway. This pathway briefly consists of a first step in which the ApoB is associated with lipids by the microsomal triglyceride transfer protein (MTP), forming the pre-beta VLDL. In endoplasmic reticulum lumen, the pre-beta VLDL are associated with the LDs, in which are located the proteins ApoE and ApoC. According to another hypothesis, the addition of lipids to VLDL might happen in the Golgi compartment [55]. Nucleocapsid-containing luLDs fuse with the pre-beta VLDL and subsequently acquire the ApoE and ApoC proteins. Finally the LVPs exit through the Golgi; mature viral particles are finally secreted in vesicles to avoid p7 and pH-dependent premature uncoating [17].

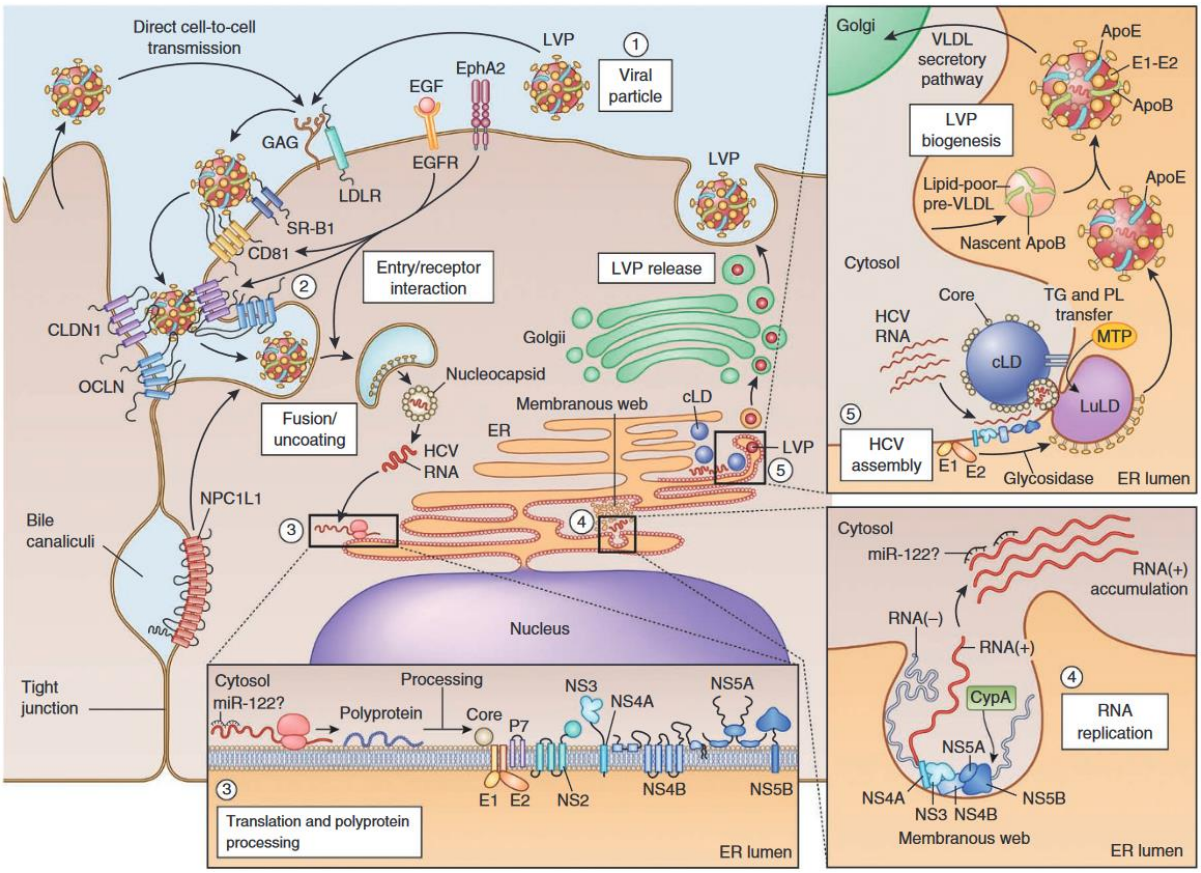

Figure 3. HCV replication cycle. From Scheel *et al.*2013 [56].

Hepatocyte innate immunity

During the viral cycle, the HCV interacts with several intracellular processes, inducing profound changes into hepatocytes. On one side, the HCV generates an intracellular environment favourable for its replication. On the other side, the infection triggers the hepatocyte antiviral systems, which are able to detect and counteract viral infection [57].

It is well known that hepatocytes are key elements of the liver immune response. In combination with other cell types (such as Kupffer cells (KCs), plasmacytoid dendritic cells (pDCs) and natural killer (NK) cells), the hepatocytes actively contribute to viral clearance [58]. However, as will be explained later, most of the HCV infected subjects fail to induce an immune response sufficient for HCV clearance. This is due to HCV-evolved mechanisms, which are able to regulate and counteract the immune response activation (**Figure 4**) [59].

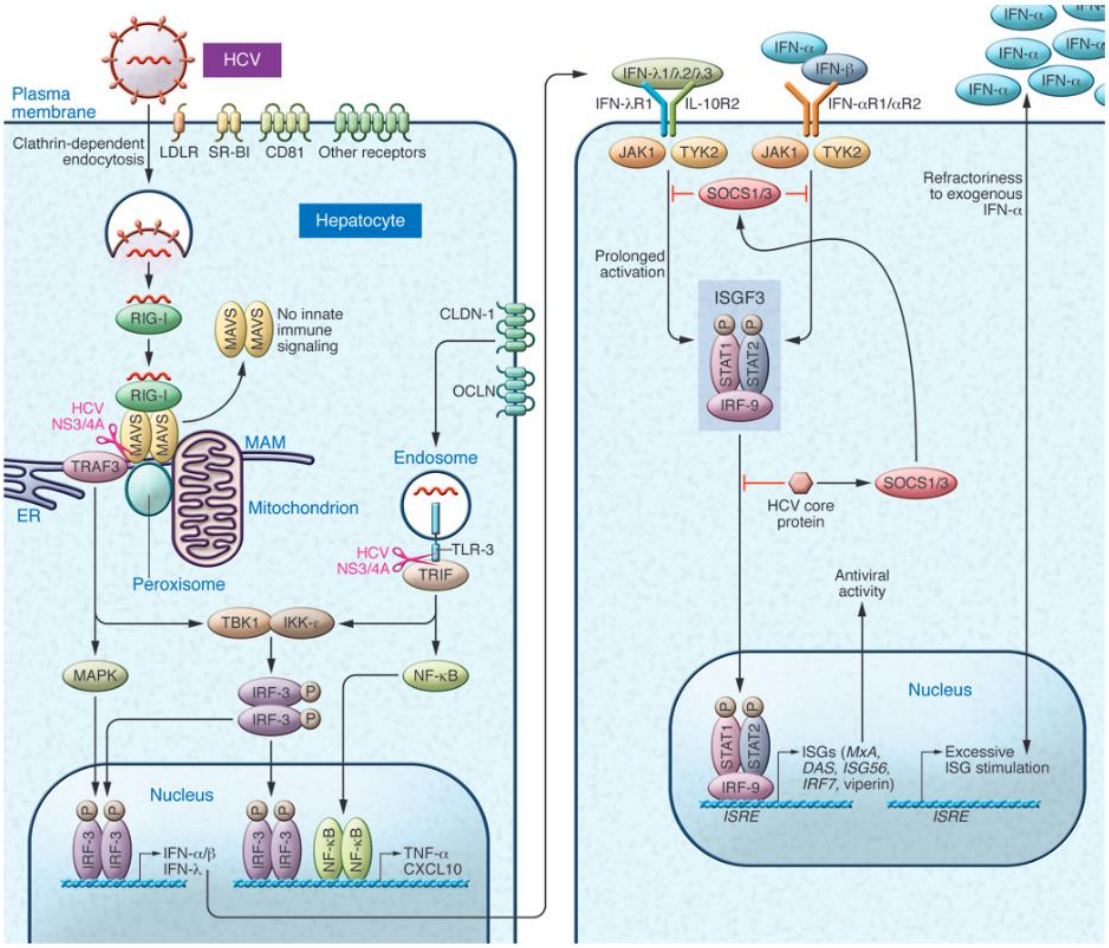

Figure 4. Hepatocyte antiviral response. From Rosen *et al.* 2013 [59].

As the first line of defense, the cellular pattern recognition receptors (PRRs) are able to recognize the generically called pathogen-associated molecular patterns (PAMPs). During HCV infection, the hepatocyte PRRs play a fundamental role in viral RNA recognition and in interferon regulatory factor (IRFs) and nuclear factor-kB (NF-kB) activation. The PRRs can be divided in three distinct families: the RIG-I–like helicases (RLHs), NOD-like receptors (NLRs; nucleotide-binding oligomerization domain-like receptors), and the toll-like receptors (TLRs) [60–62]. Further non-canonical and controversial PRRs is the interferon induced protein kinase-R (PKR), which can bind the HCV RNA IRES sequence blocking its translations. However, it has been demonstrated that HCV itself (via E2 and NS5a proteins) regulates the PKR activity, promoting the inhibition of Interferons (IFNs) and interferon-stimulated gene (ISGs) transcriptions [63,64].

RLHs are located in the cytoplasm and detect the dsRNA; they include the retinoic acid-inducible gene 1-like (RIG-I) protein, the melanoma differentiation-associated protein 5 (MDA5) and the Laboratory of genetics and physiology 2 (LGP2) protein [65,66]. RIG-I can bind both the 5′ triphosphate and the 3′-NTR regions (poly-U/UC rich) of the viral genome. It has been demonstrated *in*

vitro that MDA5 can more strongly bind the 3'-NTR compared to RIG-I [65]. The LGP2 role is not well clarified, it seems to be essential for the MDA5/HCV RNA interaction [66].
The dsRNA binding induces RLH conformational changes, which promotes protein translocation from the cytosol into intracellular membranes [67]. On mitochondria and peroxisome surfaces, the interaction of the RLHs with the mitochondrial antiviral signaling (MAVS) and the tumor necrosis factor receptor–associated factor 3 (TRAF3) induces the activation of downstream pathways. The downstream RLHs-MAVS-TRAF3 signals involved the classical kinase-related kinase (IKK) complex (IKKα/IKKβ) and the two non-classical IKK-related kinases (TANK-binding kinase 1 (TBK1) and IKKε) which induce the IRF and NF-kB activation [68]. This signaling pathway can be disrupted by the HCV protein NS3-4A, which protease activity can cleave MAVS from intracellular membranes [69,70].

NLRs are expressed on intracellular compartments. The NLR structure consist in three domains; an N-terminal effector domain, a central nucleotide-binding domain NOD (NACHT: NAIP, CIITA, HET-E, and TP-2), and a C-terminal leucine-rich repeats (LRRs) involved in ligand binding or activator sensing. These proteins are involved in the inflammasome activation pathway in combination with the adaptor protein ASC and the proteolytic enzyme caspase-1. The NLR family members can lead to NF-κB activation, stimulating pro-inflammatory cytokine production [71]. The NLRs can be activated not only by PAMPs but also by the damage-associated molecular patterns (DAMPs), which include the reactive oxygen species (ROS) highly produced during the HCV infection [72].
The NLR family is divided into the two subfamilies: NODs (NOD1 and NOD2) and NLRPs. The hepatocytes functionally express NOD1, NOD2 and NLRP3 [73]. It has been demonstrated that HCV NS5B and dsRNA can activate NOD1 signaling, leading to IL-8 and Tumor necrosis factor alpha (TNF-α) expression increase [61]. Furthermore, the NLRP3 is involved in the production of the pro-inflammatory cytokines Interleukin 1β and 18 (IL -1β, -18) in infected hepatocytes [74]. Moreover, NRL roles in HCV infection and disease progression are still elusive.

TLRs are a family of 9 transmembrane receptors located on cell surfaces (TLR1, TLR2, TLR4, TLR5 e TLR6) and in endosomes (TLR3, TLR7, TLR8 and TLR9) [75]. The TLR3 and TLR7 play a central role in HCV detection; they recognize dsRNA and RNA urine-rich ribonucleotide regions, respectively [76]. Upon binding to viral RNA, TLR3 dimerized and binds TIR-domain-containing adapter-inducing interferon-β (TRIF) leading to the activation of IRF3 and NF-kB, by the interaction with TRAF3-6 and TBK. The TLR7 exerts its function by binding to myeloid differentiation pro-inflammatory response 88 (MyD88). The TLR7-Myd88 interaction activates IL-1 receptor-associated

kinase (IRAK) and TRAF6, promoting NF-kB activation [77]. In addition, the TLR pathways can be negatively modulated and attenuated by HCV protein interactions. As mentioned for MAVS, the NS3-4A protease is also able to cleave TRIF [78]. Furthermore, in macrophage cell lines were demonstrated that NS5A can bind to MyD88 inhibiting IRAK1 recruitment [79].

The PRRs-induced pathways converge on the proteins IRFs and NF-kB, inducing their activation and translocation into the nucleus. At this level, IRFs and NF-κB induce the transcription of IFNs and proinflammatory cytokines and chemokines, respectively.

The IRFs are a large family of 9 proteins, which structure show a DNA binding domain at the N-terminus and a carboxyl (C)-terminal association domain (IAD) (except for IRF1and IRF2) [80]. Subsequently to phosphorylation, the IRF proteins can homo- or hetero- dimerize, and they translocate into the nucleus. The most important IRFs in the HCV infection context are IRF1, IRF3, IRF5, and IRF7. They are implicated in the positive regulation of type I and III IFN gene transcription. IRF1 is the first discovered member of the family, it is able to regulate not only IFN promoter but also several interferon-stimulated genes (ISGs) by binding the IFN-stimulated response element (ISRE) and interacting with IRF3 and IRF7 [57]. Ciccaglione *et al* and Pflugheber *et al*, demonstrated that Core and NS5A viral protein alone were sufficient to block IRF1 activation *in vitro* [81,82].

IRF3 can be induced by both RIG-I and TLR3 pathways and can interact with NF-kB and IRF7 inducing IFN-α/β, IFN-λ and ISG gene expression [57,83]. However, it has been demonstrated a limited IRF3 activation in subjects affected by chronic HCV infection [84]. These findings could be explained by the ability of Core and NS3-4A proteins to interfere with IRF3 activation, highlighting the ability of HCV to control the immune response [85,86].

IRF5 can induce IFNα/β expression via the TLR-My88 pathway, but principally it regulates the expression of pro-inflammatory cytokines (IL -1β, -6, -12, -23) and TNF-α [87]. Due to its ability to regulate cell proliferation, migration and apoptosis, the IRF5 protein has been proposed to be an important factor in HCC development. IRF5 is able to impair HCV-induced autophagy *in vitro*, and reduced levels of IRF5 protein were found in HCV-related HCC [88].

IRF7 protein acts as a homodimer or in combination with IRF3, inducing IFN-α/β and IFN-λ expression as previously reported. Furthermore, IRF7 itself can promote ISG expression without IFN stimulation [89,90]. *In vitro* studies shown that IRF7 is a key regulator of IFNα expression during HCV infection, and the virus can block IRF7 translocation into the nucleus modulating the host immunity response [91,92].

The IRF system induces the expression of a large number of IFNs. These proteins can be divided in three families: type I, type II and type III. The IFN-α, IFN-β, IFN-ε, IFN-κ and IFN-ω belong to the

type I family. The IFN-γ is the only type II IFN, and the IFN-λ1 (IL-29), IFN-λ2 (IL-28A), IFN-λ3 (IL-28B) and IFN-λ4 belong to the type III family [93]. The secreted type I and III IFNs bind the interferon-α/β receptor (IFNAR) and IFN-λ receptor 1 (IFNLR), respectively. The IFNAR is ubiquitously expressed on the cell surface and is composed by the two subunits IFNAR1 and IFNAR2. The IFNLR expression is mainly restricted to epithelial and dendritic cells (pDC), and it is combined with the ubiquitously expressed IL-10 receptor 2 (IL-10R2) [94].

The IFN binding on their receptors triggers the activation of Janus kinase (JAK)/signal transducer and activator of transcription (STAT) pathway (JAK-STAT). In the cytoplasm, the phosphorylated STATs (e.i. STAT1 and STAT2) can homo- or hetero- dimerize. The STAT1- homodimers translocate into the nucleus and binds the gamma interferon activation site (GAS), promoting ISG transcription. The STAT1/STAT2 heterodimer, in association with IRF9, generates the interferon stimulated gene factor 3 (ISGF3) complex. Subsequently, the ISGF3 complex translocates into the nucleus and induces the transcription of the ISGs by binding to Interferon-sensitive response elements (ISRE) [95]. The JAK/STAT induced pathway and the ISGF3 complex formation can be negatively modulated by host proteins, such as the suppressor of cytokine signaling 1/3 (SOCS1/3) and the ubiquitin specific peptidase 18 (USP18). The HCV proteins are able to interact with these suppressor pathways. It has been demonstrated that HCV Core protein induces the up-regulation of SOCS3 protein in HepG2 cells [96]. Also the HCV-induced IL-8 can suppress ISGF3 complex activity [97]. Furthermore, *in vitro* silencing of USP18 resulted in a higher IFN-α effect on HCV RNA replication, highlighting the importance of USP18 protein in IFN signaling control [98]. The IFN-induced gene pool contains a large number of ISGs; more than 300 of ISGs have been classified. A list of the most studied HCV-induced ISGs is reported in **Table 1.**

Table 1. Interferon-stimulated genes (ISGs) and HCV infection. The following list was taken and adapted from Ortega-Prieto *et al.* 2017 and Metz *et al.* 2013 [99,100].

ISGs	Gene name	Effect
Cholesterol 25-Hydroxylase	CH25H	inhibits HCV replication
Guanylate binding protein 1	GBP1	inhibits HCV release/replication
IFN alpha-inducible protein-16	IFI16	inhibits HCV release/replication
IFN alpha-inducible protein 27	IFI27	inhibits HCV replication
IFN induced transmembrane protein 1	IFITM1	inhibits HCV entry/replication
IFN induced transmembrane protein 3	IFITM3	inhibits HCV entry/replication
IFN stimulated gene 15/Ubiquitin specific peptidase 18	ISG15/USP18	IFN negative regulator
IFN stimulated gene 20	ISG20	inhibits HCV replication
Interferon-stimulated gene 56	ISG56	inhibits HCV replication
Myxovirus resistance protein A	MX1	inhibits HCV replication
Nitric oxide synthase 2	NOS2	inhibits HCV replication
2'-5'-Oligoadenylate Synthetase	OAS	inhibits HCV replication
2'-5'-Oligoadenylate Synthetase Like	OASL	inhibits HCV translation
Protein kinase-R	EIF2AK2	inhibits HCV translation
Ribonuclease L	RNaseL	inhibits HCV translation
Tetherin	BST2	inhibits HCV release
Tripartite motif family	TRIM	inhibits HCV replication
Virus inhibitory protein	RSAD2	inhibits HCV replication

Hypoxia and HCV infection

Normoxia and hypoxia are two conditions respectively based on a normal or a lower amount of oxygen reaching a tissue. The liver anatomical conformation results in the presence of an oxygen gradient in the hepatic lobule. Oxygen pressures are greater near the portal layers (60-65 mmHg, ~8%) compared to the pericentral layers (30-35 mmHg, ~4%). This oxygen gradient implies a different oxygenation and metabolic zonation of resident liver cells. Though no hypoxic response is observed in healthy liver, a liver disease onset can lead to a hypoxic state induction [101,102].

The Hypoxia-Inducible Factor (HIF) proteins are the key players of the hypoxic response. This transcription factor family includes three members with the respective subunits (α and β): HIF-1, HIF-2 and HIF-3. These proteins are heterodimers composed of the constitutively expressed subunit β and the regulated subunit α. The response to hypoxic acute conditions is principally mediated by HIF-1α. Instead HIF-2α is mainly stabilized during a chronic hypoxic state [103]. In normoxic conditions, the HIFα subunit is polyubiquitinated by specific proteins that drive HIFα degradation in the proteasome. The HIFα subunit is hydroxylated (HIFα-OH) by the prolyl hydroxylases (PHD1-3) in combination with oxygen and the co-substrates 2-oxoglutarate, iron and ascorbic acid; PHDs act as oxygen sensor. The HIFα-OH is recognized by the von Hippel-Lindau (pVhl) ubiquitin ligase complex, which induces the ubiquitin-mediated proteasome degradation. HIFα protein can also be negatively modulated by the factor inhibiting HIF (FIH), another oxygen-sensor enzyme [104]. In hypoxic or stress conditions, the HIFα subunit can be positively regulated by two different activation pathways: an oxygen-dependent and an oxygen-independent signaling pathway. In oxygen deficiency

conditions, the PHDs or the FIH cannot exert their enzymatic activity, then HIFα is stabilized and is accumulated in the cytosol [105]. The oxygen-independent pathway can be induced by ROS (linked mitochondrial dysfunctions or inflammation) and growth factor pathway; this condition is defined as pseudohypoxic state. The ROS and the growth factors induce HIFα mRNA expression and HIFα protein stabilization by phosphoinositide 3-kinase/protein kinase B (PI3K/Akt) and MAPK pathway activation. Also the IL-1β and TNF-α cytokines were found to be able to induce and stabilize HIF-1α expression, highlighting the crosstalk between inflammation and hypoxia [106–108]. Upon stabilization, the HIFα subunit translocates to the nucleus where it acts as transcription factor; in the nucleus the HIFα heterodimerizes with the HIFβ and they bind the hypoxia-responsive elements (HREs) by complexing with other factors (such as the CREB binding protein (Cbp) and the histone acetyltransferase p300). This complex induces the transcription of several genes (such as carbonic anhydrase 9 (CA9), erythropoietin (EPO), vascular endothelial growth factor (VEGF) and transforming growth factor-beta (TGF-β)), regulating angiogenesis, metabolism, cell survival and migration [109–111] (**Figure 5**). Different systems are used to recreate hypoxic conditions *in vitro*. Special incubators and hoods can regulate and maintain specific oxygen concentrations. Furthermore, the chemical inhibitors can be used such as dimethyloxalylglycine (DMOG) and cobalt (II) chloride hexahydrate ($CoCl_2 \bullet 6H_2O$). The DMOG is a synthetic analogue of 2-oxoglutarate, which acts as a PHD competitive inhibitor, inducing HIF-1α stabilization [112,113].

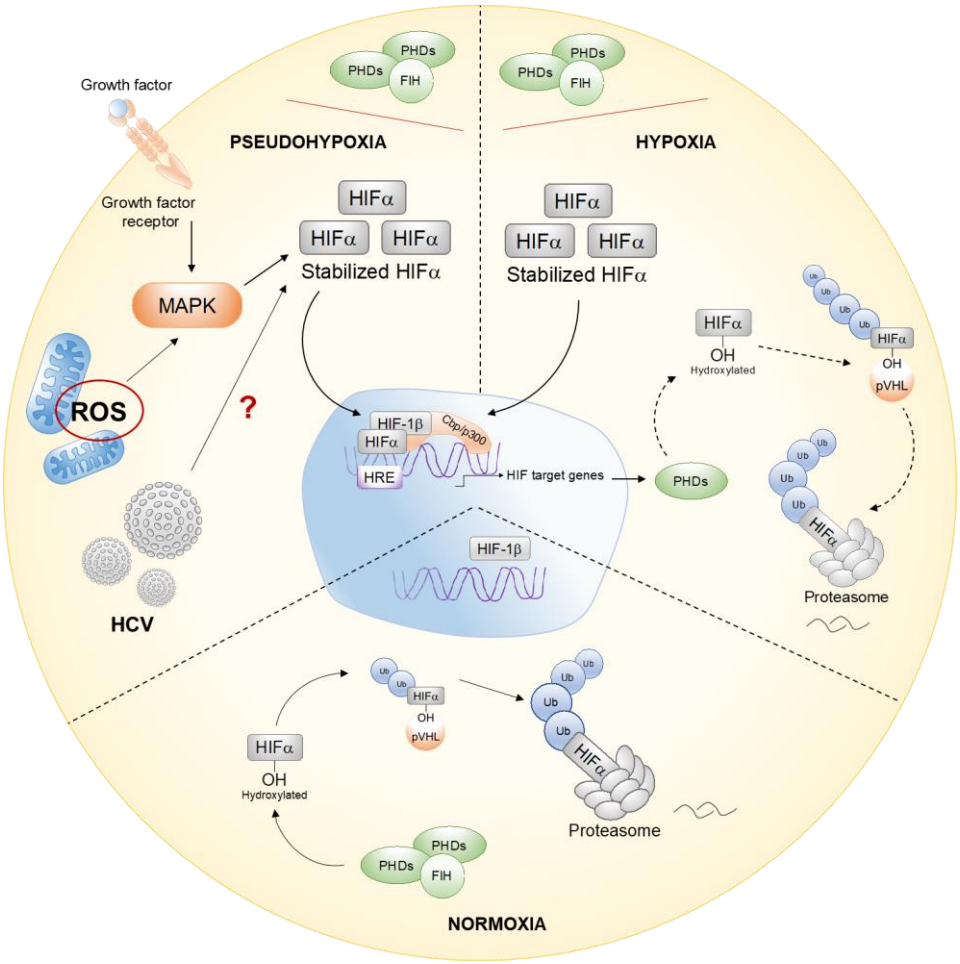

Figure 5. Hypoxia Inducible Factor alpha (HIFα) regulation in normoxia, pseudohypoxia and hypoxia conditions.

The HCV infection appears to influence the hepatocytes hypoxic state, which may play a significant role in fibrosis development and viral hepatocarcinogenesis. Hypoxic *in vitro* conditions lead to VLDL receptor (VLDLR) up-regulation, which enhances HCV viral entry [114]. Vassilaki *et al.* showed that HCV RNA replication *in vitro* is enhanced in presence of two different oxygen concentrations (3 and 12%). Despite the 12% oxygen concentration was not sufficient to induce HIF-1α stabilization, this concentration still induced a delayed HCV RNA increase compared to the increase observed in 3% oxygen condition. The HCV increased replication resulted to be independent by HIF-1α/2α activation in both oxygen concentrations tested; the enhanced replication was ascribed to glycolysis-associated oncogenes [115]. However, in other studies it has been demonstrated that the HCV infection promotes HIF-1α stabilization by the induction of mitochondrial dysfunction, oxidative stress and ROS formation [116]. The HCV Core protein itself promoted HIF-α stabilization [117]. In turn HIF-α stabilization promotes VEGF and TGF-β hepatocyte expression and the hepatocyte tight junction remodeling [118,119]. The cellular metabolic reprogramming combined with the profibrotic factor induction and the hepatocytes polarity remodeling suggest the important

role of hypoxia-HCV axis in HCC development.

Natural history of HCV infection

According to the World Health Organization (WHO), the HCV infection affects 170 millions of people globally with 3-4 million new cases/year [120]. However, these data are underestimated as the infection develops asymptomatically in a large number of cases [121]. The main way of HCV transmission is the parenteral one, in which HCV transmission occurs by intravenous drug injection [122]. The use of intravenous drugs is the major risk factor in developed countries. Transmission by the transfusion of infected blood was drastically decreased following the introduction of screening tests for blood donors since 1990. Sexual and parental transmission are rare, the latter occurs in about 5% of babies born to HCV-RNA positive mothers [123,124]. Often when the infection occurred remains unknown, due to the long disease course and the presence of asymptomatic or nonspecific symptoms. Therefore, many aspects of the natural history of this infection are incompletely understood, in particular with regard to its variability (**Figure 6**).

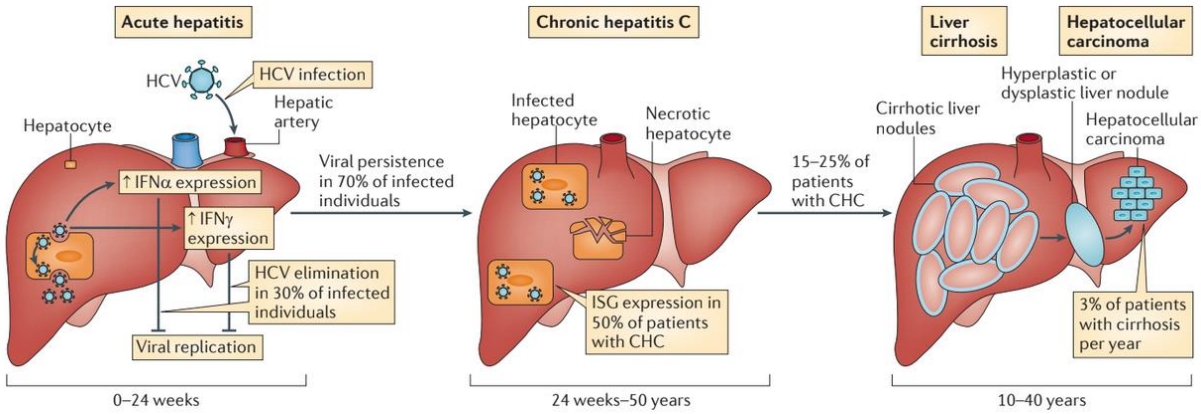

Figure 6. Natural history of HCV infection. From Heim 2013 [125].

Typically, the incubation period lasts from 20 days to 6 months. Symptoms (such as nausea, fatigue, abdominal pain, loss of appetite, and mild fever) occur in only 20-30% of acute infection cases. During the early acute phase, the IFN type I and III are the main actors of the antiviral response. After an initial peak, the IFN levels decrease at around 6 weeks. Within 6-12 weeks, post infection an alanine aminotransferase (ALT) increase can be observed. In this late acute phase, the type II IFN-γ is secreted by NK T cells and antigen-specific T cells recruited to counteract the infection [93]. Other molecules can support the antiviral activity. It has been demonstrated that TNF-α promotes and supports the IFN antiviral response, and it is also able to inhibit viral spreading directly [126–128]. The host response leads to resolution of the acute infection in 15-25% of subjects. Several factors may negatively influence the spontaneous viral clearance of the disease; age at time of infection >25

years, male sex, no jaundice or symptoms during acute infection, African American ethnicity, coinfection and immunosuppression [129]. In 70-85% of cases, the HCV infection persists becoming chronic, while cases of fulminant hepatitis are rare. The chronic infection can be defined as the presence of HCV RNA in the patient's blood longer than six months after transmission. In chronic infection, the ALT levels remain high, IFN-γ production drops, while IFN type I and type III are still expressed in 50% of subjects (**Figure 7**) [93].

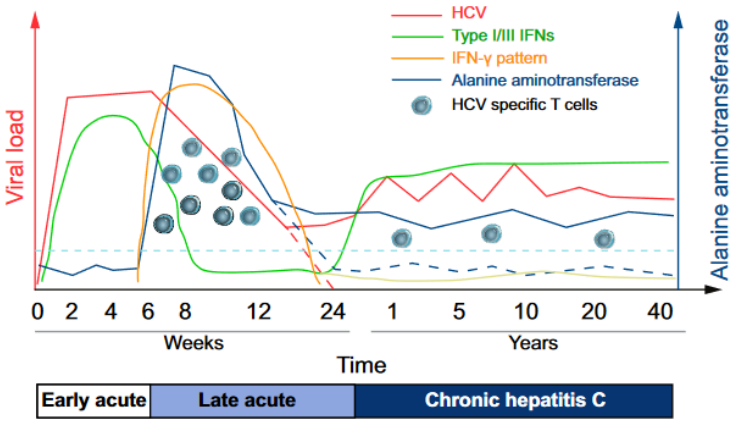

Figure 7. Progression of HCV infection and host response. From Heim 2014 [93].

Chronic infection leads to hepatic fibrogenesis, which may evolve to cirrhosis (10-20% of cases) in about 20-30 years. The establishment of hepatic cirrhosis can favour HCC development, with an annual risk rate of 1-5% [130]. The HCV-induced fibrosis is a complicated and multifactorial process, whose mechanisms are not completely understood. The most important risk factors for an advanced progression of fibrosis are related to individual factors (age >40 years, male sex, genetic), viral genotype, behavioral factors (smoking and alcohol consumption (>30 g/day in males, >20 g/day in females)), metabolic factors (insulin resistance, obesity), degree of inflammation and fibrosis on liver biopsy and coinfection with Human Immunodeficiency virus (HIV) or Hepatitis B virus (HBV).

The fibrogenesis mechanisms can be mainly ascribed to the HCV-induced antiviral response, to a hypoxic/pseudohypoxic state and to cellular metabolic changes. The synergic action of these factors promote alterations in the liver environment, leading to dysregulation of the resident liver cell type activity. It has been demonstrated that the infected hepatocytes and immune cells (such as KCs, pDCs, macrophages and NK) produce several inflammatory cytokines, which persist in the liver environment leading to fibrosis establishment. Some inflammation-related genes (such as IL6, CXCL8, CXCL10) have been found differentially expressed according to the different fibrosis grades [74,131,132]. Schulze-Krebs *et al.* demonstrated that TGF-β1 produced by HCV-infected hepatocytes is able to promote the activation of quiescent HSCs into a myofibroblast-like phenotype [133]. HSC

activation stimulates the production of fibrogenic factors such as collagen and extracellular matrix components, which induce the fibrosis onset [134]. Also HCV exposed macrophages are able to induce LX2 (immortalized human hepatic stellate cells) production of profibrogenic marks such as TGF-β1, matrix metalloproteinase 2 (MMP2) and Alpha-smooth muscle actin (α-SMA) [135].

As described above, the HCV replication induces profound metabolic changes in hepatocytes. The infection promotes hepatocyte lipid accumulation, which may lead to liver steatosis and increased fibrosis development risk. Recently, it is found that HCV genotype 3-infected subjects have a higher risk of hepatic steatosis [136,137]. Furthermore, several studies demonstrated that steatosis and fibrosis progression can be affected by the presence of genetic polymorphisms (SNPs), showing a profound interconnection between HCV infection and the host genetic factors. In this regard, the most studied SNP is the IL28B rs12979860 (C/C), which was found to be strongly associated with HCV infection resolution, steatosis progression and response to treatment [138,139].

With regard to fibrosis, the most recently studied genes are the patatin-like phospholipase domain-containing protein 3 (PNPLA3: rs738409 C>G), the 17-beta-hydroxysteroid dehydrogenase 13 (HSD17B13: rs72613567 T>TA), the transmembrane 6 superfamily member 2 (TM6SF2: rs58542926 C>T), the glucokinase regulatory protein (GCKR: rs1260326 T>C), and the membrane bound O-acyltransferase domain containing 7 (MBOAT7: rs641738 C>T). It is well known that the PNPLA3 variant induces alteration in LD synthesis and fatty acid accumulation in hepatocytes and HSCs [140]. Several studies show that the PNPLA3 SNP is a strong genetic risk factor for fibrosis severity in several liver diseases [141,142]. The HSD17B13 variant was found to be able to reduce the PNPLA3-induced risk, probably interacting with PNPLA3 protein on LD surface and regulating the lipid storage [143]. Synergistically, the GCKR allelic risk is associated with altered glucose metabolism contributing to increased de novo lipogenesis [144]. In addition, *in vitro* experiments showed that TM6SF2 inhibition led to higher accumulation of triglycerides and lipid droplets in hepatocytes and HSCs. The HSCs, carrying the TM6SF2 risk allele, are more strongly activated by TGF-β1 stimulation [145,146]. In 2016, Thabet *et al.* demonstrated an association between the MBOAT7 risk allele and a higher expression of inflammatory and oxidative stress markers in HCV-infected patient immune cells; suggesting an important role in hepatic inflammatory and fibrotic process [147]. Moreover, MBOAT7 mutation results to a reduced protein expression in hepatic cells, leading higher levels of arachidonic acid bound to phosphatidylinositol and promoting further hepatic inflammation [148,149].

Increased inflammation and fat accumulation creates a harmful environment that predisposes to enhanced oxidative stress and mitochondrial dysfunction, which in turn could be responsible for malignant hepatocyte transformation [150].

HCV therapies

The first standard therapy was based on IFN-α administration in combination with Ribavirin. The subsequent use of the PEGylated form of interferon (Peg-IFN-α), which confers longer half-life, allowed to improve the standard therapy. This therapy had to be taken for a period of 24 or 48 weeks, and the achievement of the sustained virological response (SVR: undetectable HCV RNA (<15 IU/ml) after 24 weeks of treatment) was observed in the 50-60% of cases [151]. The low response rate was due to the presence of many factors influencing this treatment: sex differences, age, ethnicity, IL28B polymorphism, viral load and genotype. Furthermore, both Peg-IFN-α and Ribavirin could lead to severe side effects such as headache, fever, severe depression, myalgia, arthralgia and hemolytic anemia [152].

In recent years, there has been a rapid evolution in HCV antiviral therapies. This was made possible by the development of *in vitro* systems (such as HCV pseudoparticles, replicon system, HCV full-length and trans-complemented particles), which allowed the deeper study of the HCV replication cycle [153]. Starting from 2011, the introduction of the novel direct anti-HCV agents (DAAs) have completely revolutionized clinical practices. The first approved DAAs were telaprevir and boceprevir, which are two NS3-4A protease inhibitors and were used in combination with Peg-IFN-α and Ribavirin. Subsequently, the growing knowledge about the HCV viral cycle has led to the development of numerous new DAAs in a short time. In 2013, the Food and Drug Administration (FDA) approved a nucleotide analogue inhibitor (sofosbuvir) and simeprevir, capable of blocking the action of the viral protein NS5B and NS3-4A, respectively. These new compounds in combination with Peg-IFN-α and Ribavirin resulted in viral eradication in 90% of cases for the viral genotypes [154]. In the last years several compounds have been developed; NS3/4A inhibitors such as grazoprevir, glecaprevir and voxilaprevir, new NS5A inhibitors (daclatasvir, elbasvir, ledipasvir, velpatasvir and pibrentasvir) and the NS5B inhibitor dasabuvir [154–156]. Using different drug combinations the success rates now exceed 95%. However, cost and the possibility of virologic resistance (principally related to the HCV genotype 3) are factors that must be considered for the future [157].

It is important to mention that new HCV therapies have also reduced the incidence of HCC. However, the hepatic inflammation can persist in a treated-chronic infection, maintaining the risk of HCC

development [158]. Furthermore, it has been demonstrated that an advanced HCV chronic infection lead to profound epigenetic and gene expression changes, which persists also in SVR-achieving patients, and these changes are associated with HCC development risk [159,160].

HCV and sex hormones

Sex-dependent biological characteristics are one of the most important factors affecting the natural history of HCV infection. The female sex is a protective factor, known to favour higher spontaneous viral clearance rates after HCV acute infection [161,162]. Moreover, disease progression is slower in females compared to males, who have a 10-fold rate of progression to fibrosis regardless of age [163]. Therefore, the female sex is a protective factor against fibrotic progression in patients with chronic liver disease [164]. However, the liver disease progression is not linear across different stages of a woman's life; specifically, a different progression rate can be observed between females in pre vs. post -menopausal period, though this issue has been debated [165,166]. In some studies, a higher SVR rate was associated with male sex; other studies did not find significant differences between females and males, while a low SVR likelihood was associated with menopause. Such differences were not observed in the DAA treatment era [167–171]. In 2004, Di Martino *et al.* evaluated the influence of menopause and hormone therapy on liver fibrosis progression in HCV-infected women. They demonstrated that fibrosis progression was faster during the menopause, and this effect was prevented by hormone replacement therapy (HRT) [164]. Similar results were obtained by other studies, proving further that chronically HCV-infected women who receive HRT have lower fibrosis stage, and that female sex influences fibrotic progression [172,173]. The main difference between the fertile and the menopausal periods is the concentration of sex hormones in the body, whose levels drop dramatically during the menopause. It has been hypothesized that the observed differences in viral clearance and disease progression could be related to sex hormones such as estrogens [174]. Nevertheless, it must be considered that in females there is a lower prevalence of obesity and lower alcohol and tobacco consumption [175].

Focusing on HCV clearance, the protective mechanisms related to female sex are unknown. A first hypothesis concerns the interplay between sex hormones and the viral entry phase. Sex hormones can modulate the host cellular receptors, which are important for the viral entry step. Testosterone is able to promote the expression of SR-B1 and CLDN in different cell types [176,177]. Conversely, E2 is able to reduce the SR-B1 expression in rat and mice livers [178]. A further hypothesis stems from the relationship between sex hormones and the immune response; some differences in IFN system induction are observed between females and males. The peripheral blood mononuclear cells

(PBMCs), isolated from untreated HCV-infected female in premenopausal period, showed higher MxA mRNA levels post IFN stimulation compared to both postmenopausal females and males. However, in the same study the IFN-stimulated PBMCs showed SOCS up-regulation and reduced JAK/STAT activation post ER agonist treatment [179]. Conversely, Fawzy *et al.* showed that the ER antagonist tamoxifen is able to decrease IFN-α production in PBMCs of HCV infected males, possibly via TLR7 suppression [180]. A further difference between female and male sex was observed evaluating the NK cell subpopulation expressing the protein p46, which is the most important member of cytotoxicity receptors. The $NKp46^{High}$ phenotype produces higher amounts of IFN-γ and their intrahepatic accumulation was found to be inversely correlated to HCV RNA levels and degree of fibrosis [181]. In a study conducted by Golden-Mason *et al.,* the HCV-infected female group had a higher amount of $NKp46^{High}$ levels compared to HCV-infected male group [182]. Several studies showed a greater viral clearance in females carrying TLR7 (rs179008-A and rs3853839-C), TLR9 (rs187084-C) and IL28B (rs12979860-C) SNPs [183–186]. With regard to the immune system cells, it is also notable that female pDCs show higher basal levels of IRF5 mRNA compared to males [187]. Moreover, pDCs isolated from healthy females produce higher IFN-α levels post TLR7 agonist stimulation compared to males [188]. Taken together, these data would suggest a greater activation of the IFN system in premenopausal females, highlighting the role of sex hormones on immune modulation.

HCV-induced cytokines and ROS production can promote the onset of a chronic inflammatory environment. As mentioned above, inflammation is a key player for fibrosis progression and HCC development. Estrogen receptors (ERs) levels are dysregulated during HCV-related fibrotic process and HCC development; HCV genotype 1b infected patients show an inverse correlation between degree of fibrosis and ER alpha (ERα) protein levels, whose expression was also found reduced in female HCV-related HCC tissues compared to male HCV-related HCC tissues [189,190]. Thus, an altered estrogen activity could be a promoting event for liver disease progression. In fact, several studies showed that estrogens can protect the liver from inflammatory injury, oxidative stress and cell death; all fundamental factors for fibrosis progression and HCC development [191–193].

In the inflammatory context, IL-6 is one of the most studied and characterised cytokines; it is considered a key component in inflammation-associated tumorigenesis [194,195]. Naugler *et al.* demonstrated that in KCs exposed to necrotic hepatocytes the IL-6 production is inhibited by 17,β-estradiol (E2) treatment. Moreover, both *in vitro* and *in vivo* the E2 was able to reduce the IL-1β activity and TNF-α levels; other two important inflammatory-associated cytokines [196,197]. It has been also demonstrated that estrogens (specifically the E2) are able to attenuate HSC activation *in*

vitro and *in vivo* [198]. Moreover, HCV infection induces an increasing oxidative stress, which in turn can lead to inflammation and liver injury [199]. The E2 is a well-known endogenous antioxidant, which could counteract the HCV-induced oxidative stress. It has also been demonstrated that 17,β-estradiol was able to reduce ROS formation in both HuH7.5 and Lx2 cell lines [200].

The use of *in vitro* HCV cell-culture systems allows a better study of the interaction between HCV infection and sex hormones directly on hepatocytes. A first interplay between the HCV and the ERα C-terminal domain was demonstrated by Watashi *et al.* and Hillung *et al.* The ER antagonist tamoxifen was able to abrogate the interaction between the viral protein NS5B and the endoplasmic reticulum. This finding suggests that ERα could play a fundamental role in the HCV replication process, favouring the NS5B-endoplasmic reticulum association [201,202]. In 2010, Hayashida *et al.* assessed the possible antiviral action of 17,β-estradiol, progesterone and ERα-, ERβ-, G protein-coupled receptor 30 (GPR30)- selective agonists; only E2 was able to significantly reduce the HCV particle production in an ERα-dependent manner [203]. Subsequently, it has been demonstrated that E2 interferes also with the entry viral step. The E2/GPR30 interaction increases the intracellular Matrix metallopeptidase 9 (MMP-9) levels, which in turn lead to OCLN cleavage, reducing viral particle entry [204]. In 2016, Magri *et al.* evaluated the antiviral activity of different sex hormones: E2, dehydroepiandrosterone sulfate (DHEA-S), progesterone and testosterone. Only E2 was able to reduce HCV infection in HuH7 cells, triggering an hepatocyte antiviral state which was able to interfere with HCV release and partially with viral entry [205]. These results suggest that the sex differences could be related not only to a higher antiviral response by the immune system cells but also by the hepatocytes. However, the E2-activated antiviral pathways in hepatocytes are not fully elucidated.

Estrogens

Biosynthesis and biological activity

Estrogens are the main female sex hormones. They are produced not only in the gonads and adrenal cortex but also in extragonadal tissues such as liver, fat, and kidney. The three primary endogenous estrogens are: estrone (E1), 17,β-estradiol (E2) and estriol (E3). These sex hormones belong to the steroid hormone family and are synthesized by cholesterol in response to the stimulus of the luteinizing hormone (LH) and follicle-stimulating hormone (FSH). Cholesterol is converted to pregnenolone by the cytochrome P450 side chain cleavage enzyme (P450scc). Then pregnenolone is converted to progesterone or DHEA by the enzymes 3-beta-hydroxysteroid dehydrogenase (3β-HSD)

or cytochrome P450 17α-hydroxylase (P45017α), respectively. The enzymes P45017α and 3β-HSD catalyze the conversion of progesterone and DHEA (respectively) to androstenedione, which is converted to testosterone by the 17-beta-hydroxysteroid dehydrogenase (HSD17B). The androstendione is the precursor of the E1, and the testosterone is the precursor of the E2; the Aromatase CYP19 catalyzes both enzymatic reactions. Then E1 can be converted to E3 through 16α-hydroxylation or to E2 through the enzyme HSD17B [206,207].

17,β-estradiol is the most abundant form of circulating estrogen [208]. However, the E2 body concentration is age-dependent; in the fertile period the range is 20-443 pg/mL (follicular phase: <20-145 pg/mL; ovulation: 112-443 pg/mL; phase luteal: <20-241 pg/mL), in menopause the E2 levels drop below 59 pg/mL [209]. In males the E2 concentration is approximately 20 pg/mL, still exerting important physiological roles [208].

17,β-estradiol exerts its biological effects via interaction with the ERs and the GPR30. There are two distinct ER forms (ERα and ERβ), which are encoded by ESR1 and ESR2 genes, respectively. The ERα is mainly expressed in the uterus, liver, kidneys and in the heart. While ERβ is mainly expressed in the ovary, prostate, lungs, gastrointestinal tract, bladder and central nervous system [210]. ERα and ERβ belong to the nuclear hormone receptor family. Their structure can be divided in five domains: the DNA binding domain, which shows highest homology sequence between ERα and ERβ, the ligand binding domain, the hinge domain containing a nuclear localization signal, and two transcriptional activation function domains. ER homo- or hetero- dimers are transcription factors located in the cytoplasm. After the interaction with their ligands, these receptors translocate to the nucleus and activate genetic transcription by binding the estrogen responsive elements (EREs) [211]. The binding to the EREs is mediated by the interaction of the ERs with coactivator proteins (such as the forkhead protein (FOXA1), the histone acetyltransferase p300 and the CBP). Furthermore, the combination of ERs with proteins such as the stimulating protein-1 (Sp-1) and the Activator protein 1 (AP-1) can promote gene transcription without the interaction with the ERE [212,213]. The bind of E2 to ER and GPR30, located on the plasma membrane, promote the fast modulation of indirect non-genomic signaling signal-transduction mechanisms; the downstream response is principally mediated by intracellular signaling molecules such as PI3K, Akt, RAS, NF-κB, endothelial nitric oxide synthase (eNOS), and MAPK [214,215]. ERs can also induce the gene transcription in a ligand independent manner; ERs interact with several growth factor receptors such as the endothelial growth factor receptor (EGFR) signaling and the insulin-like growth factor receptor 1 (IGFR1). The activated downstream response is principally mediated by PI3K/Akt, RAS/MAPK, SRC kinases and JAK/STAT signaling pathways [216].

Altogether, the estrogens can interact with a large number of intracellular signaling pathways, modulating cell proliferation, growth, migration and apoptosis. Estrogens not only promotes secondary sexual characteristic formation but also acts on a wide number of tissues and cell types; it is able to interact with the inflammatory process acting directly on immune cells, or it can modulate the metabolic processes especially in the liver, the adipose tissue and the skeletal muscle. Overall it should be considered that estrogen effects are strongly influenced by its concentration, by the exposure time and by the target cell types [217].

Estrogens and hypoxia cross-talk

Angiogenesis is a complex and highly regulated process. In normal conditions, the estrogens have a proangiogenic activity, driving principally the process in the female reproductive tract. Angiogenesis dysregulation is often observed in cancer and the interplay of estrogens and angiogenesis has been principally studied in breast cancer [218].

Hypoxic conditions lead to angiogenesis activation via the Hypoxia inducible factor 1-alpha (HIF-1α) signaling pathway, which induces proangiogenic factor production (such as VEGF, fibroblast growth factor (FGF), nitric oxide synthases (NOS), cyclooxygenase 2 (COX-2) and matrix metalloproteinases (MMPs)) [219]. The VEGF is a key molecule in the angiogenic process: it promotes cell proliferation, migration, survival, and vascular permeability. As mentioned above, a hypoxic condition can promote the establishment of an inflammatory environment and fibrosis, which may contribute to cancer development and progression. It has been hypothesized that estrogens can counteract fibrosis and inflammation establishment by the interaction with hypoxia [220]. Generally, hypoxic-induced inflammation results in a ER-α protein reduction, while oxidative stress increases the expression of ER-β [221,222]. It has been demonstrated that the E2 treatment can promote VEGF and the histone demethylase JMJD2B (KDM4B) gene transcription, which are two genes also induced by HIF-1α [223–226]. Several studies analysed the interaction between ERs and HIFs, highlighting the interconnection between the estrogen and hypoxia pathways. An ERE has also been identified in the first intron of the HIF-1α gene, the E2-activated ER-α can lead to HIF-1α production [227]. The E2/GPR30 interaction induces VEGF production via HIF-1α up-regulation in cancer-associated fibroblast (CAFs) and in the breast cancer cell line SkBr3 [228]. Transfecting the HEK 293T cells with ERE-luc and expression vectors for ER-α or ER-β, Yi *et al.* observed a synergic action of hypoxia and E2 treatment in promoting ER-α transcriptional activity. Moreover, in the MCF7 cell line, the E2 and hypoxia treatment induced a down-regulation in ER-α protein levels [229]. Another study showed that HIF-1α can interact with the unoccupied ER-α and ER-β, promoting ERs-mediated

transcription via ERE in HEK 293T. In addition, ER-β reduces VEGF levels, inhibiting HIF-1α transcription activity [230]. In the Hep3B cell line, the E2 was able to reduce hypoxic induction of HIF-1α [231]. Also in adipose tissue the E2-activated ER-α promotes the HIF-1α protein degradation, inducing PHD3 expression [232]. In prostate cancer cells the ER-β variant ERβ2 interacts with HIF-1α protein, stabilizing it and promoting an hypoxic gene expression signature [233]. However, the interplay between estrogens and hypoxia is not well understood and seems to act differently depending on ER-α or ER-β activation, cell types and diseases.

AIM

Chronic hepatitis C is one of the most widespread liver diseases in the world, with over 170 million individuals infected with the hepatitis C virus (HCV) and 3-4 million new cases every year. Several clinical studies have demonstrated that females have a greater spontaneous viral clearance after the HCV acute infection. Furthermore, HCV-induced fibrosis progression is slower in premenopausal females compared to males and postmenopausal females. These findings can also support and explain, at least in part, the lower risk of females to develop hepatocellular carcinoma. The main difference between pre- and post- menopausal age is the presence of different circulating sex hormone concentrations; so it has been hypothesized that hormonal factors can have a protective effect against HCV infection and HCV-related liver diseases [174].

In a previous study published by our group, we used different *in vitro* HCV cell culture systems to evaluate the antiviral activity of the following sex hormones: 17,β-estradiol (E2), dehydroepiandrosterone sulfate (DHEA-S), progesterone and testosterone. Only the E2 was able to counteract the viral infection in hepatocytes, acting through the intracellular estrogen receptor. Studying in depth the viral cycle phases, we found that E2 exerted its antiviral effect acting on the HCV particle release and partially with the viral entry [205]. However, the E2-activated hepatocyte antiviral mechanisms are still unknown.

During HCV infection, the hepatocytes play a central role in the innate immunity response. The interferon system, in particular, is the first-line defense mechanism against viral infections. Furthermore, the inflammatory response is one of the main modulator factors of fibrosis development and hepatocarcinogenesis. In this regard, in chronic HCV infection the inflammatory environment interacts with the HCV-induced hypoxic state, which can alter viral replication and can promote liver disease progression. In this setting, 17,β-estradiol can modulate the adaptive and innate immune responses of different cell types. It is known that estrogens can interplay with the interferon system, but most of the studies examined this interaction on immune system cells only. The possible E2-mediated interferon activity on hepatocytes is still to be clarified. Therefore, in the first part of the present study, we evaluated the E2-mediated activation of hepatocytes innate immunity. On the other hand, several studies also show the interplay between hypoxia and the estrogen signaling pathways. Therefore, in the second part of the study, we focused on the interplay between 17,β-estradiol and HCV infection in a chemically-induced pseudohypoxic state.

MATERIALS AND METHODS

Cell cultures and chemical compounds

The human hepatoma-derived HuH7 cells were grown in DMEM (1X) + GlutaMAX™-I, supplemented with 10% fetal bovine serum (FBS), 100 U/mL penicillin, 100 μg/mL streptomycin, 0.1 M non-essential amino acids, 25 mM HEPES (N-2-hydroxyethylpiperazine-N-2-ethane sulfonic acid), and 1 mM sodium pyruvate (Thermo Fisher Scientific, Milan, Italy).

According to different models described below, HuH7 cells were treated with 17,β-estradiol (E2) (Sigma-Aldrich Milan, Italy), fulvestrant (F) (Sigma-Aldrich Milan, Italy), IFN alpha-IFNAR-IN-1 hydrochloride (IFNARi) (MedChemExpress, Monmouth Junction, NJ 08852, USA), interferon alpha-2a (IFNα2a) (Roche S.P.A, Monza, Italy) and dimethyloxalylglycine (DMOG) (Sigma-Aldrich Milan, Italy). All compounds were dissolved as indicated by manufacturer's instructions and stored at -20°C.

HuH7 cells were also maintained in culture for 14 days with 17,β-estradiol (400 nM) or dimethyl sulfoxide (DMSO). In this dissertation, they were called HuH7-E2 and HuH7-DMSO, respectively. The E2 chosen concentrations are based on the previous article published by our group [205].

HCV infection

Viral particle production was performed as described by Magri *et al.* [205]. Infection was performed for 3 hours using the HCV genotype 2a JFH-1 at a multiplicity of infection (MOI) of 0.1 or 0.05 according to experiments. The compound's effects on viral infection were evaluated with the focus forming unit assay (FFU) or by intracellular HCV RNA quantification (HCV RNA). All the infection results were normalized to DMSO-treated and infected cells (drug vehicle control). The FFU assays were performed in a 96-well plate (8.000 cells/well) and the intracellular HCV RNA quantification was performed on HuH7 cells seeded in a 12-well plate (30.000 cells/well).

- In FFU assay, infected cells were fixed and permeabilized with 4% paraformaldehyde and Triton ® X-100 (0.5% in PBS 1X, Merck, Rome, Italy), respectively. After treatment with H_2O_2 (0.3% in PBS 1X), the saturation was performed with bovine serum albumin (BSA) (3% in PBS 1X-Tween®20, Sigma-Aldrich Milan, Italy). The infected cells were visualized and counted with AEC Staining Kit (Sigma-Aldrich, Milan, Italy), using as primary antibody a serum of HCV positive patient, and as secondary antibody the rabbit anti-human IgG labelled with peroxidase (Dako Denmark A/S, Produktionsvej, Denmark).
- Extracellular viral particles were measured by viral titration using the FFU assay (FFU/mL). Naïve HuH7 cells were infected with serial dilutions of the collected infective supernatants.

After 3 hours, the viral inoculum was replaced with the fresh medium for 72 hours and viral titer was evaluated by FFU assay.

- The intracellular viral particles were obtained with 4-5 freeze thaw cycles of infected cells. The viral titer (FFU/mL) was obtained as described for extracellular viral particles titration.
- The intracellular HCV RNA quantification was performed with the real-time PCR method (qPCR) by absolute quantification using a linear regression on serial dilutions of the pJFH1 plasmid at known concentrations. The RNA extraction, the revers transcription and the qPCR was performed as described below, JFH-1 primers are reported in **Table 2**.
- Viral assembly efficiency was calculated by the ratio between the intracellular viral particles (FFU/mL) and the quantified intracellular HCV RNA (copies/mL).

RNA extraction and gene expression analysis

Cells were harvested and total RNA was extracted using NucleoZOL (MACHEREY-NAGEL, Bethlehem, USA) as reported by manufacturer's instructions. Subsequently, 250 ng of RNA were retrotrascribed using High-Capacity cDNA Reverse Transcription Kit (Thermo Fisher Scientific, Milan, Italy). The qPCR was performed using the Power SYBR™ Green Master Mix (Thermo Fisher Scientific, Milan, Italy) with specific primers (**Table 2)** or using TaqMan™ Gene Expression Master Mix (Thermo Fisher Scientific, Milan, Italy) with TaqMan's probes (**Table 3**) (Thermo Fisher Scientific, Milan, Italy). We used hypoxanthine-guanine phosphoribosyltransferase (HPRT) as the housekeeping gene to calculate the ΔCt. The relative gene expression, normalized to control cells (uninfected DMSO-treated cells), was determined using the $2^{-\Delta\Delta Ct}$ method.

Table 2. Primer full sequences used for real-time qPCR. Carbonic anhydrase 9 (CA9), interleukin-8 (CXCL8), growth regulating estrogen receptor binding 1 (GREB1), hypoxanthine-guanine phosphoribosyltransferase (HPRT), interferon beta 1 (IFNB1), interferon lambda 3 (IFNL3), interleukins- (IL-1B, 18), interferon regulatory factor 3 (IRF3), interferon regulatory factor 5 (IRF5), interferon-stimulated gene 56 (ISG56), HCV RNA (JFH-1), lysine demethylase 4B (KDM4B), transforming growth factor beta (TGFB1), toll-like receptor 3 (TLR3), tumor necrosis factor alpha (TNF).

Gene	Primer Forward	Primer Revers
CA9	5'-GTGCCTATGAGCAGTTGCTGTC-3'	5'-AAGTAGCGGCTGAAGTCAGAGG-3'
CXCL8	5'-CCAGGAAGAAACCACCGGA-3	5'-GAAATCAGGAAGGCTGCCAAG-3
GREB1	5'-GGTCTGCCTTGCATCCTGATCT-3'	5'-TCCTGCTCCAAGGCTGTTCTCA-3'
HPRT	5'-GATTTGGAAAGGGTGTTTAT-3'	5'-TCCCATCTCCTTCATCACAT-3'
IFNB1	5'-CAGCAATTTTCAGTGTCAGAAGC-3'	5'-TCATCCTGTCCTTGAGGCAGT-3'
IFNL3	5'-TCGCTTCTGCTGAAGGACTGCA-3'	5'-CCTCCAGAACCTTCAGCGTCAG-3'
IL1B	5'-ACAGATGAAGTGCTCCTTCCA-3'	5'-GTCGGAGATTCGTAGCTGGAT-3'
IL18	5'-GACCAAGGAAATCGGCCTCTA-3'	5'-ACCTCTAGGCTGGCTATCTTTATACATAC-3'
IRF3	5'-ACCAGCCGTGGACCAAGAG-3'	5'-TACCAAGGCCCTGAGGCAC-3'
IRF5	5'-TATGCCATCCGCCTGTGTCAGT-3'	5'-GCCCTTTTGGAACAGGATGAGC-3'
ISG56	5'-GCCTTGCTGAAGTGTGGAGGAA-3'	5'-ATCCAGGCGATAGGCAGAGATC-3'
JFH-1	5'-TCCCGGGAGAGCCATAGTG-3'	5'-TCCAAGAAAGGACCCAGTC-3'
KDM4B	5'-ATCTTGACCATGTCCTTCCG-3'	5'-TCAACTGCGCAGAATCTACC-3'
TGFB1	5'-CCCAGCATCTGCAAAGCTC-3'	5'-GTCAATGTACAGCTGCCGCA-3'
TLR3	5'-GCGCTAAAAAGTGAAGAACTGGAT-3'	5'-GCTGGACATTGTTCAGAAAGAGG-3'
TNF	5'-CCCAGGGACCTCTCTCTAATC-3'	5'-ATGGGCTACAGGCTTGTCACT-3'

Table 3. TaqMan probes used for real-time qPCR. Eukaryotic translation initiation factor 2 alpha kinase 2 (EIF2AK2), hypoxia inducible factor 1 alpha (HIF1A), hypoxanthine-guanine phosphoribosyltransferase (HPRT), interferon alpha 1 (IFNA1), interleukin-6 (IL6), interferon regulatory factor (IRF7), interferon-stimulated gene 15 (ISG15), myxovirus (influenza) resistance 1 (MX1), 2'-5'-oligoadenylate synthetase 2 (OAS2).

Gene	TaqMan probe	GenBank
EIF2AK2	Hs00169345_m1	AK290655.1
HIF1A	Hs00153153_m1	AB073325.1
HPRT	Hs02800695_m1	AK313435.1
IFNA1	Hs00256882_s1	AB578886.1
IL6	Hs00985639_m1	A09363.1
IRF7	Hs00185375_m1	AF076494.1
ISG15	Hs00192713_m1	BM712238.1
MX1	Hs00182073_m1	AK096355.1
OAS2	Hs00942643_m1	AK292796.1

Re-sensitising to infection

HuH7 cells were seeded in a 96-well plate; the next day cells were treated with E2 according to two different hormone-treatment exposure: short- and long- term treatment.

Regarding the short-term treatment model (**Figure 8A**), HuH7 cells were incubated overnight (ON) with two different E2 concentrations (400 and 200 nM) or DMSO (control group), the next day treatment was removed and replaced with the fresh medium for different time points (0, 2, 3, 4, 5, 6 and 24 hours) before the 3 hours infection (MOI 0.1).

In the long-term treatment model, HuH7 cells were cultured in a flask for 14 day in presence of E2 at the concentration of 400 nM (HuH7-E2) or DMSO (HuH7-DMSO). These cells were seeded in a 96-

well plate still in presence of hormone and the next day treatment was removed and replaced with the fresh medium for 0, 1, 2, 3, 4 and 5 days before 3 hours infection (MOI 0.1) (**Figure 8B**).
In each model, the cells were maintained 72 hours post infection in the fresh medium and the antiviral activity was evaluated by FFU assay.

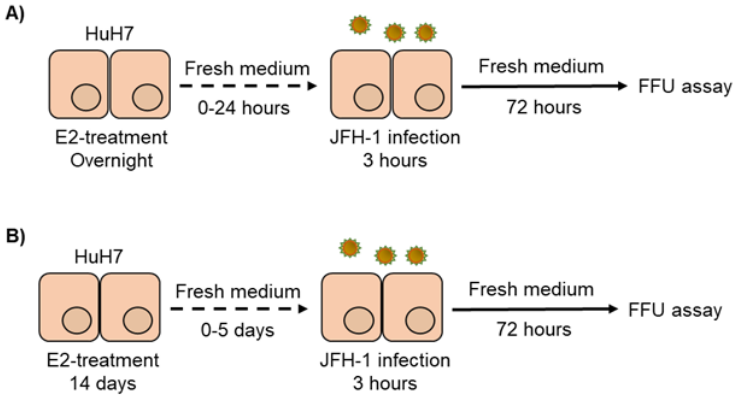

Figure 8. Re-sensitisation models. A) Short-term treatment model. **B)** Long-term treatment model.

Time course gene expression

HuH7 cells were seeded in a 12-well plate, the next day cells were treated 1 hour with E2 (400 nM) (HCVcc+E2) or DMSO (HCVcc) and then infected for 3 hours (MOI 0.1) still in presence of treatments (**Figure 9A**). Control treatment (E2-treated cells) and control cell conditions were performed incubating cells for 1+3 hours in E2 or DMSO, respectively (**Figure 9B**). Afterwards, all the conditions were maintained in the fresh medium and we performed gene expression analysis at different time points (0, 6, 24, 48 and 72 hours). The analysed genes are shown in **Table 2** and **Table 3**; CA9 and HIF1A genes were not evaluated in this experimental models.

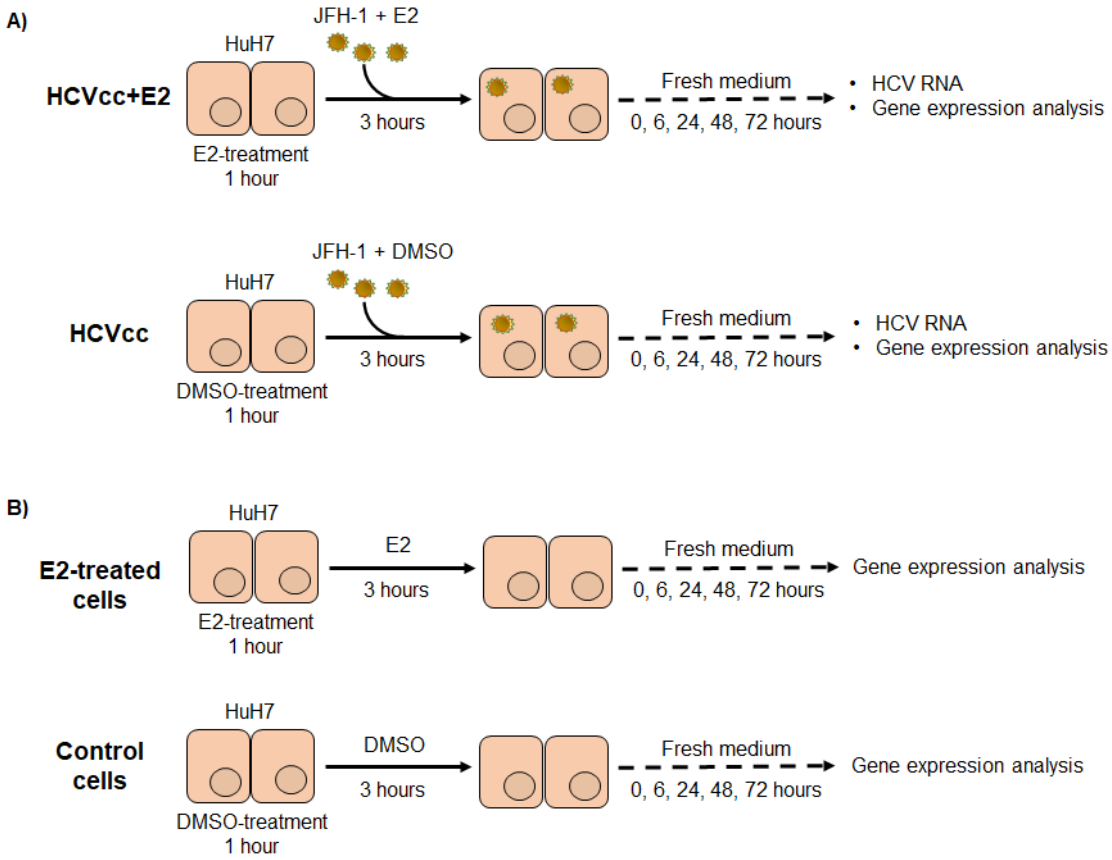

Figure 9. HCVcc and 17,β-estradiol-treatment models. A) HCVcc model with and without E2 treatment. **B)** Treatment control models.

Combination treatment models

The antiviral activities of the estrogen receptor modulators (E2 and fulvestrant) and of IFNα2a were tested in combination with IFNARi at the concentration of 500 nM.

IFNα2a + IFNARi:

- Cells were infected for 3 hours (MOI 0.1), then they were incubated for 72 hours in presence of serial dilution (1:10) of IFNα2a (from 10^{3} to 10^{-4} MUI/mL) or DMSO with or without IFNARi. Viral infection was evaluated by FFU assay (**Figure 10**).

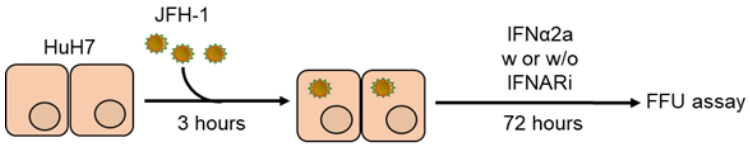

Figure 10. IFNα2a and IFN alpha-IFNAR-IN-1 hydrochloride (IFNARi) combination treatment model.

17,β-estradiol or fulvestrant + IFNARi:

- HuH7 cells were treated for 1 hour with different compounds; E2, fulvestrant, the combination E2+F and DMSO (control), all combined with or without IFNARi. Infection was performed for

3 hours (MOI 0.1) still in the presence of treatments. After infection, viral inoculum was removed and cells were incubated with IFNARi or DMSO. At 72 hours, viral infection was evaluated by FFU assay. Real-time qPCR analysis on intracellular HCV RNA was performed only for E2±IFNARi and DMSO±IFNARi treatment conditions (**Figure 11A**).

- HuH7 cells were incubated for 1 hour with E2 or DMSO and infected for 3 hours (MOI 0.1) still in the presence of treatment. Afterwards, viral inoculum was removed and IFNARi was added immediately (0), 24 or 48 hours post infection until 72 hours. Viral infection was evaluated by FFU assay (**Figure 11B**).

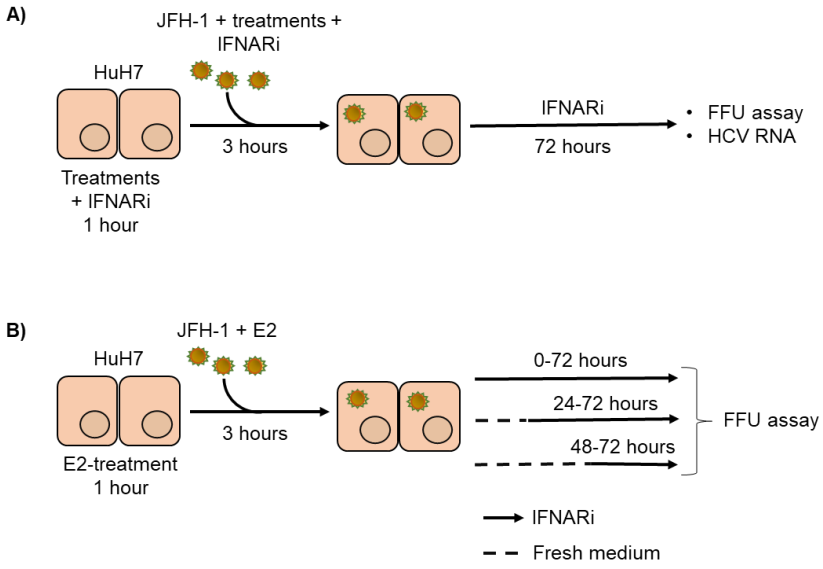

Figure 11. HCVcc+treatment models in combination with IFN alpha-IFNAR-IN-1 hydrochloride (IFNARi). A) Treatments (E2, fulvestrant (F) and E2+F) in combination with IFNARi. **B)** IFNARi was added at different time points post E2-treatment and infection.

Conditioned medium (CM) production and antiviral activity evaluation

HuH7 cells were seeded in a 6-well plate (75.000 cells/well), next they were treated for 4 hours with E2 (400 nM) or DMSO (control media). Subsequently, treatment was removed and replaced with fresh medium. Separately for each timing, the conditioned medium (CM) was collected at the corresponding time point (24, 48 or 72 hours) and stored in -80°C until use (**Figure 12**).

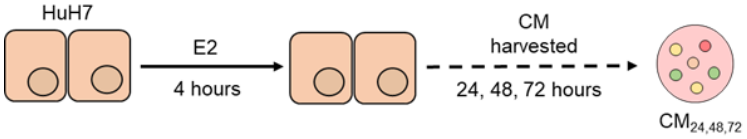

Figure 12. Conditioned medium (CM) production.

To test the antiviral action of the CM_{24}, HuH7 cells were seeded in a 96-well plate. The next day, cells were treated for 4 hours with E2 (400 nM) or DMSO and maintained in the fresh medium for 24 hours before infection (MOI 0.1). Then, viral inoculum was removed and CM_{24} or fresh medium were added for 72 hours. The antiviral activity was evaluated performing the FFU assay (**Figure 13A**).

To test the antiviral action of the conditioned medium harvested at 48 and 72 hours (CM_{48} and CM_{72}), HuH7 cells were seeded in a 6-well plate (75.000 cells/well). These cells were treated 1 hour with the respective CM with or without IFNARi supplementation. In the next 3 hours, infection (MOI 0.1) occurs still in the presence of treatments. Subsequently, viral inoculum was removed and replaced with the fresh medium for 72 hours (**Figure 13B**). The infective supernatant was then titrated as previously described by FFU assay.

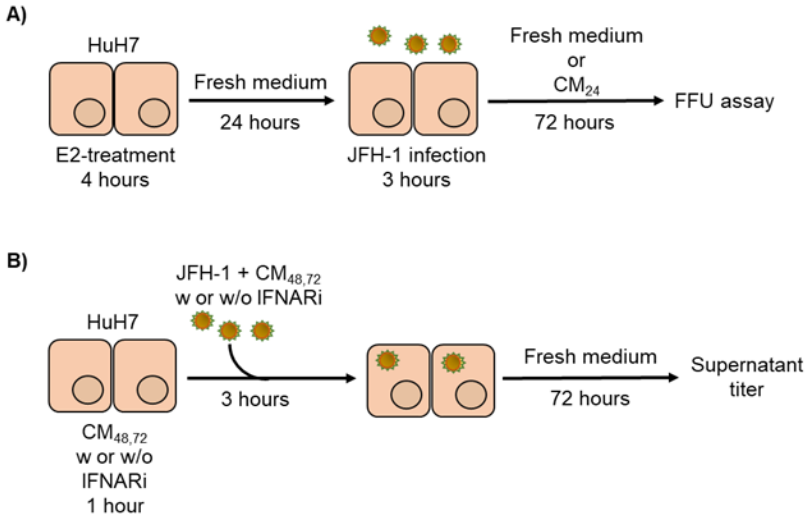

Figure 13. Evaluation models of conditioned medium (CM) antiviral activity. Models used to test the antiviral activity of the CM_{24} (**A**) and the CM_{48} and CM_{72} (**B**)

DMOG treatment models

DMOG was used at concentrations of 80 µM and with serial dilutions from 40 to 0.064 µM (1:5). The DMOG serial dilutions were tested also in combination with 17,β-estradiol (400 nm) or fulvestrant (400 nm). The 17,β-estradiol and fulvestrant serial dilutions (1:2: from 400 to 6.25 nM) were tested in combination with DMOG (1.6 and 8 µM). HuH7 cells were treated according to two different Models (**Figure 14**) with or without JFH-1infection. In Model 1 cells were treated overnight, JFH-1 infection was performed for 3 hours and cells were then incubated for 72 hours in the fresh medium (**Figure 14A**). In Model 2, post 3 hours infection cells were incubated for 72 hours in presence of treatment (**Figure 14B**). Infection was performed at a MOI of 0.1 or 0.05 according to experiments. At 72 hours, the HCV infection was evaluated by FFU assay and by HCV RNA

quantification. The gene expression analysis of the hypoxia-related gene CA9 and HIF1A (**Table 2**) was performed as previously described in the "RNA extraction and gene expression analysis" section.

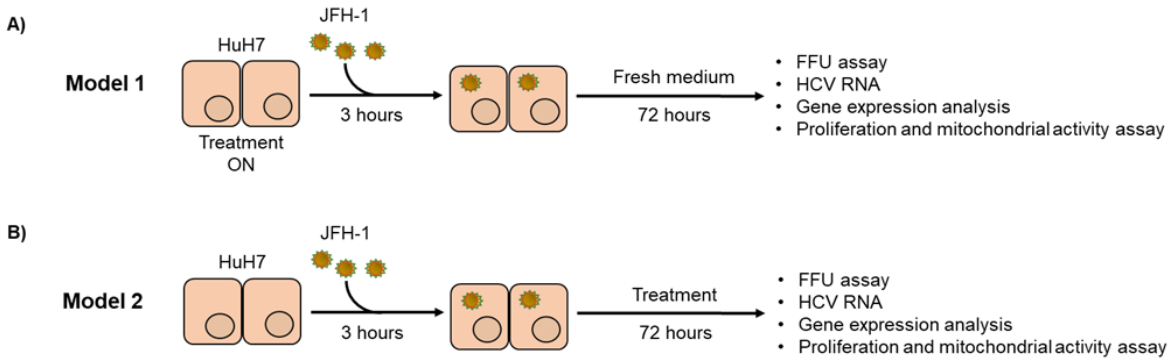

Figure 14. DMOG treatment models. Treatment model 1 **(A)** and treatment model 2 **(B)**.

Proliferation and mitochondrial activity assay

The IFNARi effects on cell proliferation were tested using crystal violet (CV) assay. HuH7 cells were seeded in a 96 well plate (8.000 cells/well) and the next day cells were treated for 72 hours with IFNARi serial dilutions (1:3: 20-0.01 µM). Then, cells were fixed with glutaraldehyde (11,5%) and, after washing steps, crystal violet (0,1%) was added. Following washing steps and acetic acid (10%) addition, the absorbance values (OD) were measured at 570 nm using the instrument VICTOR Multilabel Plate Reader (PerkinElmer, Milan, Italy).

According to the Models shown in **Figure 14,** the CV assay was also used to test the effect on cell proliferation of DMOG serial dilutions (1:5: 40 -0.064 µM) or DMOG at 80 µM in presence or absence of infection. DMSO was used as control treatment and OD values were obtained as previously described.

The Model 2 (**Figure 14B**) was used to test the effect on cell mitochondrial activity of E2 (400 nM), F (400 nM) and DMOG (8 µM), alone or in combination. In this experiment, HuH7 cells were seeded in two 96-well plates, the next day cells were infected or not (w infection, w/o infection) for 3 hours. Subsequently, cells were incubated with the compound combinations for 24, 48 or 72 hours: E2, F, DMOG, E2+DMOG, F+DMOG (DMSO was used as control treatment). At the corresponding time point, CV assay was performed in one plate as previously described. At the same time point, MTT assay was performed in the other plate, cells were incubated 2 hours at 37°C with the chemical compound 3-(4,5-dimethylthiazol-2-yl)-2,5-diphenyltetrazolium bromide (MTT). Subsequently, DMSO was added to each well and the OD values (570 nm) were measured. The mitochondrial activity was calculated performing the ratio between the MTT OD and the CV OD (OD ratio).

Statistical analysis

Statistical analysis was performed with GraphPad Prism 8 (GRAPHPAD SOFTWARE, LLC San Diego, CA). Each experiment was performed at least three times in duplicate. The statistical significance level was setted at 0.05. The results obtained in the FFU assays, in the HCV RNA quantifications and in the gene expressions showed a normal distribution.

FFU assay experiments were analysed using the Two-way ANOVA for three or more group comparisons; post-hoc pairwise multiple comparison tests were performed by Bonferroni's method.

Intracellular HCV RNA were analysed with the T test for two group comparisons. The Two-way ANOVA was used for three or more group comparisons; post-hoc pairwise multiple comparison tests were performed by Bonferroni's method. Each time point was analysed separately.

Also in the gene expression analysis, each time point was analysed separately. The statistical analysis was performed using the multiple T test for two group comparison. The Two-way ANOVA was used for three or more group comparisons; post-hoc pairwise multiple comparison tests were performed by Bonferroni's method. Crystal violet and mitochondrial activity assays were evaluated using the Two-way ANOVA; post-hoc pairwise multiple comparison tests were performed by Bonferroni's method. The IC50 difference between groups was evaluated using the Mann-Whitney test.

RESULTS

1st part: 17,β-estradiol - HCV - Hepatocyte innate immunity

17,β-estradiol long-term treatment and re-sensitising to infection

In literature, it has been hypothesized that, in the female sex, the progressive loss of sexual hormones (from pre- to post- menopause period) could lead to a higher susceptibility to HCV infection [174]. Initially, we investigated the antiviral effect of a prolonged 17,β-estradiol treatment time and we assessed how long the estrogen antiviral activity persists *in vitro*. For these purposes, HuH7 were cultured in presence of 17,β-estradiol (HuH7-E2) or DMSO (HuH7-DMSO) for 14 days and subsequently to infection (3 hours) cells were incubated for 72 hours still in presence of E2 or DMSO. We found a significant reduction of viral infection in HuH7-E2 cells compared to control: HuH7-E2 without E2-treatment post infection 59.7% FFU ±15.4 (p<0.001), HuH7-E2 with E2-treatment post infection 54.6% FFU ±16.3 (p<0.001) (**Figure 15**). No difference was found between HuH-E2 cells with or without treatment post infection. As expected, HuH7-DMSO cells treated with E2 post infection showed a reduction of 38.9% FFU ±19.1 (p<0.001) compared to control, no difference was found against long-treated cells.

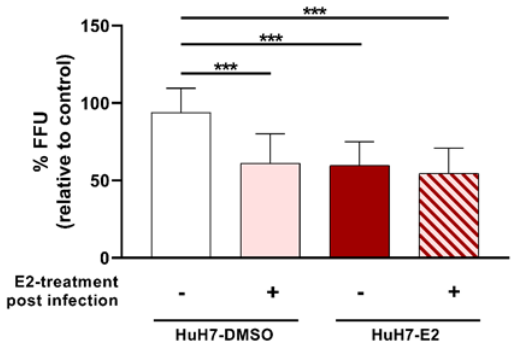

Figure 15. Long-term 17,β-estradiol (E2) exposure and HCV infection. HuH7 cells were cultured in presence of E2 or DMSO for 14 days, post 3h infection they were incubated for 72 hours in the fresh medium with or without E2 and viral infection was evaluated by FFU assay. Data are shown as mean±SD normalized to HuH7-DMSO infected control, ***= $p\leq0.001$.

In order to assess how long the estrogen antiviral activity persists in HuH7 cells, we performed an infection susceptibility experiment in which cells were treated with E2 and incubated in the fresh medium without treatment before the infection for different time. We used a short and a long -term treatment model in which HuH7 were cultured overnight (ON) or for 14 days respectively.

In short-term treatment, cells were exposed to two different estrogen concentrations, then treatment was replaced with the fresh medium and cells were infected every hour from 0 to 6h or after 24h after

E2 removal. As shown in **Figure 16A**, we observed a progressive loss of the antiviral effect over time, with an estimated 50% decrease at around 3h (E2 400 nM: 72.6% FFU ±6.6, $p<0.001$; E2 200 nM: 72.7% FFU ±14.5, $p<0.001$) and a full recovery observed after 5 and 6 hours in cells treated with E2 at 200 and 400 nM, respectively.

In long-term treatment, HuH7 cells were maintained in presence of 400 nM of E2 for 14 consecutive days and then re-sensitised with normal media from 0 to 5 days before infection. In line with the short exposure data, we observed a time-dependent increase in viral susceptibility with a 50% recovery at 2.4 days and a full recovery after 3 days **Figure 16B**.

In each treatment model, we observed a comparable antiviral effect when infection was performed immediately post treatment. However, different treatment duration leads to different timing in normal infection condition restoration.

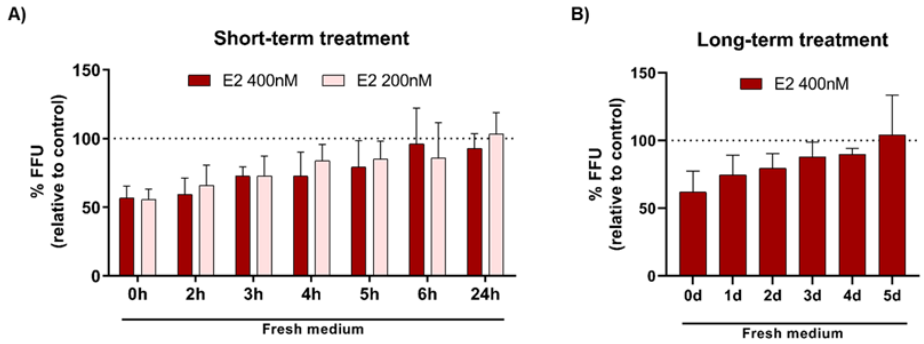

Figure 16. Re-sensitising to infection. A) Short-term 17,β-estradiol exposure (ON): cells were maintained in the fresh medium for different hours (0-24h) before 3h infection. **B)** Long-term 17,β-estradiol exposure (14 days): HuH7-E2 cells were maintained in the fresh medium for different days (0-5d) before 3h infection. In both models cells were incubated in the fresh medium post infection for 72h, and cellular susceptibility was evaluated by FFU assay. Data were normalized to DMSO-treated cells (dot line) and are presented as mean±SD.

17,β-estradiol and hepatocyte innate immunity

The 17,β-estradiol (E2) antiviral effect against HCV was demonstrated to be directly mediated by the nuclear estrogen receptor Alpha and Beta (ER) [205]. ER is a well-characterised transcriptional modulator and E2 binding can lead to transcription of a variety of genes belonging to several classes. According to the E2-treated cell model (**Figure 9B**), we evaluated the mRNA fold change (FC) of interferon- and inflammation- related genes (**Table 2** and **Table 3**) relative to control cells. We focused on interferon-related genes assuming that the estrogen-mediated antiviral status could be mainly ascribed to an interferon signaling pre-activation.

Firstly, we assess the early activation of ER-mediated gene transcription evaluating two well known estrogen receptor-regulated genes, GREB1 and KDM4B. HuH7 cells were treated for 4 hours with E2 and fulvestrant alone or in combination (E2+F) (**Figure 17**). No differences were detected at 0 hours post treatment in all the conditions tested, while at 6 hours we observed an up-regulation of GREB1 and KDM4B mRNA fold change (FC) in E2 treated cells, instead these increase is completely aborted in E2+F treated cells (GREB1: 1.8 FC ±0.6 vs. 1.15 FC ±0.3, p=0.02; KDM4B 1.3 FC ±0.2 vs. 0.9 FC ±0.3, p=0.008). These findings suggested the ability of 17,β-estradiol to induce a fast activation of gene transcription mediated by ER activation in HuH7 cells.

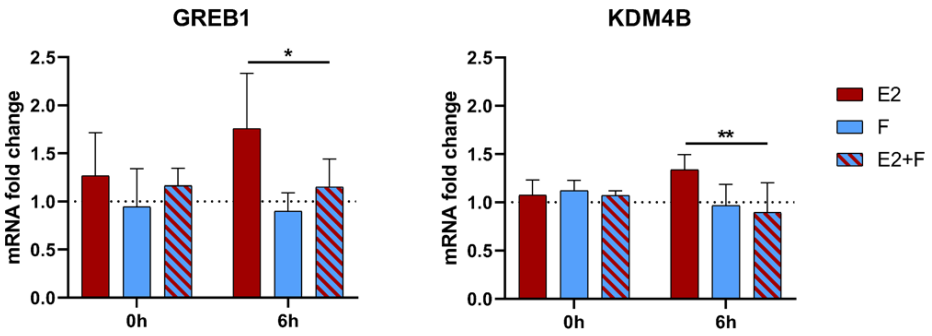

Figure 17. Induction of estrogen-regulated genes in HuH7 cells. HuH7 cells were treated for 4 hours with 17,β-estradiol (E2, 400 nM), fulvestrant (F, 400 nM) and their combination (E2+F). GREB1 and KDM4B mRNA fold change (FC) were evaluated at 0 and 6h post treatment. Data are reported as mean±SD normalized to control (dot line). *= $p \leq 0.05$, **= $p \leq 0.01$

Focusing on E2-treated cells, we performed a differential gene expression analysis at 0, 6, 24, 48 and 72 hours post treatment (**Figure 18A**).

The greatest gene expression differences were found in interferon- and inflammation -related gene classes. Immediately post treatment (0 hours), IFNA1 and IL18 were up-regulated of 2.85 FC ±1.63 (p=0.03) and 1.25 FC ±0.13 (p=0.006), respectively. Their mRNA levels were still increased at 6 hours (IFNA1: 12.15 FC ±5.49, p<0.001; IL18: 1.38 FC ±0.07, p<0.001) reaching a first peak along with the interferon gene IFNB1 (2.55 FC ±1.13, p=0.03), while IFNL3 gene expression was similar to control cells. At the same time point, the mRNA of molecules related to the interferon induction pathway such as the TLR3 (1.63 FC ±0.58, p=0.008), IRF5 (4.20 FC ±1.67, p=0.002), IRF7 (2.05 FC ±0.15, p<0.001), MX1 (1.67 FC ±0.5, p=0.04) and EIF2AK2 (2.20 FC ±0.92, p=0.04) were found to be up-regulated. Conversely IL1B (0.59 FC ±0.11, p<0.001) and IRF3 (0.80 FC ±0.07, p=0.002) were found to be down-regulated.

At 24 hours post treatment, most of the above mentioned genes were expressed at the same levels of control cells. CXCL8, IL18 and IRF5 mRNA were down-regulated and showed values of 0.48 FC

±0.27 (p=0.02), 0.57 FC ±0.20 (p=0.002) and 0.66 FC ±0.24 (p=0.04), respectively. Subsequently to this refractory period, at 48 hours post treatment we observed a second increase in gene transcription of IRF5 (2.30 FC ±0.66, p<0.001), IFNA1 (9.57 FC ±8.65, p=0.02), IFNB1 (3.86 FC ±1.94, p=0.03), IL18 (1.75 FC ±0.72, p=0.02) and TNF (2.59 FC ±1.22, p=0.04). This up-regulation was also maintained at 72 hours for IFNA1 (2.63 FC ±1.88, p=0.007), IFNB1 (1.61 FC ±0.31, p=0.003), TLR3 (1.74 FC ±0.87, p=0.04) and TNF (1.80 FC ±0.99, p=0.007) compared to control cells. The analysed interferon-stimulated genes (ISG15, ISG56, and OAS2) and the genes IL6 and TGFB1 did not show significant expression differences at all the time points.

In **Figure 18B** were shown the fold changes of genes modulated by E2 treatment in a minimum of two time points. Interestingly, kinetic analysis showed E2-mediated antiviral status induced a first peak between 0-6 hours post treatment, a refractory period at around 24 hours, followed by a second prolonged period between 48 and 72 hours.

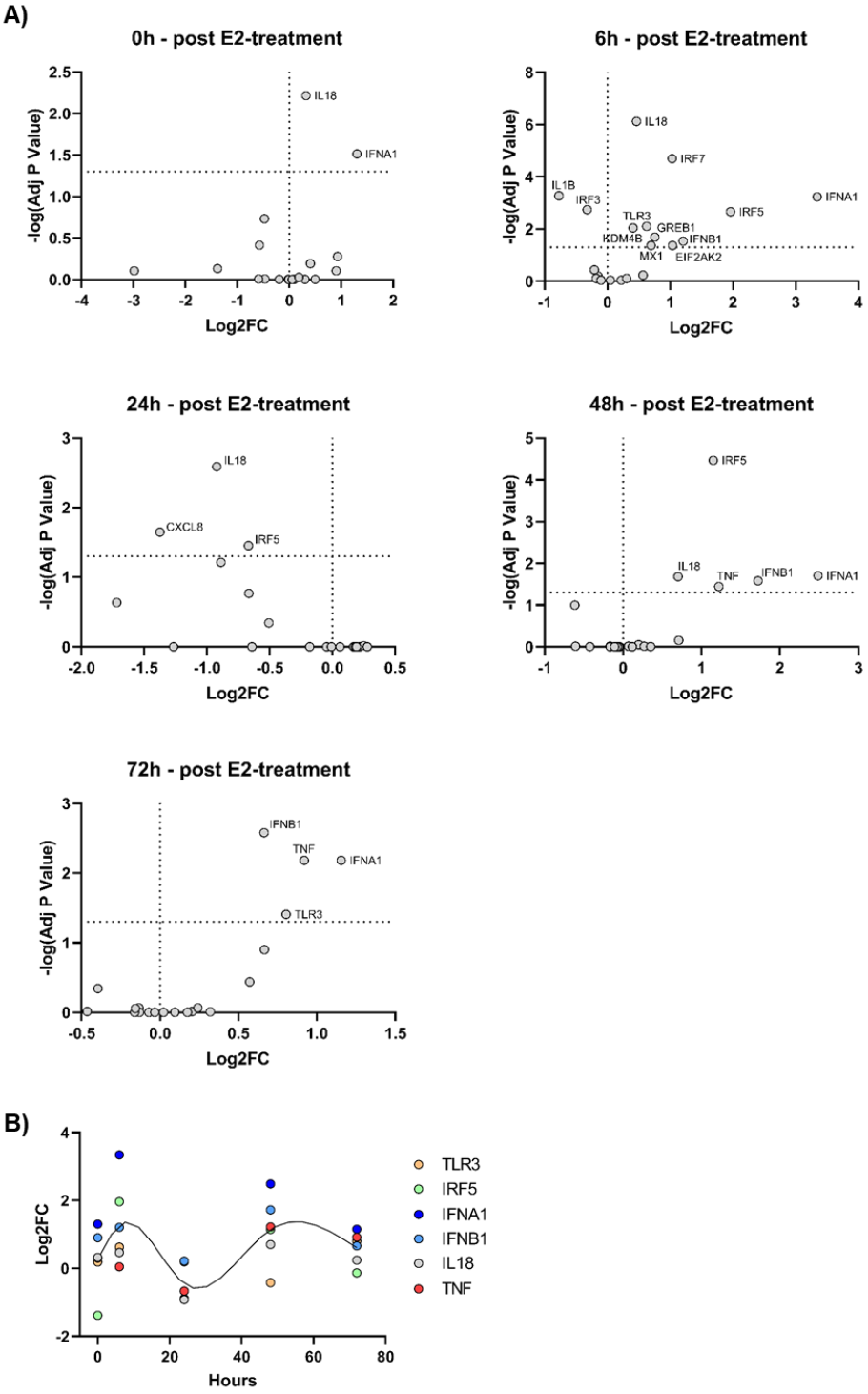

Figure 18. 17,β-estradiol-modulated gene expression profile. HuH7 cells were treated 4 hours with 17,β-estradiol (E2) (400 nM) and the relative gene expression was evaluated at different time points post treatment (0, 6, 24, 48 and 72 hours). **A)** Volcano plots of the Log2 mRNA fold change (Log2FC) in E2-treated cells normalized to control. Up- and down- regulated genes are delimited by the vertical dotted line, significant values ($p \leq 0.05$) are delimited by the horizontal dotted line. **B)** Time course gene expression of six E2-modulated genes in a minimum of two time points. The mRNA levels of each gene are reported as Log2FC normalized to control. The reported line interpolates the gene set mRNA expression means measured at each time point.

HCVcc vs. HCVcc+17,β-estradiol gene expression analysis

To assess if the E2-induced mRNA expression changes also occur in an infection context we performed the differential gene expression analysis using the HCV cell culture (HCVcc) system. Based on a previously published HCVcc model, HuH7 cells were pretreated for 1 hour with E2 (HCVcc+E2) or DMSO (control infection: HCVcc) and then exposed to treatment during the 3 hours of infection (**Figure 9A**) [205].

Firstly, we tested the E2 antiviral action quantifying the intracellular HCV RNA in HCVcc+E2 compared to HCVcc (**Figure 19**). No significant differences were found in the first 24 hours post infection. However, starting from 48 hours we observed a significant viral RNA reduction in the HCVcc+E2 model (68.5% ±22.8, p=0.03) and the HCV RNA levels were also lower at 72 hours (69.2% ±27.1, p=0.007) compared to HCVcc.

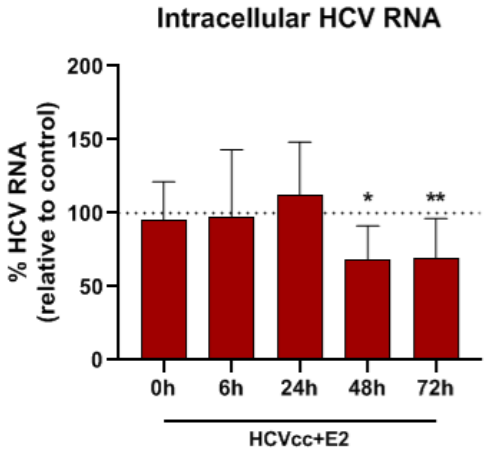

Figure 19. Intracellular HCV RNA quantification in HCVcc and HCVcc+E2 models. Percentage of intracellular HCV RNA in treated-infected cells (HCVcc+E2) normalized to infected cells (HCVcc) (dot line) at 0, 6, 24, 48 and 72 hours post infection. Asterisks are referred to the statistical analysis performed between HCVcc+E2 vs. HCVcc groups and data are presented as mean±SD, *= $p \leq 0.05$, **= $p \leq 0.01$.

We then proceeded to analyse the gene expression profile in HCVcc and HCVcc+E2 models at 0, 6, 24, 48 and 72 hours post infection. Overall, as shown in the heatmap in **Figure 20**, in HuH7 infected cells (both HCVcc and HCVcc+E2) we observed an early response of interferon system genes, which recurs slightly higher at 48 and 72 hours post infection. The expression of cytokines-related genes was found to increase only in the late time points and 12 genes did not shown significant difference relative to control cells (IL1B-6-18, TGFB1, IRF3, IFNL3, ISG56, MX1, EIF2AK2, OAS2, KDM4B, GREB1) (**Figure 20**).

More in detail, in both conditions we found an early higher expression of IFNA1 mRNA at 0 and 6 hours compared to control cells (0h: HCVcc: 3.63 FC ±0.56, p<0.001 and HCVcc+E2: 3.65 FC ±3.43,

p<0.001; 6h: HCVcc: 7.55 FC ±5.74, *p*<0.001 and HCVcc+E2: 10.47 FC ±6.64, *p*<0.001). At 0 hours, IFNB1 mRNA was found to be up-regulated in HCVcc+E2 compared to uninfected control cells (0h: 2.68 FC ±1.67, *p*=0.007).

After the initial response, IFNA1 mRNA levels decrease at 24 hours in both conditions, remaining slightly higher in the HCVcc condition (2.06 FC ±2.37, *p*=0.01). At the same time point, in both infection conditions we found the activation of IRF5 (HCVcc: 2.36 FC ±1.28, *p*<0.001; HCVcc+E2: 2.03 FC ±0.90, *p*=0.01) and ISG15 (HCVcc: 3.47 FC ±0.73, *p*<0.001; HCVcc+E2: 4.57 FC ±2.50, *p*<0.001) gene transcription. Instead, IFNB1 mRNA levels were increased only in HCVcc+E2 model relative to control (3.94 FC ±2.08, *p*<0.001).

At 48 hours post infection, TNF were found to be up-regulated both in HCVcc (TNF: 4.77 FC ±4.08, *p*<0.001) and HCVcc+E2 (4.36 FC ±2.42, *p*<0.001. Instead, compared to uninfected control the ISG15 mRNA levels remained higher in HCVcc (3.25 FC ±1.48, *p*=0.03) and IFNA1 was strongly expressed in HCVcc+E2 (9.56 FC ±9.72, *p*<0.001).

At the last time point (72h), the cytokines-related genes TNF and CXCL8 were highly expressed in HCVcc+E2 (TNF: 3.32 FC ±1.96, *p*<0.001; CXCL8: 3.04 FC ±2.90, *p*<0.001). While the interferon related genes ISG15, IRF7 and IFNA1 were up-regulated in both infection conditions compared to control (ISG15: HCVcc 3.47 FC ±2.04, *p*<0.001 and HCVcc+E2 3.45 FC ±0.95, *p*<0.001; IRF7: HCVcc 4.93 FC ±4.57, *p*<0.001 and HCVcc+E2 4.48 FC ±2.40, *p*<0.001; IFNA1: HCVcc 4.82 FC ±3.02, *p*<0.001 and HCVcc+E2 2.40 FC ±1.70, *p*=0.005).

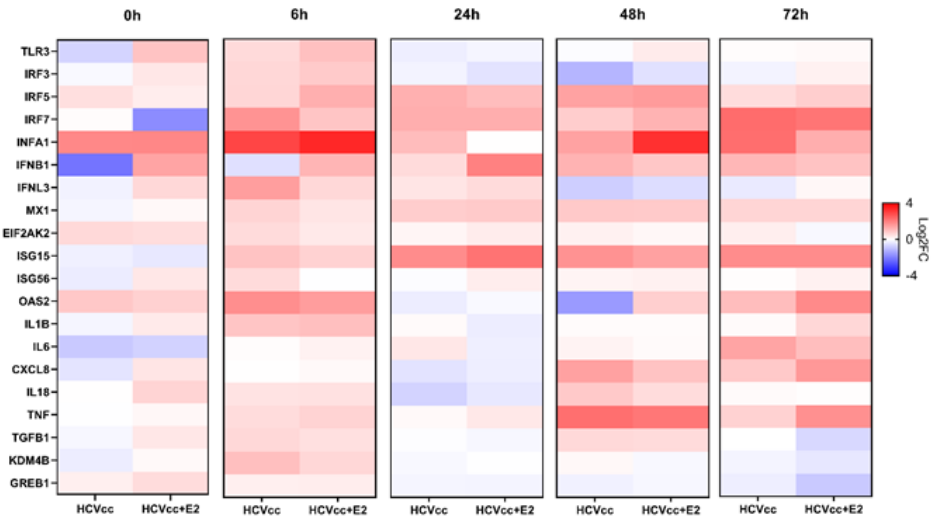

Figure 20. Gene expression profiling in the HCVcc and the HCVcc+E2 models. The heatmap show the gene expression mean values obtained in HCVcc and HCV+E2 models at 0, 6, 24, 48 and 72h post infection. Data are shown as Log2 mRNA fold change (Log2FC) normalized to control cells.

As shown in **Figure 21**, some of the observed changes in the HCVcc+E2 model partially mimicked the gene expression trends noticed in E2-treated cells (**Figure 18B**). Immediately after infection, in the HCVcc+E2 model we found a significant up-regulation of IFNB1 ($p<0.001$) and TLR3 ($p=0.04$) mRNA compared to HCVcc. As observed in E2-treated cells, also in the HCVcc+E2 model the IFNA1 mRNA reached a peak at 6 hours post treatment/infection, which was higher compared to normal infection condition ($p=0.003$). In all the conditions IFNA1 gene expression decreased at 24 hours remaining slightly higher in HCVcc compared to HCVcc+E2 ($p=0.01$).

However, at 24 hours the HCVcc+E2 model showed higher mRNA levels of IFNB1 ($p<0.001$) and ISG15 ($p=0.007$) compared to HCVcc. Furthermore, we previously reported that in E2-treated cells IFNA1 mRNA reached a second peak at 48h and also the HCVcc+E2 model showed increased IFNA1 mRNA levels at this time point compared to HCVcc ($p<0.001$). As happened in E2-treated cells at 72 hours, IFNA1 mRNA remained higher in HCVcc+E2 compared to control but slightly lower compared to HCVcc model ($p<0.001$), conversely CXCL8 resulted more expressed ($p=0.02$). TNF mRNA exhibited a similar kinetics between E2-treated cells and HCV+E2 model showing an increase at 48 hours and a significant up-regulation compared to HCVcc at 72 hours ($p=0.002$).

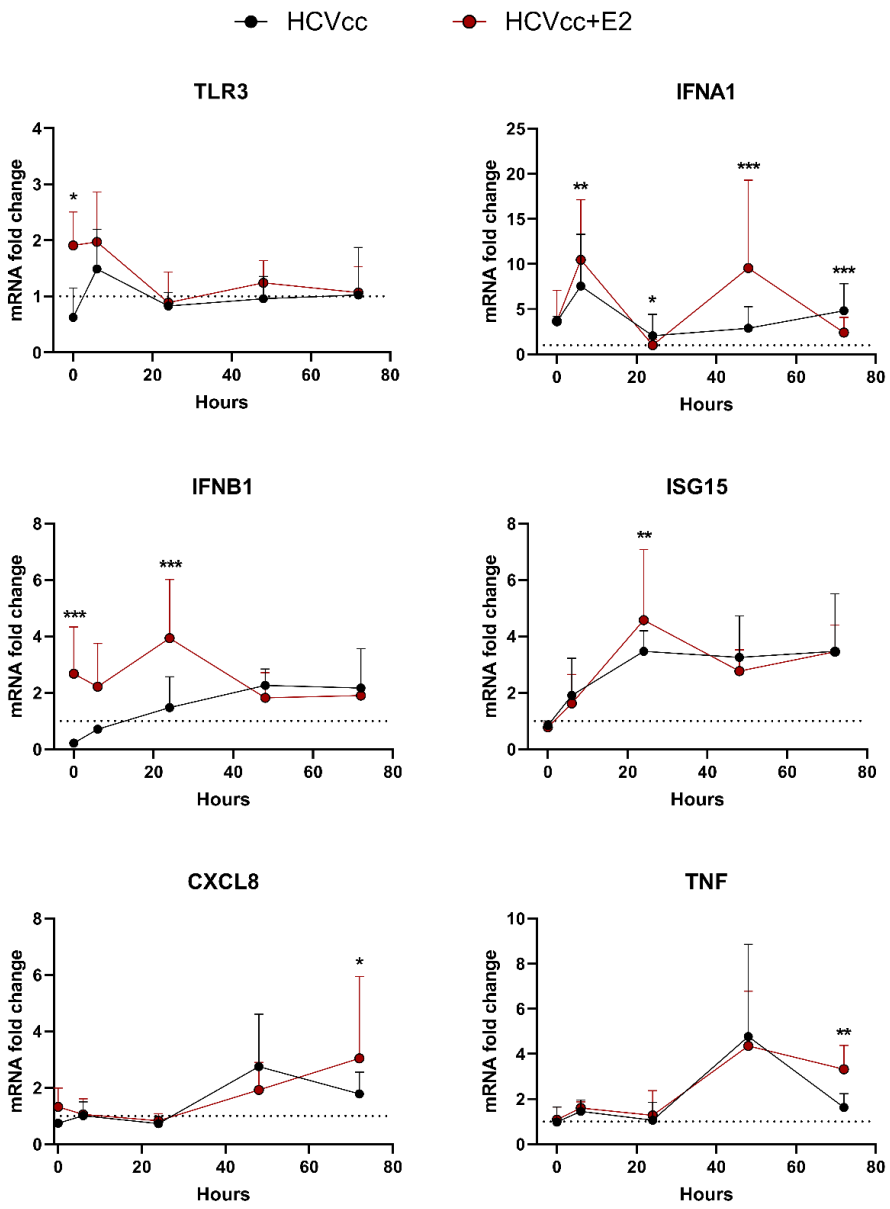

Figure 21. Gene expression comparisons between the HCVcc and the HCVcc+E2 models. HCVcc (Black line), HCVcc+E2 (Red line). Results are shown as mRNA fold change normalized to control cells (dot line). Asterisks are referred to the statistical analysis performed between HCVcc+E2 vs. HCVcc groups and data are presented as mean±SD, *= $p \leq 0.05$, **= $p \leq 0.01$, ***= $p \leq 0.001$.

17,β-estradiol and type I interferon antiviral response

Previous data together suggested that type I interferon response could be the key regulator for estrogen-mediated antiviral activity. To confirm this hypothesis, 17,β-estradiol treatment was tested in combination with the IFN alpha-IFNAR-IN-1 hydrochloride (IFNARi) compound, an inhibitor of the interaction between Interferon alpha (IFN-α) and interferon alpha receptor (IFNAR) [234,235].

In order to assess the better inhibitor concentration to use during experiments, we firstly tested the effect of IFNARi treatment on cell proliferation. HuH7 cells were treated for 72 hours with serial

dilution of the compound and, as reported in **Figure 22A**. The IC50 value was equal to 5.09 µM [4.31-6.32], and for next experiments we chose the concentration of 500 nM which was in a concentration range with no anti-proliferative effect.

In order to confirm the ability of IFNARi to counteract the action of type I interferons, we tested the ability of the chosen concentration (500 µM) to attenuate the IFNα2a pharmacological activity. According to the model shown in **Figure 10**, HuH7 infected cells were incubated for 72 hours in presence of IFNα2a in combination with DMSO or IFNARi. As shown in **Figure 22B**, the IFNα2a IC50 value resulted to be 0.02 MUI/mL [0.01-0.04], instead in combination with IFNARi the obtained IC50 value was significantly higher (0.11 MUI/mL [0.03-0.38], p=0.04).

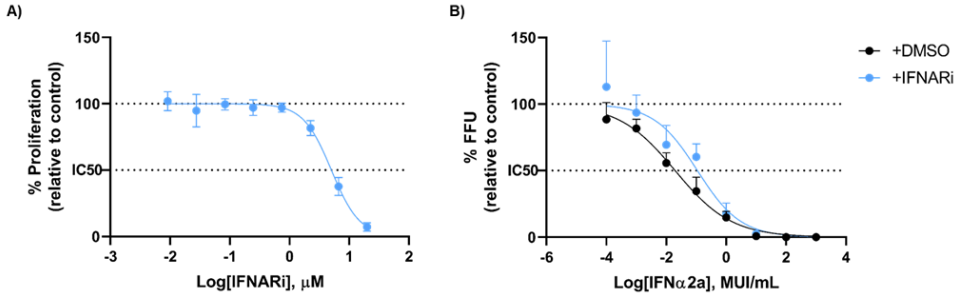

Figure 22. IFN alpha-IFNAR-IN-1 hydrochloride (IFNARi) activity evaluation. **A)** HuH7 cells were incubated for 72h in presence of IFNARi serial dilutions. Proliferation was evaluated by crystal violet assay and results were normalized to control (upper dot line). **B)** HuH7 cells were infected for 3 hours and then incubated for 72h with IFNα2a serial dilutions in combination with DMSO (Black curve) or IFNARi (Blue curve). Infection was evaluated by FFU assay and results were normalized to infected control (upper dot line). IC50 thresholds are reported in graphs (lowest dot lines) and data data are shown as mean±SD.

To test if the 17,β-estradiol antiviral action was dependent by type I interferon signaling we used the HCVcc model shown in **Figure 11A**. This model is similar to the one used for gene expression analysis, HuH7 cells were pretreated for 1 hours with E2 (400 nM) or DMSO and infected for 3 hours still in the presence of treatment. IFNARi was added in combination with E2 and DMSO and in the incubation period of 72 hours post infection.

As shown in **Figure 23**, we found that IFNARi in combination with DMSO did not alter the viral infection in both FFU assay and intracellular HCV RNA quantification compared to infected control cells (FFU: 90.1% ±11.7, p=0.74; intracellular HCV RNA: 114.6% ±29.9, p=0.34). As expected, E2 treatment without IFNARi induced a reduction of 38.4% ±8.5 in FFU (p<0.001) and of 37.2% ±16.4 in intracellular HCV RNA levels (p<0.001). On the contrary, the E2 antiviral effect was completely abolished when we performed E2 treatment in presence of IFNARi. In the HCVcc+E2+IFNARi model, on one hand FFU and HCV RNA levels (94.9% ±8.6 and 93.1% ±6.0, respectively) were

significantly higher compared to HCVcc+E2 model (FFU: p=0.002; intracellular HCV RNA: p=0.008). On the other hand, no differences were found between the HCVcc+E2+IFNARi model to the HCVcc+DMSO model added with the IFNARi (FFU: p>0.999; intracellular HCV RNA: p=0.108, respectively).

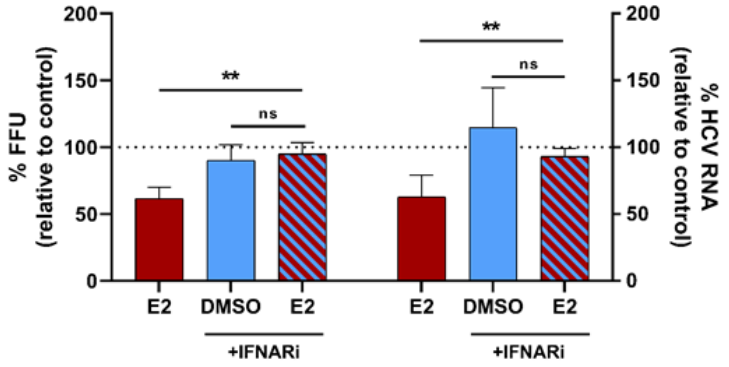

Figure 23. 17,β-estradiol (E2) antiviral effect in combination with IFN alpha-IFNAR-IN-1 hydrochloride (IFNARi). HuH7 cells were treated and infected according to the HCVcc model shown in **Figure 11A**. Viral infection was evaluated at 72 hours post infection by FFU assay and intracellular HCV RNA performed. Results are shown as the percentage mean±SD normalized to control (dot line). ns= not significant, **= $p \leq 0.01$.

The same FFU assay experiment was performed also in presence of fulvestrant (F) in combination with E2 (E2+F) with or without IFNARi (**Figure 24**). Fulvestrant control treatment (104.4% FFU ±8.8) or in combination with IFNARi (86.1% FFU ±23.9) had no significant differences compared to control infected cells (p>0.999 and p=0.397, respectively) and DMSO+IFNARi condition (p=0.343 and p>0.999, respectively). Also the E2+F treatment abolished the antiviral effect of E2 without or with IFNARi (91.8% FFU ±8.3 and 92.4% FFU ±9.9, respectively) without differences with infected control cells (p=0.920 and p=0.997, respectively) and DMSO+IFNARi condition (p>0.999).

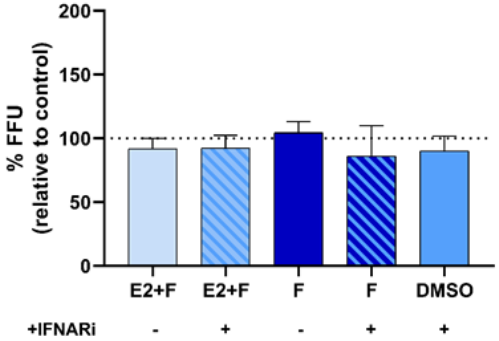

Figure 24. Antiviral effect evaluation of fulvestrant with or without 17,β-estradiol (E2) and IFN alpha-IFNAR-IN-1 hydrochloride (IFNARi). HuH7 cells were treated and infected according to the HCVcc model shown in **Figure 11A**. Viral infection was evaluated at 72 hours post infection by FFU assay. Results are shown as the percentage mean±SD normalized to control (dot line).

Based on our previous results showing time-dependency of the estrogen-mediated interferon induction (**Figure 18B and Figure 21**), we investigated the role of each interferon peak on anti-HCV activity (6 vs. 48 hours). Based on the model shown in **Figure 11B**, we treated HuH7 cells with E2 (400 nM) for 1h, and then we infected them still in presence of E2. After 3 hours, the viral inoculum was removed and IFNARi was added at different times post infection, 0, 24 or 48h, respectively. Adding the inhibitor immediately post infection (0-72h), resulting in a block for both peaks, showed a complete rescue of viral infection compared to E2 treated infected cells (102.7% FFU ±25.7 vs. 60.6% FFU ±13.9, p=0.002) without significant differences compared to IFNARi treated cells (p>0.999). Similarly, when the inhibitor was added at 24h post infection (24-72h), after the first peak passed and during the refractory period, we still observed a full infection restoration (105.8% FFU ±35.7, p<0.001). Adding IFNARi at 48h post infection (48-72h), during the second peak, was not sufficient to revert antiviral phenotype, showing FFU levels similar to E2 control (60.9% ±18.6 vs. 60.6% ±13.9, p>0.999) and significantly lower compared to IFNARi treatment control (p=0.03), suggesting that the first peak was essential to induce a strong antiviral response (**Figure 25**).

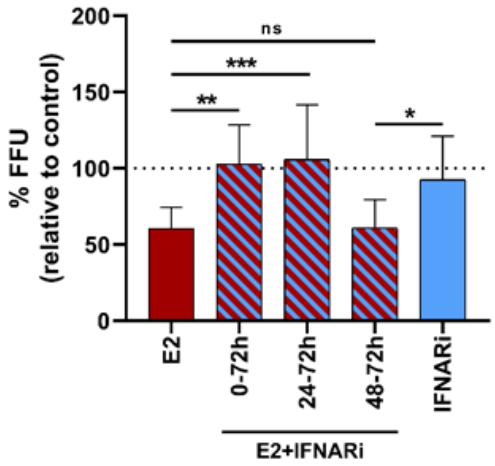

Figure 25. 17,β-estradiol (E2)-induced antiviral activity loss. HuH7 cells were treated according to the HCVcc+E2 model shown in **Figure 11B.** IFN alpha-IFNAR-IN-1 hydrochloride (IFNARi) was added to the HCVcc+E2 model immediately (0-72h), 24h (24-72h) or 48h (48-72h) post infection, and viral presence was evaluated at 72h by FFU assay. Results are shown as the percentage mean±SD normalized to control (dot line). ns= not significant, *= p≤0.05, **= p≤0.01, ***= p≤0.001

17,β-estradiol-conditioned medium antiviral effect

Our findings showed that 17,β-estradiol was able to early stimulate a type I interferon gene expression and the estrogen antiviral activity could be reverted by blocking IFN type I signaling pathway. Furthermore, as shown in the re-sensitising experiment (**Figure 15A**), in the short-term treatment

model the first 24 hours post treatment was crucial to preserve the E2 antiviral effect. All of these results led us to hypothesize that the E2-stimulated cells could early release molecules in the cell culture media able to induce a pre-activated antiviral status in HuH7 and to exert an antiviral effect.

To assess the hypothesis we focused on the conditioned medium (CM) obtained 24, 48 and 72 hours post an E2 treatment of 4 hours (CM_{24}, CM_{48} and CM_{72}) (**Figure 12**). We initially tested whether our short model phenotype could still be reverted by 24h re-sensitisation as observed in the short-term treatment; the used model is shown in **Figure 13A**. We obtained a significant difference between E2 treated cells without or with 24 hour re-sensitisation before infection (63.0% FFU ±14.3 vs. 92.8% FFU 8.5±, p<0.001) demonstrating that E2 treated cells were completely re-sensitised if infected 24 hours post treatment (**Figure 26A**).

Using the same model, we tested if the CM_{24} was essential to maintain the estrogen induced antiviral effect. As shown in **Figure 26B**, when untreated and infected cells were incubated for 72 hours post infection in CM_{24} we obtained a partial reduction of infection compared to control (74.7% FFU ±11.9, p<0.001), first showing that CM_{24} has an antiviral activity. Similarly, when E2-treated and re-sensitised cells were incubated post infection in the CM_{24}, we observed the antiviral effect restoration (51.1% FFU ±19.1) with a significant difference compared to infected control (p<0.001). Surprisingly, despite these cells were re-sensitised, we found a significant difference compared to cells incubated in CM_{24} post infection without a previous E2 treatment (p<0.001), demonstrating an E2-induced pre-activation status in HuH7 which was able to maximise CM_{24} antiviral activity.

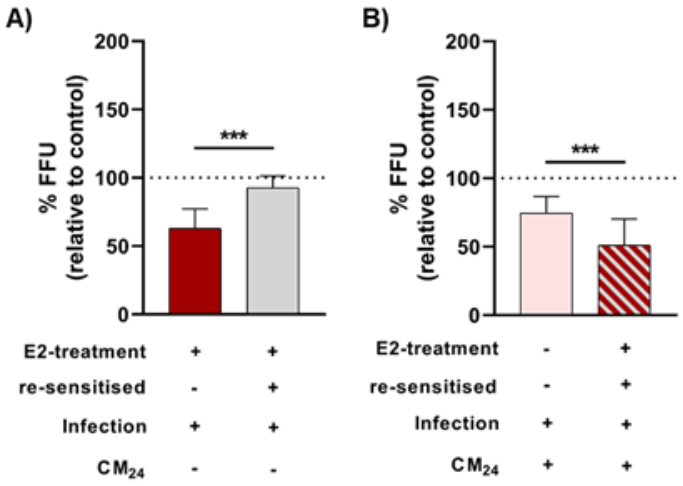

Figure 26. Antiviral effect evaluation of conditioned medium (CM) harvested at 24 hours post 17,β-estradiol (E2) treatment. HuH7 cells were treated for 4 hours with E2 or DMSO (control). Post treatment cells were maintained in the fresh medium for 24h (re-sensitised) and then infected for 3 hours. **A)** post infection cells were incubated in the fresh medium. **B)** post infection, cells were incubated in the conditioned

medium collected at 24h (CM_{24}). FFU assay was performed 72h post infection. Results are shown as the percentage mean±SD normalized to control (dot line). ***= $p \leq 0.001$.

The hypothesized antiviral action of CM_{48} and CM_{72} was tested according to the HCVcc model reported in **Figure 13B**. To evaluate if the antiviral activity could be mediated by type I interferon molecules, HuH7 cells were treated with the CM with or without IFNARi.

Both CM_{48} and CM_{72} were able to reduce supernatant viral titer (FFU/mL) with significant difference compared to infection control (CM_{48}: 59.8% ±24.9, $p<0.001$; CM_{72}: 58.4% ±16.8, $p<0.001$) (**Figure 27**). Whereas, adding IFNARi to the conditioned medium we obtained the nullification of CM antiviral activity (CM_{48}: 100.3% FFU/mL ±29.9; CM_{72}: 112.8% FFU/mL ±17.3) with a significant difference compared to CM treated cells without the inhibitor (CM_{48} vs. CM_{48}+IFNARi: $p=0.008$; CM_{72} vs. CM_{72}+IFNARi: $p<0.001$).

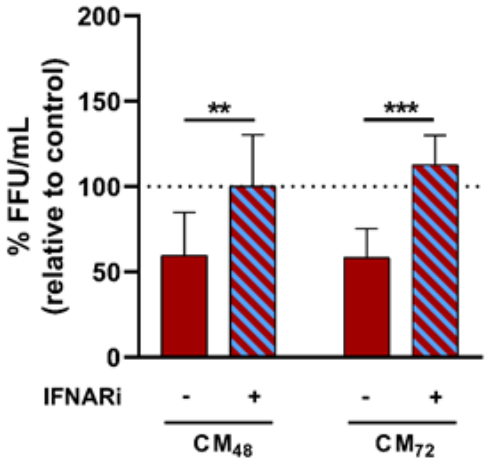

Figure 27. Antiviral effect evaluation of conditioned medium (CM) harvested at 48 and 72 hours post 17,β-estradiol (E2) treatment. The conditioned medium was collected at 48 and 72h (CM_{48} and CM_{72}) post E2 treatment. Naïve HuH7 cells were treated 1 hour with CM_{48} and CM_{72} added with or without IFNARi, then infection was performed for 3 hours still in the presence of treatments. Cells were incubated in the fresh medium and supernatant viral titers were quantified at 72 hours post infection by FFU assay (FFU/mL). Results are shown as the percentage mean±SD normalized to control (dot line). **= $p \leq 0.01$, ***= $p \leq 0.001$

2nd part: 17,β-estradiol - HCV - Pseudohypoxic state

HCV infection and DMOG treatment

A cellular hypoxic state is able to influence the HCV infection and may play a significant role in viral hepatocarcinogenesis. Moreover, several studies showed the relationship between hypoxia and estrogens, so we evaluated the 17,β-estradiol antiviral effect in combination with dimethyloxalylglycine (DMOG). The DMOG is a chemical compound often used to mimic an artificial hypoxic state (pseudohypoxic condition) [112]. The experiments were performed using several DMOG concentrations and two different treatment models shown in **Figure 14**. In the short treatment model HuH7 cells were incubated with DMOG overnight before infection (Model 1), instead in the long treatment model HuH7 cells were treated for 72 hours post infection (Model 2). The effect on cell proliferation was tested for all DMOG concentrations with or without JFH-1 infection. In Model 1 without infection we found a slight proliferation reduction using the concentrations of 40 and 80 μM (-11.9% OD ±8.2, p=0.008; -16.8% OD ±8.2, p=0.02). In Model 2 there was a modest proliferation reduction incubating cells with DMOG at 40 μM without and with infection (-16.2% ±3.5, p=0.03; -11.0% ±13.9, p=0.04) (**Figure 28**).

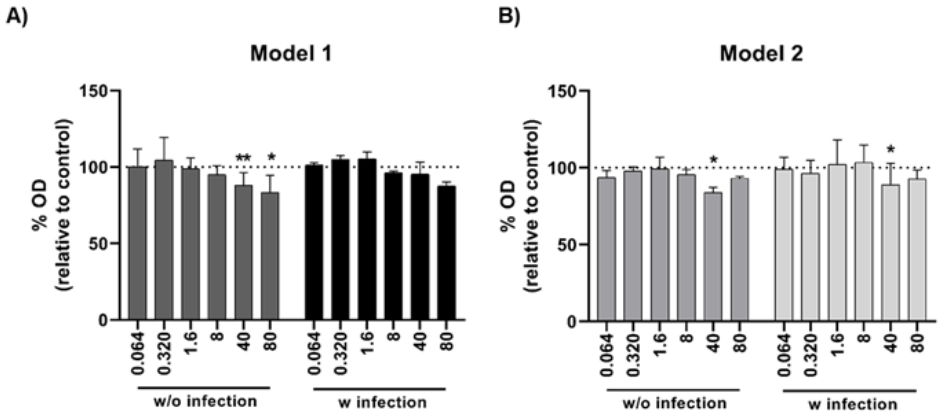

Figure 28. DMOG proliferation assay. HuH7 cells were treated with the reported DMOG concentrations with or without infection (MOI 0.1) according to Model 1 and 2. Cellular proliferation was evaluated by crystal violet assay at 72 hours, optical density (OD) results are shown as percentage mean±SD normalized to DMSO-treated control (dot line). Asterisks are referred to the statistical analysis performed between treatment vs. control groups. *= $p \leq 0.05$, **= $p \leq 0.01$.

To assess if Model 1 and Model 2 were able to induce a pseudohypoxic condition we evaluated the mRNA levels of two hypoxia-related genes (HIF1A and CA9) in cells treated with DMOG (80 μM) without or with JFH-1 infection (**Figure 29**). As shown in **Figure 29A**, ON exposure (Model 1) did not induce an hypoxia-related response at 72 hours post treatment compared to control cells (HIF1A:

1.26 FC ±0.47, p=0.256; CA9: 1.76 FC ±1.61, p=0.274), instead the 72h-long DMOG exposure (Model 2) was able to slightly up-regulate the HIF1A mRNA (1.33 FC ± 0.14, p<0.001) and a trend was observed in CA9 mRNA levels (4.67 FC ±5.55, p=0.06) compared to control cells. We did not find significant differences evaluating HIF1A and CA9 mRNA expressions in presence of JFH-1 infection (HCVcc vs. HCVcc+DMOG) (**Figure 29B**).

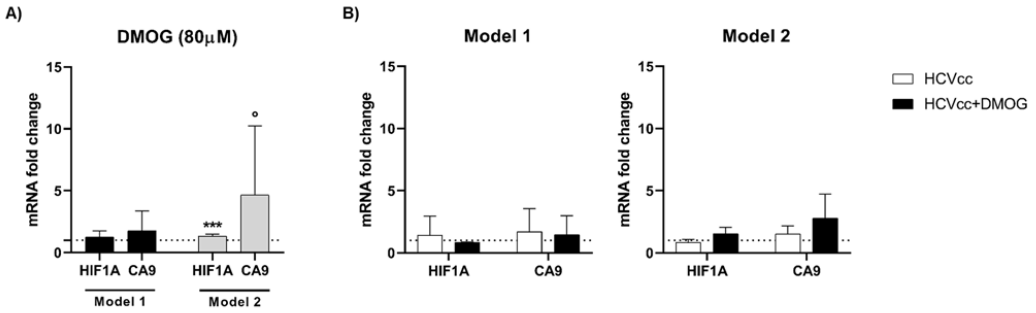

Figure 29. DMOG-induced hypoxic-gene evaluation. A) HuH7 cells were treated with DMOG at 80 μM overnight (Model 1(Black)) or for 72 hours (Model 2 (Grey)). **B)** The HCVcc system was performed according to Model 1 and Model 2 with or without DMOG treatment (80 μM) (HCVcc+DMOG and HCVcc, respectively). Gene expression analysis was performed at 72 hours and mRNA levels are shown as FC normalized to DMSO-treated control (dot line). Asterisks and circles are referred to the statistical analysis performed between treatment vs. control groups. °= p=0.06, ***= p≤0.001.

Although Model 1 and Model 2 showed no gene expression differences in an infective context, assessing intracellular HCV RNA we found two different infection kinetics between the two treatment models (**Figure 30A**). In Model 1, we observed a progressive increase of intracellular viral RNA over time reaching a peak at 72 hours post infection compared to control (72h: 338.6% ±130.7, p<0.001), while in Model 2 HCV RNA levels remained similar to control (79.8% ±45.9, p>0.999). Viral RNA kinetics resulted to be significantly different between Model 1 and Model 2 at 72 hours post infection (p<0.001). Similar results were obtained treating cells with DMOG serial dilutions, we found significant differences in FFU count between Model 1 and 2 in the highest tested concentrations (40 μM: 189.8% ±15.0 vs 89.5% ±38.9, p<0.001; 8 μM: 169.5% ±23.9 vs. 104.7% ±21.4, p<0.001) (**Figure 30B**).

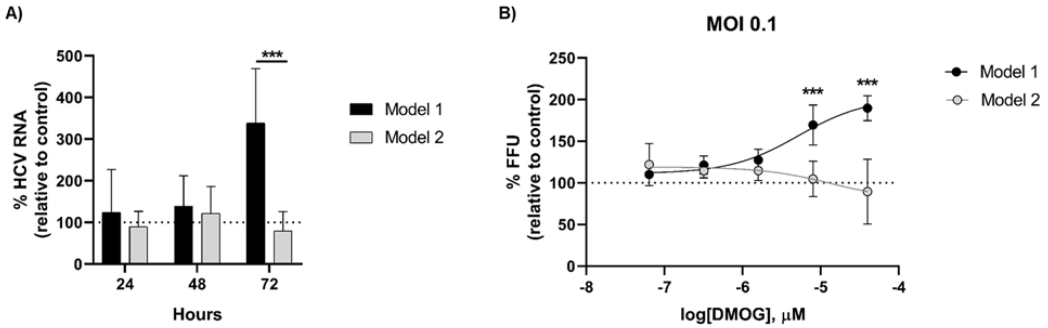

Figure 30. DMOG treatment effects on viral infection (MOI 0.1). According to Model 1 (Black) and 2 (Grey), HuH7 cells were treated with DMOG at 80 μM **(A)** or DMOG serial dilutions (0.064-40 μM) **(B)** and were infected with a MOI of 0.1. Infection was evaluated by intracellular HCV RNA quantification at 24, 48 and 72 hours post infection **(A)** or by FFU assay at 72 hours post infection **(B)**. Results are shown as the percentage mean±SD normalized to infected control (dot line). Asterisks are referred to the statistical analysis performed between Model 1 vs. Model 2 groups. ***= $p \leq 0.001$.

Reducing the JFH-1 MOI from 0.1 to 0.05, the infection differences between the two Models resulted deeper (**Figure 31**). Comparing Model 1 and 2, we found significant differences in three DMOG concentrations tested (1.6 μM: 121.4% FFU ±22.6 vs. 77.7% FFU ±23.4, $p<0.001$; 8 μM: 136.0% FFU ±14.9 vs. 69.9% FFU ±18.3, $p<0.001$; 40 μM: 132.9% FFU ±17.9 vs. 43.0% FFU ±15.6, $p<0.001$). Moreover, focusing on Model 2 the same three concentrations were able to reduce viral infection compared to infected control (1.6 μM: $p=0.02$; 8 μM: $p=0.01$; 40 μM: $p<0.001$). DMOG treatment performed before infection had a positive effect on JFH-1 infection, instead a prolonged post infection treatment induced a concentration-dependent reduction of viral infection.

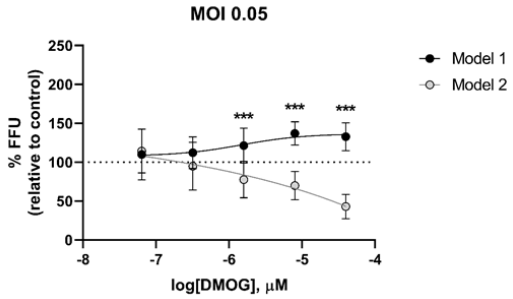

Figure 31. DMOG treatment effects on viral infection (MOI 0.05). HuH7 cells were treated with serial dilutions of DMOG (0.064-40 μM) and infected with a MOI of 0.05 according to Model 1 (Black) and 2 (Grey). Infection was evaluated by FFU assay at 72 hours post infection and results are shown as the percentage mean±SD normalized to infected control (dot line). Asterisks are referred to the statistical analysis performed between Model 1 vs. Model 2 groups. ***= $p \leq 0.001$.

17,β-estradiol antiviral effect in combination with DMOG

To assess if the 17,β-estradiol antiviral activity persisted also in DMOG-induced conditions, we tested E2 (400 nM) in combination with serial dilutions of DMOG in both models. Treating cells before

infection (Model 1) the E2 antiviral effect (E2 treatment control: 48.5% FFU ±8.8) resulted partially lost when estrogen was used in combination with DMOG concentrations (0.064 μM: 73.9% FFU ±19.9, p=0.03; 0.32 μM: 77.6% FFU ±26.1, p=0.008; 8 μM: 83.0% FFU ±23.1, p<0.001; 40 μM: 107.0% FFU ±28.1, p<0.001), the combination of E2 with DMOG at 1.6 μM showed a trend (67.0% FFU ±17.8, p=0.06) (**Figure 32A**). However, the E2 combined with all the DMOG concentrations was still able to induced an infection reduction compared to the DMOG-treated group (0.064 μM: p=0.001; 0.32 μM: p=0.002; 1.6 μM: p<0.001; 8 μM: p<0.001; 40 μM: p<0.02) (**Figure 32A**).

Similarly, evaluating the effect of the combination DMOG+E2 vs. DMOG in Model 2, we observed an infection reduction in E2-treated cells only in combination with the lowest DMOG concentrations: 0.064 μM (68.7% FFU ±15.5 vs. 108.5% FFU ±20.0, p<0.001), 0.32 μM (76.5% FFU ±20.5 vs. 97.6% FFU ±30.1, p=0.02) and 1.6 μM (62.4% FFU ±15.0 vs. 77.7% FFU ±23.5, p=0.008). No differences were found combining E2 with DMOG at 8 and 40 μM (**Figure 32B**). Compared to E2-treated cells (51.9% FFU ±12.7), viral infection was significantly higher in cells treated with E2 in combination of DMOG at 0.32 μM (76.5% FFU ±20.5, p=0.02) and 8 μM (71.4% FFU ±19.2, p=0.03) (**Figure 32B**).

Overall, in Model 1 the infection promoting activity of DMOG was partially counteracted by E2 (400 nM) and in Model 2 the 17,β-estradiol antiviral action was present only in combination with the lowest DMOG concentrations. Since in Model 2 the DMOG antiviral action increased with increasing concentration, the E2 antiviral effect progressively overlapped the DMOG effect.

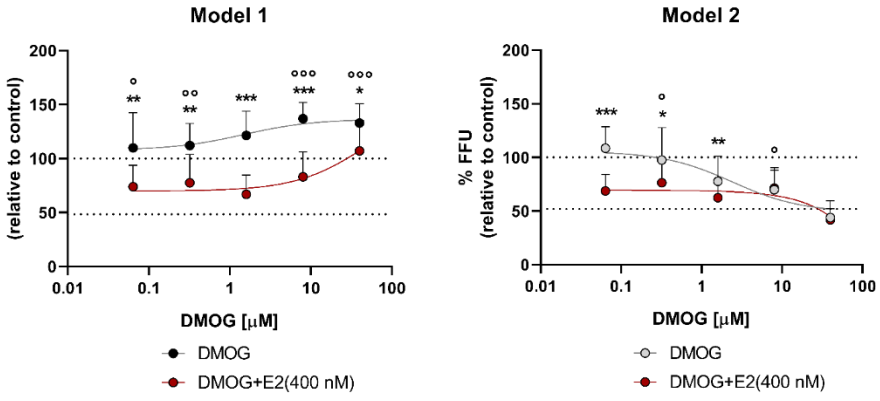

Figure 32. 17,β-estradiol (E2) antiviral activity in combination with DMOG serial dilutions. HuH7 cells were treated and infected according to Model 1 **(A)** and Model 2 **(B)**. Serial dilutions of DMOG (0.064-40 μM) were used with or without E2 at 400 nM (DMOG+E2 and DMOG, respectively). Infection was evaluated at 72 hours by FFU assay and results are shown as the percentage mean±SD normalized to infected control (upper dot line). E2 control treatment value was reported as the lower dot line. Asterisks are referred to the statistical analysis performed between DMOG+E2 vs. DMOG groups, white circles are referred to the

statistical analysis performed between DMOG+E2 vs. E2 groups. */°= $p \leq 0.05$, **/°°= $p \leq 0.01$, ***/°°°= $p \leq 0.001$.

Based on these data, we focused on the two DMOG concentrations of 1.6 and 8 μM, which in Model 2 presented opposite results comparing DMOG+E2 vs. DMOG treatment conditions. Treating cells before or post infection, the antiviral effect of E2 serial dilutions (from 400 nM to 6.25 nM) were tested in combination of the two DMOG concentrations (1.6 or 8 μM).

As shown in **Figure 33A**, in Model 1 the DMOG concentration of 1.6 μM combined with E2 concentrations did not alter estrogen antiviral effect; no differences were found compared to E2 treatment controls. Instead, compared to DMOG treatment (1.6 μM: 121.4% FFU ±22.6), significant differences were found when DMOG was used in combination with E2 at 50, 100, 200 and 400 nM (50 nM: 86.8% FFU ±18.8, p=0.006; 100 nM: 88.5% FFU ±33.8, p=0.01; 200 nM: 84.2% FFU ±17.7 p=0.003; 400 nM 67.0% FFU ±17.8, p<0.001). Increasing DMOG concentration to 8 μM, we noticed a partial loss of the estrogen antiviral activity in the whole E2+DMOG conditions tested compared to E2 (6.25 nM: 120.2% FFU ±12.5 vs. 89.3% FFU ±16.4, p=0.01; 12.5 nM: 125.7% FFU ±17.2 vs. 89.2% FFU ±16.4, p<0.001; 25 nM: 111.7% FFU ±17.7 vs. 73.0% FFU ±14.0, p<0.001; 50 nM: 121.6% FFU ±38.4 vs. 72.5% FFU ±26.1, p<0.001; 100 nM: 117.8% FFU ±35.6 vs. 59.9% FFU ±12.6, p<0.001; 200 nM: 102.3% FFU ±21.6 vs. 58.7% FFU ±31.4, p<0.001; 400 nM: 83.0% FFU ±23.1 vs. 48.5% FFU ±8.8, p=0.001) (**Figure 33B**). In combination with DMOG only the two highest E2 concentration tested (200 and 400 nM) were able to significantly reduce viral infection compared to DMOG control (8 μM: 137.0% FFU ±14.9) (200 nM: p=0.006; 400 nM: p<0.001).

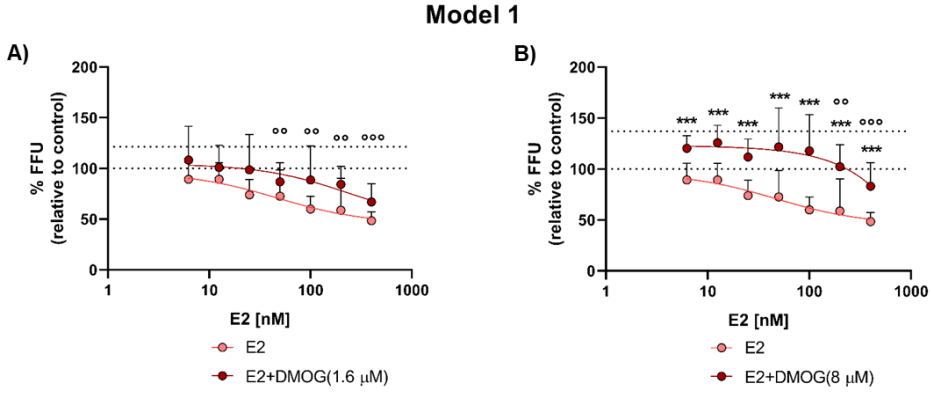

Figure 33. 17,β-estradiol (E2) serial dilution antiviral activity in combination with DMOG (Model 1). HuH7 cells were treated overnight before infection (Model 1) with E2 serial dilutions (6.25-400 nM) with or without DMOG (E2+DMOG and E2, respectively) at 1.6 μM **(A)** and 8 μM **(B)**. Infection was evaluated by FFU assay at 72 hours post infection and results are shown as the percentage mean±SD normalized to infected control (lower dot line). In each graph, DMOG control values were reported as the upper dot line. Asterisks

are referred to the statistical analysis performed between E2+DMOG vs. E2 groups, white circles are referred to the statistical analysis performed between E2+DMOG vs. DMOG groups. °°= $p \leq 0.01$, ***/°°°= $p \leq 0.001$.

Observing the post infection treatment model (Model 2) (**Figure 34A**), no significant differences were found between E2+DMOG(1.6 μM) and estrogen treatment control, except using E2 at 6.25 nM (67.3% FFU ±17.4 vs. 96.4% FFU ±11.3, p=0.009). Moreover, combining E2 at 400 nM with DMOG we observed significant lower levels in FFU compared to DMOG control (67.3% ±17.4 vs. 77.7% ±23.5, p=0.03). When the DMOG concentration was increased to 8 μM, the combined treatments were equal to E2 treatment for all the concentrations tested excluding the one at 400 nM (71.4% FFU ±19.2 vs. 51.9% FFU ±12.7, p=0.04). The combination of E2 at 6.25 nM with DMOG (8 μM) slightly increased the FFU levels compared to DMOG control (89.0% ±17.1 vs. 69.9% ±18.3, p=0.03) (**Figure 34B)**.

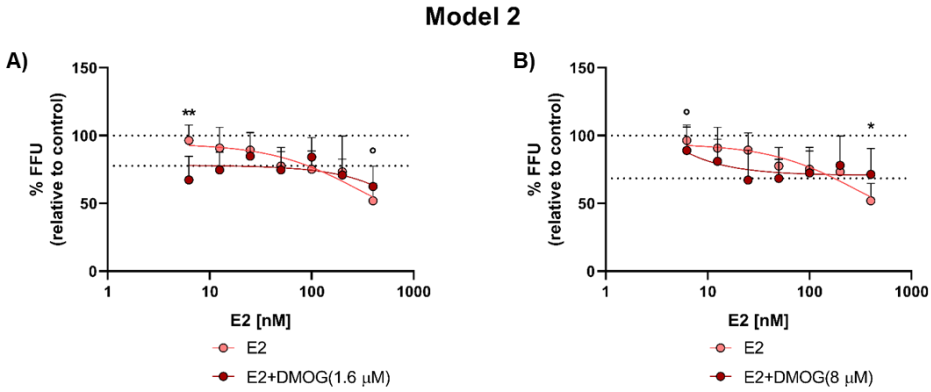

Figure 34. 17,β-estradiol (E2) serial dilution antiviral activity in combination with DMOG (Model 2). HuH7 cells were treated 72 hours post infection with E2 serial dilutions (6.25-400 nM) with or without DMOG (E2+DMOG and E2, respectively) at 1.6 μM **(A)** and 8 μM **(B)**. Infection was evaluated by FFU assay at 72 hours post infection and results are shown as the percentage mean±SD normalized to infected control (upper dot line). In each graph, DMOG control values were reported as the lower dot line. Asterisks are referred to the statistical analysis performed between E2+DMOG vs. E2 groups, white circles are referred to the statistical analysis performed between E2+DMOG vs. DMOG groups. */°= $p \leq 0.05$, ***= $p \leq 0.001$.

Observing the post infection treatment model, individually DMOG and E2 treatments induced a reduction of viral infection but the combined effects of the two compounds did not result in a higher antiviral effect. So we hypothesized that the DMOG and the E2 antiviral effect could be exerted activating a common estrogen receptor (ER)-mediated molecular pathway. To evaluate this hypothesis, we tested the antiviral action of DMOG in presence of the ER antagonist fulvestrant.

As shown in **Figure 35**, we noticed a full recovery of viral infection when both DMOG concentrations were used in combination with fulvestrant serial dilutions. We found significant differences between

DMOG (1.6 μM) control (77.7% FFU ±23.5) and DMOG with fulvestrant at 400 nM (107.8% FFU ±42.8, p=0.04), 200 nM (115.6% FFU ±46.3, p=0.02) and 100 nM (126.6% FFU ±34.3, p<0.001). A reduction of the DMOG antiviral effect was also found using fulvestrant at 400 and 200 nM in combination with DMOG at 8 μM (400 nM: 106% FFU ±31.8, p=0.002; 200 nM: 110.3% FFU ±23.9, p<0.001) compared to DMOG control (69.9% FFU ±18.3).

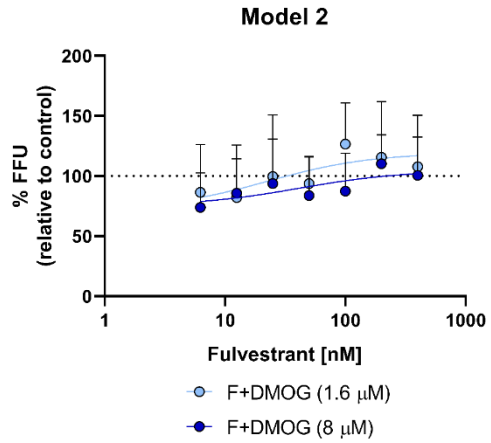

Figure 35. DMOG antiviral effect in combination with fulvestrant serial dilutions (Model 2). HuH7 cells were treated 72 hours post infection with fulvestrant serial dilutions (6.25-400 nM) in combination with DMOG at 1.6 μM and 8 μM. Infection was evaluated at 72 hours post infection by FFU assay and results are shown as the percentage mean±SD normalized to infected control (dot line).

In order to better characterise the relationship between ER, DMOG and viral infection we assessed the interactions between DMOG, E2 and fulvestrant on viral products: intracellular HCV RNA, intra and extra -cellular viral particles and viral assembly efficiency. Looking at our previous experiments, we focused on the Model 2, in which the E2 treatment (400 nM) combined with DMOG (8 μM) resulted in an antiviral effect reduction if compared to the E2 treatment control (**Figure 34B**).

Firstly, we evaluated the mitochondrial activity in cells, with or without previous infection, treated with DMOG (8 μM), E2 (400 nM), fulvestrant (400 nM) and the respective combinations (E2+DMOG and F+DMOG) for 24, 48 and 72 hours. As reported in **Figure 36**, no differences were found between all the conditions tested in presence or not of JFH-1 infection.

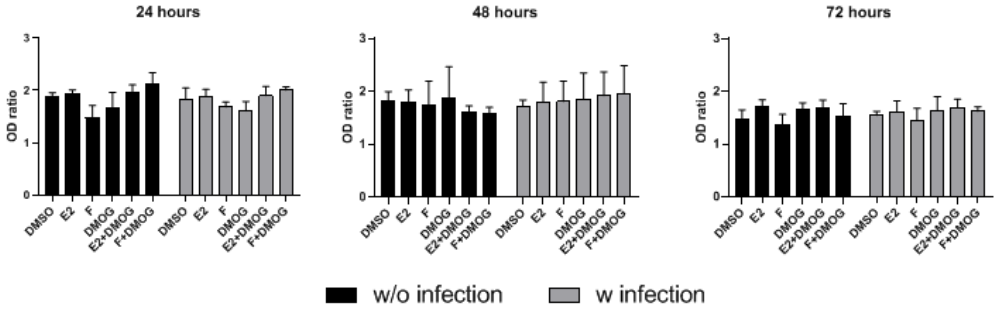

Figure 36. Mitochondrial activity assay. HuH7 cells were treated with DMOG, 17,β-estradiol (E2) or fulvestrant (F) and the respective combinations (E2+D, F+D) with or without previous infection, DMSO was used as treatment control. MTT and Crystal violet (CV) assays were performed at 24, 48 and 72 hours from the beginning of the treatment. The OD ratios (OD MTT/OD CV) are shown as mean±SD.

Evaluating viral infection products we observed similar levels in intracellular HCV RNA in the control DMOG treatment condition compared to the infected control (128.8% ±39.8, p=0.250) (**Figure 37A**). However, both intracellular and extracellular viral particles were found to have significantly lower levels in the control DMOG treatment condition (49.5% ±22.9, p=0.003 and 64.6% ±25.9, p=0.006, respectively) (**Figure 37B-C**). In agreement, virion assembly efficiency was found to be lower in the DMOG treated cells compared to control (40.4% ±10.6, p=0.002,) (**Figure 37D**).

When the ER agonist 17,β-estradiol was used in presence of DMOG treatment (E2+DMOG), the intracellular HCV RNA resulted to be higher if compared to E2 control (111.3% ±48.6 vs. 65.3% ±18.4, p=0.01) without significant differences compared to DMOG control (p<0.999) (**Figure 37A**). The intra- and extra- cellular viral particles had similar levels in E2-treated cells with or without DMOG showing significant lower levels compared to infected control (E2+DMOG: 66.9% ±28.4 intracellular viral particles, and 53.5% ±31.1 extracellular viral particles; p<0.05 and p<0.001, respectively; E2: 51.3% ±17.3 intracellular viral particles, and 60.3% ±26.6 extracellular viral particles; p=0.02 and p<0.01, respectively). Evaluating the virion assembly efficiency no differences were found between E2 treatments with or without DMOG (81.2% ± 24.7 vs. 70.8% ±16.2, p>0.999) (**Figure 37B-C-D**).

Using the ER antagonist fulvestrant in combination with DMOG (F+DMOG), we found a significant reduction of intracellular HCV RNA compared to DMOG control (88.65% ±28.7, p=0.004) with similar level to fulvestrant control treatment (86.7% ±10.0, p<0.999) (**Figure 37A**). Furthermore, the intra- and extra- cellular viral particles were not affected by fulvestrant treatment with or without DMOG compared to infected control (F+DMOG: 70.6% ±21.5 intracellular viral particles, and 87.6% ±49.2 extracellular viral particles; p=0.408 and p<0.999, respectively; F: 109.1% ±6.9 intracellular

viral particles and 82.7% ±48.1 extracellular viral particles, $p<0.999$ and $p<0.999$, respectively). The virion assembly efficiency in F+DMOG treated cells resulted significantly higher compared to DMOG control (86.5% ±29.3 vs. 40.4% ±10.6, $p=0.03$) (**Figure 37B-C-D**).

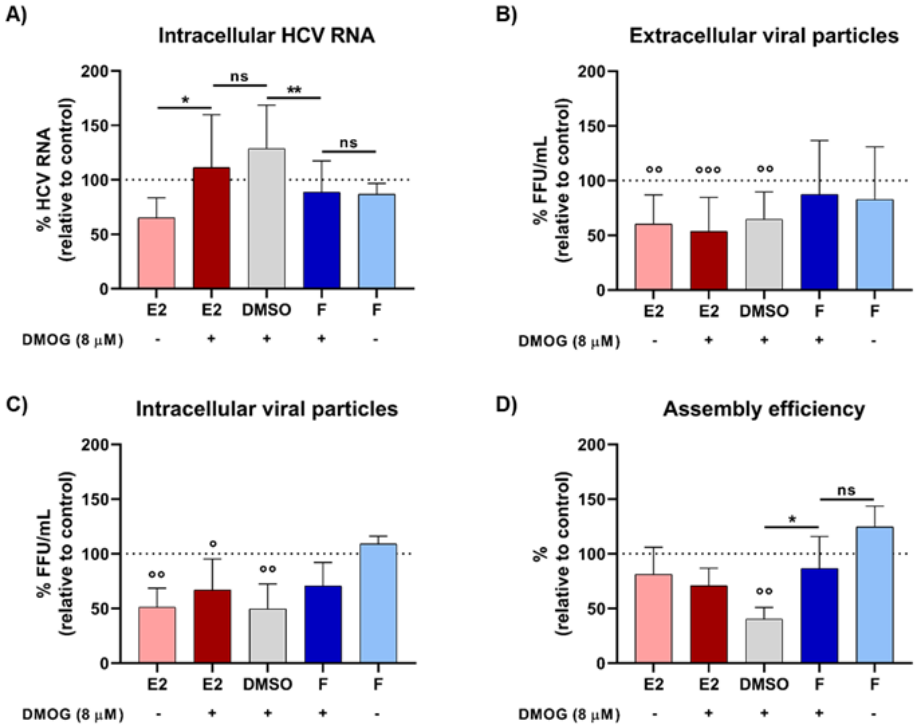

Figure 37. DMOG treatment antiviral effect in combination with estrogen receptor ligands. HuH7 cells were treated post JFH-1 infection (MOI 0.05) for 72 hours with 17,β-estradiol (E2), fulvestrant (F) with or without DMOG (8 µM) . Intracellular HCV RNA **(A)**, extra **(B)** and intra **(C)** -cellular viral particles and assembly efficiency **(D)** were evaluated by qPCR and FFU assay. Results were shown as mean±SD normalized to infected control (dot line). Asterisks are referred to the statistical analysis performed between treatment vs. treatment groups, white circles are referred to the statistical analysis performed between treatment vs. infected control groups. ns= not significant, */°= $p\leq0.05$, **/°°= $p\leq0.01$, °°°=$p\leq0.001$.

DISCUSSION

Affecting more than 170 millions of people globally, the HCV is the leading cause of several liver diseases [236]. The wide study of the virus led to the development of the Direct Antiviral Agents (DAAs), which have revolutionized the disease treatment [237]. Nevertheless, some topics about the natural history of HCV infection are still unclear. Principally, the relationship between sex differences and HCV infection is an object of debate even in the DAAs era [238]. Indeed, females show a higher spontaneous viral clearance rate, and the progression of HCV-associated liver diseases is slower in women compared to men [162,239,240]. Particularly, the female sex is a protective factor against fibrotic progression in patients with chronic liver disease [164]. Moreover, the male sex resulted to be a strong risk factor for hepatocellular carcinoma (HCC) development; the HCC is 3 fold common in males compared to females. However, the HCV infection persistence and the liver disease progression in females are age-related, depending on whether females are in pre- or post- menopausal period [164,172,174]. In a previous study published by our group, using different *in vitro* HCV cell culture systems we demonstrated that 17,β-estradiol (E2) exerts its antiviral effect acting on the HCV particles release and partially with the viral entry. However, the E2-activated hepatocyte antiviral mechanisms were still unknown [205]. Moreover, estrogen activity can also cross-talk with hypoxia-induced conditions, which is an important factor in cirrhosis and HCC development [105,227]. Characterising the E2-dependent hepatocyte modulation in different environmental conditions can lead to better understanding the female sex protective role observed in several liver diseases.

In the present study, we demonstrated that 17,β-estradiol (E2) stimulates the hepatocytes innate immunity, inducing the generation of an intra- and extra- cellular environment with antiviral properties. Moreover, we demonstrated that the E2-induced antiviral agents are linked to the interferon type I system. In the second part of the study, we found that the dimethyloxalylglycine (DMOG) treatment (a synthetic analogue of alpha-ketoglutarate used to mimic hypoxic conditions) exerts opposite effects on viral infection, depending on exposure timing. Using the estrogen receptor (ER) agonist (17,β-estradiol) and antagonist (fulvestrant (F)) compounds in DMOG-treatment condition, we demonstrated a mutual interaction between the ER pathway and DMOG treatment effect on viral infection.

Initially we focus on the clinical data about the progressive loss of HCV infection protection in females during menopause period [174]. To explore this observation we evaluated the presence of a re-sensitisation to infection in E2-treated hepatocytes. To better mimic physiological conditions, hepatocytes were maintained in E2 treatment not only for a short period but also for a long one. The

long-treatment period demonstrated an antiviral effect similar to a shorter model, highlighting an antiviral effect threshold of approximately 50% (**Figure 15**). Performing the re-sensitisation experiments, we evaluated the persistence of the estrogen-mediated antiviral status after removal of the receptor stimulation and its impact on the infection susceptibility. The E2 antiviral activity loss resulted to be time-treatment dependent. In fact, the infection susceptibility in the overnight (ON) treatment model was recovered in approximately a few hours. While the prolonged treatment period (14 days) showed a longer persistence of the antiviral effect up to a couple of days, and a full recovery of viral infection after three days (**Figure 16**). These results are in line with the clinical observations, showing a progressive loss over time of the E2 protective antiviral effect. The progressive antiviral action loss could be related not only to a reduced direct estrogen effect on hepatocytes, but it also could be ascribed to the removal of antiviral molecules present in the medium produced by the E2 treatment. In fact, it should be noted that the extracellular medium (E2-conditioned medium) was removed before the infection, and the E2 could promote both intra- and extra- cellular antiviral environments.

The hepatocyte innate immunity shows several molecular mechanisms (pathogen-associated molecular patterns (PAMPs)) which are able to detect the HCV viral infection. PAMP activation stimulates IFN molecule production, which exert an autocrine and paracrine action inducing interferon-stimulated gene (ISGs) transcription and suppressing viral infection [59]. A different immune response between females and males is well documented in literature. It has also been reported that 17,β-estradiol can promote the interferon signaling during viral infections [241,242]. Also healthy female immune cells show higher IFN signaling pathway activation compared to male, mainly linked to IRF5 and TLR signaling pathway [187,188]. So we hypothesized that the estrogen-mediated antiviral status could be ascribed to an interferon signaling pre-activation. To test this hypothesis, we performed a time course gene expression analysis, firstly focusing on interferon- and inflammation- related genes in E2-treated hepatocytes without HCV infection. We observed a fast transcription of the two estrogen-regulated genes (GREB1 and KDM4B), and we also demonstrated that their transcription is mediated by the ER activation (**Figure 17**). In fact, treating cells with E2 in combination with the ER antagonist fulvestrant the GREB1 and KDM4B mRNA levels remain similar to control. The faster E2-induced gene transcription could be related to the estrogen lipophilic nature, which allows them to easily cross cell membranes and bind intracellular receptors. Furthermore, the presence of ER on plasma membranes can lead to a faster intracellular response activation (indirect non-genomic signaling) [243]. HuH7 cells, treated for 4 hours with E2, showed a particular gene expression profile. An early gene transcription activation at 0 and 6 hours post

treatment is followed by a refractory period at 24 hours, at 48 hours we found a subsequent second gene transcription activation, which partially persists at 72 hours (**Figure 18A**). The two well-known inflammation-related genes IL1B and CXCL8 were found to be down-regulated, highlighting the potential role of estrogens to control inflammation. Conversely, we observed profound changes in IFN-related genes, a strong transcription activation was found at 6 hours post treatment concurrently to GREB1 and KDM4B induction. Five genes (IL18, IRF5, IFNA1, IFNB1, TLR3 and TNF) were found highly modulated in at least two time points (**Figure 18B**). These data demonstrate that the innate immune gene transcription can be modulated in naïve HuH7 cells by 17,β-estradiol.

Observing the infection context, in the HCVcc and the HCVcc+E2 models we found a general up-regulation of interferon- and cytokines- related genes (**Figure 20)**. However, the mRNA levels of IFNL3 and the evaluated ISGs (excluding ISG15) did not show significant differences compared to control cells in each time point. These findings could be due by the low MOI used during the experiment (0.1), and by the negative regulation exerted by the HCV suppressing innate immunity. Also the choice of HuH7 cell line can explain our findings; in fact HuH7 cells have a defective innate immunity, although exogenous IFN-α-stimulation can anyway lead to normal ISG induction [244]. Moreover, despite HuH7 cell line shows up-regulated IFN mRNA levels during viral infections, it is still debated if this cell line can produce a higher amount of IFN molecules [91,245,246].
As expected, the E2 treatment induced a reduction of intracellular HCV RNA, starting from 48 hours (**Figure 19)**. Comparing the HCVcc+E2 and HCVcc models, the higher gene expression differences were found in the early 0-24 hours post treatment and infection, consistent with the E2-induced early response. At these time points, TLR3 and IFNB1 genes showed up-regulated mRNAs levels. In the HCVcc+E2 model, IFNA1 mRNA showed a kinetic similar to the one observed in E2-treated cells, resulting significantly differently compared to the HCVcc model at 6 and 48 hours post infection. These data are in line with the reported ability of estrogens to induce and promote IFN response in different cell types and during viral infections [242,247,248].
At 24 hours, we also found a slight increase in ISG15 mRNA. The ISG15 protein is one of the most IFN type I-induced ISGs, but its role is controversial [249]. During *in vitro* HCV infection it has been demonstrated that ISG15, combined with USP18, acts as a negative feedback loop of IFN response [250]. It has been also demonstrated that ISG15 can be secreted from infected cells and can activate T and NK cells, inducing IFN-γ production [251]. The $NKp46^{High}$ cells produce higher amounts of IFN-γ and are highly expressed in HCV-infected female subjects; these cells are also inversely correlated to HCV RNA levels and fibrosis degree [182]. Intriguingly, we could speculate that released ISG15 acts as an inflammation regulator: on one hand, it could recruit immune system cells,

which lead to viral clearance, and on the other hand, it could dump hepatocyte interferon stimuli to control local inflammation.

Looking at the later time point (72 hours), the two CXCL8 and TNF mRNAs were up-regulated in the HCVcc+E2 model compared to the control infection condition. Despite their harmful role as proinflammatory agents in chronic infection, several findings support their positive role to counteract the infection establishment. It has been proposed that a low replicative virus acute infection can induce these two cytokines release stimulating innate antiviral pathways; an IFN-stimulated response element (ISRE) binding site was located in the CXCL8 promoter region, and the toll-like receptor (TLR) signaling activation can promote TNF transcription [126,252]. In an *in vitro* HCV replicon system the CXCL8 mRNA inversely correlated with IL8 protein and HCV RNA replication [253]. Furthermore, Laidlaw *et al.* found that TNF-α, independently and in combination with IFNs, can inhibit HCV particle release [128].

Based on gene expression data, we hypothesized that the 17,β-estradiol antiviral effect could be mediated by type I IFN system. The type I IFN family comprises a wide number of different molecules, which exert their activity by binding to a single receptor complex (IFNAR1/IFNAR2). Therefore, we evaluated the E2 treatment in combination with the compounds IFN alpha-IFNAR-IN-1 hydrochloride (IFNARi), which is an inhibitor of the IFN-α/IFNAR interaction [235]. The chosen inhibitor concentration did not affect cell proliferation and was able to blunt the pharmacological action of the IFNα2a. Furthermore, the chosen IFNARi concentration did not alter basal HCV viral infection; in line with a published result showing that JAK-STAT pathway inhibition did not alter HCV infection in HuH7 cell lines [244]. Adding the IFNARi to the HCVcc + E2 model, we obtained the complete E2-antiviral effect loss (**Figure 23**). Based on our previous results showing time-dependency of the estrogen-mediated interferon induction, we investigated the role of each interferon peak on anti-HCV activity (**Figure 25**). We have added the IFNARi at different timelines to the HCVcc+E2 model, and we found a viral infection full restoration only in cells treated with the IFNARi immediately (0h) or 24h post infection. Adding the IFNARi at 48h post infection, during the second peak, was not sufficient to revert antiviral phenotype. These data suggest that the first E2-induced interferon peak is essential to induce a strong antiviral response.

Therefore, we assumed that E2-stimulated HuH7 cells could produce a conditioned medium (CM) able to interfere with the HCV viral infection. Furthermore, the presence of early-released antiviral molecules in the medium, post the E2 treatment, could also explain the restoration of infection observed in re-sensitising experiments. In fact, we found an E2 antiviral effect loss when four hours-treated cells were incubated for 24 hours in fresh medium, which was subsequently removed before

the infection (**Figure 26A**). The CM produced in the first 24 hours (CM_{24}) was sufficient to induce a modest infection reduction. Surprisingly, when the re-sensitised cells were incubated for 72 hours in the CM_{24} post infection, we obtained the complete restoration of the antiviral (**Figure 26B**). The significant difference between the above-mentioned conditions suggests that the previously E2-treated cells have a higher sensitivity to extracellular antiviral factors. These data are in line with other published observations, which demonstrate a greater IFN-related response in female isolated cells compared to male ones [179,187,188]. The late-harvested CM (CM_{48} and CM_{72}) showed a strong antiviral effect (**Figure 27**). This could be explained by a higher accumulation of E2-induced antiviral molecules during time. Moreover, the IFNARi addition to the CM completely abrogated the CM antiviral activity, confirming the presence of IFN-related molecules in the medium, which are able to interfere with viral infection.

Taken together, these findings demonstrate a role of the type I interferon system in estrogen-mediated antiviral activity in hepatocytes. Hence, we also demonstrated that the E2 antiviral effect is not only limited to hepatocyte intracellular level, but it also acts at an extracellular level. The hepatocyte-released antiviral molecules also modulates other cell type behavior. It is well aware that the HCV infection context and liver disease progression is not restricted only to the hepatocyte function. The antiviral response against HCV infection is a complex event, which is orchestrated by the interaction of the hepatocytes with the non-parenchymal liver cells (Kupffer cells (KCs), hepatic stellate cells (HSCs) and liver sinusoidal endothelial cells (LSECs)) and other immune cells [254]. The persistence of HCV infection and a insufficient antiviral response promotes the establishment of an inflammatory environment, which can lead to a chronic infection and the onset of liver diseases such as cirrhosis and hepatocellular carcinoma. In the future, we aim to deeply characterise the interferon intracellular response in order to find the ISGs involved in viral clearance. We also aim to evaluate the conditioned medium effect on liver non-parenchymal cells. Co-culture experiments would be the best conditions to deeply understand the estrogen protective role in liver disease progression.

Considering the entire hepatic context is a fundamental step to study and evolve new strategies against liver disease progression. In this sight, a factor that is increasingly being taken into consideration is the hypoxic condition [105]. An oxygen gradient is physiologically present in the liver lobule, and the onset of liver disease (such as the HCV infection) can promote the establishment of a hypoxic environment. The cellular hypoxic state appears to influence the HCV infection itself and may play a significant role in viral hepatocarcinogenesis, interplaying with chronic inflammation. Several studies show a cross-talk between hypoxia and estrogen signaling pathway [227]. Hence, in the

second part of our study, we focused on the interplay between 17,β-estradiol and HCV infection in a chemically-induced pseudohypoxic state.

To establish a pseudohypoxic state we used the compound dimethyloxalylglycine (DMOG), a synthetic analogue of 2-oxoglutarate that acts as a PHD competitive inhibitor, inducing HIF-1α stabilization. However, being an 2-oxoglutarate the DMOG activity is not specific, and this compound can modulate the signaling pathway mainly linked to metabolism [112]. We used two different treatment models, which are based on an ON treatment before infection (Model 1) and a 72 hours treatment post infection (Model 2). The DMOG is normaly used at 1-2 mM concentrations [255,256], but some published work showed a DMOG dose-dependent reduction in cell growth in long-time treatment experiments [257–259]. We used low DMOG concentrations (0.064 - 80 µM) to avoid a detrimental impact on cell proliferation, which could affect viral infection analysis. The chosen concentrations did not markedly affect HuH7 cell proliferation (**Figure 28**). To assess the pseudohypoxic state induction, we did not evaluate HIF-1α protein stabilization, but we performed a gene expression analysis of two hypoxia-related genes (HIF1A and CA9). Treating cells for 72 hours with the higher DMOG concentration tested (80 µM) we observed a slightly HIF1A mRNA up-regulation at 72 hours, while a trend was observed in CA9 mRNA levels. Conversely, no HIF1A and CA9 mRNA level differences were observed treating cells ON, probably due the restricted time of exposure (**Figure 29A**). No gene expression differences were also found using both models in combination with the HCV infection (**Figure 29B**). Therefore, we cannot assert the reaching of a complete pseudohypoxic state under HCVcc conditions. The low used MOI was insufficient to induce mitochondrial impairment (**Figure 36**).

However, we found a significantly different viral infection kinetic between the two DMOG treatment models, evaluating the intracellular HCV RNA (**Figure 30**). More marked results were obtained using a lowest MOI and DMOG serial dilutions in FFU assay (**Figure 31**). Viral infection promotion or impairment resulted in dose and timing dependent. Our data demonstrated that a short DMOG treatment before infection promotes late HCV RNA up-regulation, while a prolonged DMOG treatment post infection compromises viral infection. These DMOG double effects lead us to assume that a hypoxic or pseudohypoxic environment could be a double edge sword for HCV viral infection. A low oxygen tension can enhance viral replication and can promote viral entry by VLDLR up-regulation [115,260]. However, Magri *et al.* observed the HCV infection reduction under 72h-long strong hypoxic conditions [261]. Under hypoxic conditions, the histone demethylase family (KDMs) is transcriptionally activated and is an important transcription regulator. The N-Myc downstream-regulated gene 1 (NDRG1) gene can be regulated by KDM4B, and NDRG1 expression is enhanced by high hypoxic conditions (1.5% O_2) and by DMOG treatment in normoxic conditions (µM

concentration) [262–264]. Conversely, the HCV can promote NDRG1 down-regulation to favour its particle formation. In fact, it has been demonstrated that NDRG1 can modulate lipid droplet formation, negatively affecting the HCV assembly phase [265]. These data would support the idea of two distinct effects exerted by hypoxic conditions on the viral replication cycle.

The KDM family transcription can be activated not only by hypoxia but also by estrogens, underling a common signaling pathway between hypoxia and estrogen signaling pathway [226]. Therefore, we focused on the ER-mediated antiviral activity evaluation in DMOG treatment model conditions. We found that in Model 1 the DMOG infection-promoting activity was partially counteracted by E2 in a concentration-dependent manner. In fact, the highest E2 concentration (400 nM) partially counteracted DMOG-related infection up-regulation (**Figure 32A**). While, the E2 serial dilution antiviral activity was dependent by the DMOG concentration tested. The DMOG concentration of 1.6 μM combined with E2 concentrations did not alter antiviral estrogen effects. Increasing the DMOG concentration to 8 μM, we found the E2 antiviral activity maintenance only in the highest tested concentrations (**Figure 33**). Observing the post infection treatment model (Model 2), individually DMOG and E2 treatments induced a reduction of viral infection, but the combined effects of the two compounds did not result in a higher antiviral effect. Furthermore, we found a slight reduction in E2 (400 nM) antiviral activity in combination with DMOG at 8 μM (**Figure 32B** and **Figure 34B**). Based on these data, we assumed that the DMOG and the E2 antiviral effect could be exerted activating a common estrogen receptor-mediated molecular pathway. To evaluate this hypothesis we tested the ER antagonist fulvestrant in combination with DMOG, and we found that the ER inhibition compromised the DMOG antiviral action in a dose-dependent manner (**Figure 35**).

Finally, we better characterised the interplay between ER agonist (E2), ER antagonist (F) and DMOG treatment on HCV viral cycle (**Figure 37**). The treatment combination E2+DMOG induced an up-regulation of the intracellular HCV RNA compared to E2 control treated cells, explaining the partial loss of E2 antiviral activity previously reported. However, in the three treatment conditions (E2, E2+DMOG and DMOG) we found a profound decrease of the intra- and the extra- cellular viral particles. While the viral assembly efficiency resulted unbalanced only in the DMOG treatment control condition; these findings are in line with previously reported data, which demonstrated that E2 mainly affected the viral particle release [205]. The unbalanced viral assembly efficiency leads us to hypothesize that the DMOG treatment on one hand could promote viral replication; on the other hand, it could generate a harmful intracellular environment, which negatively affects viral particle assembly/release. The DMOG proviral activity on HCV RNA seems to be dependent on an activated or unoccupied ER, although the E2 presence still reduces the viral infection. In fact, blocking the ER activity with fulvestrant, we observed the HCV RNA decrease in F+DMOG condition compared to

DMOG treatment control, and we found the partial restoration of viral assembly efficiency. However, the HCV replicon system should be used to better study the interaction between ER, DMOG treatment and HCV replication.

It has been demonstrated that fulvestrant is able to alter hypoxia-induced gene transcription in breast cancer cells [266]. Furthermore, an E2-activated ER-α/β can promote HIF-1α transcription, while Tamoxifen-blocked ER exters an opposite effect [266]. Some studies showed that the hypoxia-activated transcription factors and the ER-α/β can interplay modulating the gene transcription by binding to estrogen responsive elements (EREs) or to hypoxia-responsive elements (HREs) [230,233]. We can suppose a different DMOG-induced gene transcription regulation in an ER status-dependent manner, which may lead to different effects on viral infection. Nevertheless, the DMOG use showed some limitations in inducing a pseudohypoxic state. In future, we aim to investigate the interaction between estrogen and HCV under not chemical-induced hypoxic conditions.

To conclude, we can affirm that 17,β-estradiol promotes the *in vitro* hepatocyte IFN-related gene expression and the conditioned medium production with IFN type I system-mediated antiviral activity. In addition, the 17,β-estradiol induces an hepatocyte pre-activation status that emphasizes the antiviral conditioned medium activity.

The 17,β-estradiol antiviral effect can be altered under DMOG treatment conditions, in a mutual concentration-dependent manner. The DMOG also exert opposite effects on the HCV viral infection, depending on the exposure timing. Moreover, the DMOG antiviral action can be blocked by the ER antagonist fulvestrant, demonstrating an interplay between ER activation and DMOG treatment effect on the HCV viral infection.

During the PhD period, I collaborated on several projects in the epathology field. These projects were related to the research of liquid biopsy-based biomarkers implicated in liver diseases and potentially related to HCC risk development. In most of the studies, I worked on the experimental setting of the single nucleotide polymorphisms (SNPs) analysis and for serological marker quantification. The project-related articles include:

- Severity of Nonalcoholic Fatty Liver Disease in Type 2 Diabetes Mellitus: Relationship between Nongenetic Factors and PNPLA3/HSD17B13 Polymorphisms [267].

- Periostin Circulating Levels and Genetic Variants in Patients with Non-Alcoholic Fatty Liver Disease [268].

- Interplay of PNPLA3 and HSD17B13 Variants in Modulating the Risk of Hepatocellular Carcinoma among Hepatitis C Patients [269].

- Genes modulating liver fat accumulation and lipogenesis predict development of hepatocellular carcinoma among DAA treated cirrhotics C with and without viral clearance (Manuscript under review).

Furthermore, I actively participated in the organisation of a multicentric study in collaboration with "Università degli studi Milano - Bicocca", "Ospedale San Gerardo" (Monza), "ASST Grande Ospedale Metropolitano Niguarda" (Milano). The project is entitled "Finding the seed of recurrence: the role of the liquid biopsy to detect circulating tumor cells as markers of advanced disease and prognosis in hepatocarcinoma". I worked on the isolation and characterisation of circulating tumor cells (CTCs) in enrolled patients. Currently the preliminary results were exposed at the EASL - Liver Cancer Summit, 5-6 February 2021 [270]. The acquired knowledge in the "HCC and CTC" field allowed us to write a review (Manuscript under review).

BIBLIOGRAPHY

1. Thrift, A.P.; El-Serag, H.B.; Kanwal, F. Global epidemiology and burden of HCV infection and HCV-related disease. *Nat. Rev. Gastroenterol. Hepatol.* **2017**, *14*, 122–132, doi:10.1038/nrgastro.2016.176.
2. Petruzziello, A.; Marigliano, S.; Loquercio, G.; Cacciapuoti, C. Hepatitis C virus (HCV) genotypes distribution: an epidemiological up-date in Europe. *Infect. Agent. Cancer* **2016**, *11*, 53, doi:10.1186/s13027-016-0099-0.
3. Murphy, D.G.; Sablon, E.; Chamberland, J.; Fournier, E.; Dandavino, R.; Tremblay, C.L. Hepatitis C Virus Genotype 7, a New Genotype Originating from Central Africa. *J. Clin. Microbiol.* **2015**, *53*, 967–972, doi:10.1128/JCM.02831-14.
4. Salmona, M.; Caporossi, A.; Simmonds, P.; Thélu, M.-A.; Fusillier, K.; Mercier-Delarue, S.; De Castro, N.; LeGoff, J.; Chaix, M.-L.; François, O.; et al. First next-generation sequencing full-genome characterization of a hepatitis C virus genotype 7 divergent subtype. *Clin. Microbiol. Infect.* **2016**, *22*, 947.e1-947.e8, doi:10.1016/j.cmi.2016.07.032.
5. Borgia, S.M.; Hedskog, C.; Parhy, B.; Hyland, R.H.; Stamm, L.M.; Brainard, D.M.; Subramanian, M.G.; McHutchison, J.G.; Mo, H.; Svarovskaia, E.; et al. Identification of a Novel Hepatitis C Virus Genotype From Punjab, India: Expanding Classification of Hepatitis C Virus Into 8 Genotypes. *J. Infect. Dis.* **2018**, *218*, 1722–1729, doi:10.1093/infdis/jiy401.
6. Budkowska, A. Intriguing structure of the HCV particle. *Gut* **2017**, *66*, 1351–1352, doi:10.1136/gutjnl-2016-313184.
7. Wrensch, F.; Crouchet, E.; Ligat, G.; Zeisel, M.B.; Keck, Z.-Y.; Foung, S.K.H.; Schuster, C.; Baumert, T.F. Hepatitis C Virus (HCV)-Apolipoprotein Interactions and Immune Evasion and Their Impact on HCV Vaccine Design. *Front. Immunol.* **2018**, *9*, 1436, doi:10.3389/fimmu.2018.01436.
8. Lindenbach, B.D.; Rice, C.M. The ins and outs of hepatitis C virus entry and assembly. *Nat. Rev. Microbiol.* **2013**, *11*, 688–700, doi:10.1038/nrmicro3098.
9. Bartenschlager, R.; Lohmann, V.; Penin, F. The molecular and structural basis of advanced antiviral therapy for hepatitis C virus infection. *Nat. Rev. Microbiol.* **2013**, *11*, 482–496, doi:10.1038/nrmicro3046.
10. Gawlik, K.; Baugh, J.; Chatterji, U.; Lim, P.J.; Bobardt, M.D.; Gallay, P.A. HCV Core Residues Critical for Infectivity Are Also Involved in Core-NS5A Complex Formation. *PLoS One* **2014**, *9*, e88866, doi:10.1371/journal.pone.0088866.
11. Shavinskaya, A.; Boulant, S.; Penin, F.; McLauchlan, J.; Bartenschlager, R. The Lipid Droplet

Binding Domain of Hepatitis C Virus Core Protein Is a Major Determinant for Efficient Virus Assembly. *J. Biol. Chem.* **2007**, *282*, 37158–37169, doi:10.1074/jbc.M707329200.

12. Wang, Y.; Wang, J.; Wu, S.; Zhu, H. The unexpected structures of hepatitis C virus envelope proteins. *Exp. Ther. Med.* **2017**, *14*, 1859–1865, doi:10.3892/etm.2017.4745.
13. Forns, X.; Thimme, R.; Govindarajan, S.; Emerson, S.U.; Purcell, R.H.; Chisari, F. V.; Bukh, J. Hepatitis C virus lacking the hypervariable region 1 of the second envelope protein is infectious and causes acute resolving or persistent infection in chimpanzees. *Proc. Natl. Acad. Sci.* **2000**, *97*, 13318–13323, doi:10.1073/pnas.230453597.
14. Prentoe, J.; Bukh, J. Hypervariable Region 1 in Envelope Protein 2 of Hepatitis C Virus: A Linchpin in Neutralizing Antibody Evasion and Viral Entry. *Front. Immunol.* **2018**, *9*, 2146, doi:10.3389/fimmu.2018.02146.
15. Madan, V.; Bartenschlager, R. Structural and Functional Properties of the Hepatitis C Virus p7 Viroporin. *Viruses* **2015**, *7*, 4461–4481, doi:10.3390/v7082826.
16. Gentzsch, J.; Brohm, C.; Steinmann, E.; Friesland, M.; Menzel, N.; Vieyres, G.; Perin, P.M.; Frentzen, A.; Kaderali, L.; Pietschmann, T. Hepatitis C Virus p7 is Critical for Capsid Assembly and Envelopment. *PLoS Pathog.* **2013**, *9*, e1003355, doi:10.1371/journal.ppat.1003355.
17. Wozniak, A.L.; Griffin, S.; Rowlands, D.; Harris, M.; Yi, M.; Lemon, S.M.; Weinman, S.A. Intracellular Proton Conductance of the Hepatitis C Virus p7 Protein and Its Contribution to Infectious Virus Production. *PLoS Pathog.* **2010**, *6*, e1001087, doi:10.1371/journal.ppat.1001087.
18. Jones, C.T.; Murray, C.L.; Eastman, D.K.; Tassello, J.; Rice, C.M. Hepatitis C Virus p7 and NS2 Proteins Are Essential for Production of Infectious Virus. *J. Virol.* **2007**, *81*, 8374–8383, doi:10.1128/JVI.00690-07.
19. Yao, N.; Reichert, P.; Taremi, S.S.; Prosise, W.W.; Weber, P.C. Molecular views of viral polyprotein processing revealed by the crystal structure of the hepatitis C virus bifunctional protease–helicase. *Structure* **1999**, *7*, 1353–1363, doi:10.1016/S0969-2126(00)80025-8.
20. Belon, C.A.; Frick, D.N. Helicase inhibitors as specifically targeted antiviral therapy for hepatitis C. *Future Virol.* **2009**, *4*, 277–293, doi:10.2217/fvl.09.7.
21. Hu, B.; Li, S.; Zhang, Z.; Xie, S.; Hu, Y.; Huang, X.; Zheng, Y. HCV NS4B targets Scribble for proteasome-mediated degradation to facilitate cell transformation. *Tumor Biol.* **2016**, *37*, 12387–12396, doi:10.1007/s13277-016-5100-4.
22. Hu, B.; Xie, S.; Hu, Y.; Chen, W.; Chen, X.; Zheng, Y.; Wu, X. Hepatitis C virus NS4B protein induces epithelial-mesenchymal transition by upregulation of Snail. *Virol. J.* **2017**, *14*, 83,

doi:10.1186/s12985-017-0737-1.

23. Brass, V.; Bieck, E.; Montserret, R.; Wölk, B.; Hellings, J.A.; Blum, H.E.; Penin, F.; Moradpour, D. An Amino-terminal Amphipathic α-Helix Mediates Membrane Association of the Hepatitis C Virus Nonstructural Protein 5A. *J. Biol. Chem.* **2002**, *277*, 8130–8139, doi:10.1074/jbc.M111289200.
24. Tellinghuisen, T.L.; Marcotrigiano, J.; Gorbalenya, A.E.; Rice, C.M. The NS5A Protein of Hepatitis C Virus Is a Zinc Metalloprotein. *J. Biol. Chem.* **2004**, *279*, 48576–48587, doi:10.1074/jbc.M407787200.
25. Asabe, S.I.; Tanji, Y.; Satoh, S.; Kaneko, T.; Kimura, K.; Shimotohno, K. The N-terminal region of hepatitis C virus-encoded NS5A is important for NS4A-dependent phosphorylation. *J. Virol.* **1997**, *71*, 790–796, doi:10.1128/JVI.71.1.790-796.1997.
26. Macdonald, A.; Harris, M. Hepatitis C virus NS5A: tales of a promiscuous protein. *J. Gen. Virol.* **2004**, *85*, 2485–2502, doi:10.1099/vir.0.80204-0.
27. Gale, M.J.; Korth, M.J.; Tang, N.M.; Tan, S.L.; Hopkins, D.A.; Dever, T.E.; Polyak, S.J.; Gretch, D.R.; Katze, M.G. Evidence that hepatitis C virus resistance to interferon is mediated through repression of the PKR protein kinase by the nonstructural 5A protein. *Virology* **1997**, *230*, 217–27, doi:10.1006/viro.1997.8493.
28. François, C.; Duverlie, G.; Rebouillat, D.; Khorsi, H.; Castelain, S.; Blum, H.E.; Gatignol, A.; Wychowski, C.; Moradpour, D.; Meurs, E.F. Expression of Hepatitis C Virus Proteins Interferes with the Antiviral Action of Interferon Independently of PKR-Mediated Control of Protein Synthesis. *J. Virol.* **2000**, *74*, 5587–5596, doi:10.1128/JVI.74.12.5587-5596.2000.
29. Masaki, T.; Suzuki, R.; Murakami, K.; Aizaki, H.; Ishii, K.; Murayama, A.; Date, T.; Matsuura, Y.; Miyamura, T.; Wakita, T.; et al. Interaction of Hepatitis C Virus Nonstructural Protein 5A with Core Protein Is Critical for the Production of Infectious Virus Particles. *J. Virol.* **2008**, *82*, 7964–7976, doi:10.1128/JVI.00826-08.
30. Boyce, S.E.; Tirunagari, N.; Niedziela-Majka, A.; Perry, J.; Wong, M.; Kan, E.; Lagpacan, L.; Barauskas, O.; Hung, M.; Fenaux, M.; et al. Structural and Regulatory Elements of HCV NS5B Polymerase – β-Loop and C-Terminal Tail – Are Required for Activity of Allosteric Thumb Site II Inhibitors. *PLoS One* **2014**, *9*, e84808, doi:10.1371/journal.pone.0084808.
31. Simmonds, P. Genetic diversity and evolution of hepatitis C virus – 15 years on. *J. Gen. Virol.* **2004**, *85*, 3173–3188, doi:10.1099/vir.0.80401-0.
32. Barth, H.; Schnober, E.K.; Zhang, F.; Linhardt, R.J.; Depla, E.; Boson, B.; Cosset, F.-L.; Patel, A.H.; Blum, H.E.; Baumert, T.F. Viral and Cellular Determinants of the Hepatitis C Virus Envelope-Heparan SulfateInteraction. *J. Virol.* **2006**, *80*, 10579–10590,

doi:10.1128/JVI.00941-06.

33. Zahid, M.N.; Turek, M.; Xiao, F.; Dao Thi, V.L.; Guérin, M.; Fofana, I.; Bachellier, P.; Thompson, J.; Delang, L.; Neyts, J.; et al. The postbinding activity of scavenger receptor class B type I mediates initiation of hepatitis C virus infection and viral dissemination. *Hepatology* **2013**, *57*, 492–504, doi:10.1002/hep.26097.
34. Lupberger, J.; Zeisel, M.B.; Xiao, F.; Thumann, C.; Fofana, I.; Zona, L.; Davis, C.; Mee, C.J.; Turek, M.; Gorke, S.; et al. EGFR and EphA2 are host factors for hepatitis C virus entry and possible targets for antiviral therapy. *Nat. Med.* **2011**, *17*, 589–595, doi:10.1038/nm.2341.
35. Sainz, B.; Barretto, N.; Martin, D.N.; Hiraga, N.; Imamura, M.; Hussain, S.; Marsh, K.A.; Yu, X.; Chayama, K.; Alrefai, W.A.; et al. Identification of the Niemann-Pick C1–like 1 cholesterol absorption receptor as a new hepatitis C virus entry factor. *Nat. Med.* **2012**, *18*, 281–285, doi:10.1038/nm.2581.
36. Coller, K.E.; Berger, K.L.; Heaton, N.S.; Cooper, J.D.; Yoon, R.; Randall, G. RNA Interference and Single Particle Tracking Analysis of Hepatitis C Virus Endocytosis. *PLoS Pathog.* **2009**, *5*, e1000702, doi:10.1371/journal.ppat.1000702.
37. Sharma, N.R.; Mateu, G.; Dreux, M.; Grakoui, A.; Cosset, F.-L.; Melikyan, G.B. Hepatitis C Virus Is Primed by CD81 Protein for Low pH-dependent Fusion*. *J. Biol. Chem.* **2011**, *286*, 30361–30376, doi:10.1074/jbc.M111.263350.
38. Paul, D.; Bartenschlager, R. Flaviviridae Replication Organelles: Oh, What a Tangled Web We Weave. *Annu. Rev. Virol.* **2015**, *2*, 289–310, doi:10.1146/annurev-virology-100114-055007.
39. Camus, G.; Vogt, D.A.; Kondratowicz, A.S.; Ott, M. Lipid Droplets and Viral Infections. In *Methods in cell biology*; 2013; Vol. 116, pp. 167–190.
40. Wang, L.; James Ou, J. Hepatitis C virus and autophagy. *Biol. Chem.* **2015**, *396*, 1215–1222, doi:10.1515/hsz-2015-0172.
41. Yang, W.; Hood, B.L.; Chadwick, S.L.; Liu, S.; Watkins, S.C.; Luo, G.; Conrads, T.P.; Wang, T. Fatty acid synthase is up-regulated during hepatitis C virus infection and regulates hepatitis C virus entry and production. *Hepatology* **2008**, *48*, 1396–1403, doi:10.1002/hep.22508.
42. Levy, G.; Habib, N.; Guzzardi, M.A.; Kitsberg, D.; Bomze, D.; Ezra, E.; Uygun, B.E.; Uygun, K.; Trippler, M.; Schlaak, J.F.; et al. Nuclear receptors control pro-viral and antiviral metabolic responses to hepatitis C virus infection. *Nat. Chem. Biol.* **2016**, *12*, 1037–1045, doi:10.1038/nchembio.2193.
43. Lerat, H.; Kammoun, H.L.; Hainault, I.; Mérour, E.; Higgs, M.R.; Callens, C.; Lemon, S.M.; Foufelle, F.; Pawlotsky, J.-M. Hepatitis C Virus Proteins Induce Lipogenesis and Defective

Triglyceride Secretion in Transgenic Mice. *J. Biol. Chem.* **2009**, *284*, 33466–33474, doi:10.1074/jbc.M109.019810.

44. Meyers, N.L.; Fontaine, K.A.; Kumar, G.R.; Ott, M. Entangled in a membranous web: ER and lipid droplet reorganization during hepatitis C virus infection. *Curr. Opin. Cell Biol.* **2016**, *41*, 117–124, doi:10.1016/j.ceb.2016.05.003.
45. Blackham, S.; Baillie, A.; Al-Hababi, F.; Remlinger, K.; You, S.; Hamatake, R.; McGarvey, M.J. Gene Expression Profiling Indicates the Roles of Host Oxidative Stress, Apoptosis, Lipid Metabolism, and Intracellular Transport Genes in the Replication of Hepatitis C Virus. *J. Virol.* **2010**, *84*, 5404–5414, doi:10.1128/jvi.02529-09.
46. Hsu, S.; Wang, B.; Kota, J.; Yu, J.; Costinean, S.; Kutay, H.; Yu, L.; Bai, S.; La Perle, K.; Chivukula, R.R.; et al. Essential metabolic, anti-inflammatory, and anti-tumorigenic functions of miR-122 in liver. *J. Clin. Invest.* **2012**, *122*, 2871–2883, doi:10.1172/JCI63539.
47. Li, Y.; Masaki, T.; Yamane, D.; McGivern, D.R.; Lemon, S.M. Competing and noncompeting activities of miR-122 and the 5' exonuclease Xrn1 in regulation of hepatitis C virus replication. *Proc. Natl. Acad. Sci.* **2013**, *110*, 1881–1886, doi:10.1073/pnas.1213515110.
48. Jirasko, V.; Montserret, R.; Lee, J.Y.; Gouttenoire, J.; Moradpour, D.; Penin, F.; Bartenschlager, R. Structural and Functional Studies of Nonstructural Protein 2 of the Hepatitis C Virus Reveal Its Key Role as Organizer of Virion Assembly. *PLoS Pathog.* **2010**, *6*, e1001233, doi:10.1371/journal.ppat.1001233.
49. Popescu, C.-I.; Callens, N.; Trinel, D.; Roingeard, P.; Moradpour, D.; Descamps, V.; Duverlie, G.; Penin, F.; Héliot, L.; Rouillé, Y.; et al. NS2 Protein of Hepatitis C Virus Interacts with Structural and Non-Structural Proteins towards Virus Assembly. *PLoS Pathog.* **2011**, *7*, e1001278, doi:10.1371/journal.ppat.1001278.
50. Stapleford, K.A.; Lindenbach, B.D. Hepatitis C Virus NS2 Coordinates Virus Particle Assembly through Physical Interactions with the E1-E2 Glycoprotein and NS3-NS4A Enzyme Complexes. *J. Virol.* **2011**, *85*, 1706–1717, doi:10.1128/JVI.02268-10.
51. Counihan, N.A.; Rawlinson, S.M.; Lindenbach, B.D. Trafficking of Hepatitis C Virus Core Protein during Virus Particle Assembly. *PLoS Pathog.* **2011**, *7*, e1002302, doi:10.1371/journal.ppat.1002302.
52. Menzel, N.; Fischl, W.; Hueging, K.; Bankwitz, D.; Frentzen, A.; Haid, S.; Gentzsch, J.; Kaderali, L.; Bartenschlager, R.; Pietschmann, T. MAP-Kinase Regulated Cytosolic Phospholipase A2 Activity Is Essential for Production of Infectious Hepatitis C Virus Particles. *PLoS Pathog.* **2012**, *8*, e1002829, doi:10.1371/journal.ppat.1002829.
53. Herker, E.; Harris, C.; Hernandez, C.; Carpentier, A.; Kaehlcke, K.; Rosenberg, A.R.; Farese,

R. V.; Ott, M. Efficient hepatitis C virus particle formation requires diacylglycerol acyltransferase-1. *Nat. Med.* **2010**, *16*, 1295–1298, doi:10.1038/nm.2238.

54. Dubuisson, J.; Cosset, F.-L. Virology and cell biology of the hepatitis C virus life cycle – An update. *J. Hepatol.* **2014**, *61*, S3–S13, doi:10.1016/j.jhep.2014.06.031.
55. Olofsson, S. Intracellular Assembly of VLDL Two Major Steps in Separate Cell Compartments. *Trends Cardiovasc. Med.* **2000**, *10*, 338–345, doi:10.1016/S1050-1738(01)00071-8.
56. Scheel, T.K.H.; Rice, C.M. Understanding the hepatitis C virus life cycle paves the way for highly effective therapies. *Nat. Med.* **2013**, *19*, 837–849, doi:10.1038/nm.3248.
57. Wong, M.-T.; Chen, S.S.-L. Emerging roles of interferon-stimulated genes in the innate immune response to hepatitis C virus infection. *Cell. Mol. Immunol.* **2016**, *13*, 11–35, doi:10.1038/cmi.2014.127.
58. Rosen, H.R. Hepatitis C pathogenesis: mechanisms of viral clearance and liver injury. *Liver Transpl.* **2003**, *9*, S35-43, doi:10.1053/jlts.2003.50253.
59. Rosen, H.R. Emerging concepts in immunity to hepatitis C virus infection. *J. Clin. Invest.* **2013**, *123*, 4121–4130, doi:10.1172/JCI67714.
60. SAITO, T.; Gale Jr., M. RIG-I mediated hepatic innate immune signaling that controls HCV infection. *Uirusu* **2008**, *58*, 105–116, doi:10.2222/jsv.58.105.
61. Vegna, S.; Gregoire, D.; Moreau, M.; Lassus, P.; Durantel, D.; Assenat, E.; Hibner, U.; Simonin, Y. NOD1 Participates in the Innate Immune Response Triggered by Hepatitis C Virus Polymerase. *J. Virol.* **2016**, *90*, 6022–6035, doi:10.1128/JVI.03230-15.
62. Eksioglu, E.A.; Zhu, H.; Bayouth, L.; Bess, J.; Liu, H.; Nelson, D.R.; Liu, C. Characterization of HCV Interactions with Toll-Like Receptors and RIG-I in Liver Cells. *PLoS One* **2011**, *6*, e21186, doi:10.1371/journal.pone.0021186.
63. Garaigorta, U.; Chisari, F. V. Hepatitis C Virus Blocks Interferon Effector Function by Inducing Protein Kinase R Phosphorylation. *Cell Host Microbe* **2009**, *6*, 513–522, doi:10.1016/j.chom.2009.11.004.
64. Arnaud, N.; Dabo, S.; Maillard, P.; Budkowska, A.; Kalliampakou, K.I.; Mavromara, P.; Garcin, D.; Hugon, J.; Gatignol, A.; Akazawa, D.; et al. Hepatitis C Virus Controls Interferon Production through PKR Activation. *PLoS One* **2010**, *5*, e10575, doi:10.1371/journal.pone.0010575.
65. Cao, X.; Ding, Q.; Lu, J.; Tao, W.; Huang, B.; Zhao, Y.; Niu, J.; Liu, Y.-J.; Zhong, J. MDA5 plays a critical role in interferon response during hepatitis C virus infection. *J. Hepatol.* **2015**, *62*, 771–778, doi:10.1016/j.jhep.2014.11.007.

66. Hei, L.; Zhong, J. Laboratory of genetics and physiology 2 (LGP2) plays an essential role in hepatitis C virus infection-induced interferon responses. *Hepatology* **2017**, *65*, 1478–1491, doi:10.1002/hep.29050.

67. Kolakofsky, D.; Kowalinski, E.; Cusack, S. A structure-based model of RIG-I activation. *RNA* **2012**, *18*, 2118–2127, doi:10.1261/rna.035949.112.

68. Paz, S.; Vilasco, M.; Werden, S.J.; Arguello, M.; Joseph-Pillai, D.; Zhao, T.; Nguyen, T.L.-A.; Sun, Q.; Meurs, E.F.; Lin, R.; et al. A functional C-terminal TRAF3-binding site in MAVS participates in positive and negative regulation of the IFN antiviral response. *Cell Res.* **2011**, *21*, 895–910, doi:10.1038/cr.2011.2.

69. Li, X.-D.; Sun, L.; Seth, R.B.; Pineda, G.; Chen, Z.J. Hepatitis C virus protease NS3/4A cleaves mitochondrial antiviral signaling protein off the mitochondria to evade innate immunity. *Proc. Natl. Acad. Sci.* **2005**, *102*, 17717–17722, doi:10.1073/pnas.0508531102.

70. Bellecave, P.; Sarasin-Filipowicz, M.; Donzé, O.; Kennel, A.; Gouttenoire, J.; Meylan, E.; Terracciano, L.; Tschopp, J.; Sarrazin, C.; Berg, T.; et al. Cleavage of mitochondrial antiviral signaling protein in the liver of patients with chronic hepatitis C correlates with a reduced activation of the endogenous interferon system. *Hepatology* **2010**, *51*, 1127–1136, doi:10.1002/hep.23426.

71. Kim, Y.K.; Shin, J.-S.; Nahm, M.H. NOD-Like Receptors in Infection, Immunity, and Diseases. *Yonsei Med. J.* **2016**, *57*, 5, doi:10.3349/ymj.2016.57.1.5.

72. Lupfer, C.; Kanneganti, T.-D. The expanding role of NLRs in antiviral immunity. *Immunol. Rev.* **2013**, *255*, 13–24, doi:10.1111/imr.12089.

73. Xu, T.; Du, Y.; Fang, X.-B.; Chen, H.; Zhou, D.-D.; Wang, Y.; Zhang, L. New insights into Nod-like receptors (NLRs) in liver diseases. *Int. J. Physiol. Pathophysiol. Pharmacol.* **2018**, *10*, 1–16.

74. Shrivastava, S.; Mukherjee, A.; Ray, R.B.; Ray, R.B. Hepatitis C Virus Induces Interleukin-1 (IL-1)/IL-18 in Circulatory and Resident Liver Macrophages. *J. Virol.* **2013**, *87*, 12284–12290, doi:10.1128/jvi.01962-13.

75. O'Neill, L.A.J.; Golenbock, D.; Bowie, A.G. The history of Toll-like receptors — redefining innate immunity. *Nat. Rev. Immunol.* **2013**, *13*, 453–460, doi:10.1038/nri3446.

76. Yang, D.-R. Hepatitis C virus and antiviral innate immunity: Who wins at tug-of-war? *World J. Gastroenterol.* **2015**, *21*, 3786, doi:10.3748/wjg.v21.i13.3786.

77. Wong, M.-T.; Chen, S.S.L. Emerging roles of interferon-stimulated genes in the innate immune response to hepatitis C virus infection. *Cell. Mol. Immunol.* **2016**, *13*, 11–35, doi:10.1038/cmi.2014.127.

78. Li, K.; Foy, E.; Ferreon, J.C.M.; Nakamura, M.; Ferreon, A.C.M.; Ikeda, M.; Ray, S.C.; Gale, M.; Lemon, S.M. Immune evasion by hepatitis C virus NS3/4A protease-mediated cleavage of the Toll-like receptor 3 adaptor protein TRIF. *Proc. Natl. Acad. Sci.* **2005**, *102*, 2992–2997, doi:10.1073/pnas.0408824102.

79. Abe, T.; Kaname, Y.; Hamamoto, I.; Tsuda, Y.; Wen, X.; Taguwa, S.; Moriishi, K.; Takeuchi, O.; Kawai, T.; Kanto, T.; et al. Hepatitis C Virus Nonstructural Protein 5A Modulates the Toll-Like Receptor-MyD88-Dependent Signaling Pathway in Macrophage Cell Lines. *J. Virol.* **2007**, *81*, 8953–8966, doi:10.1128/JVI.00649-07.

80. Honda, K.; Taniguchi, T. IRFs: Master regulators of signalling by Toll-like receptors and cytosolic pattern-recognition receptors. *Nat. Rev. Immunol.* **2006**, *6*, 644–658, doi:10.1038/nri1900.

81. Pflugheber, J.; Fredericksen, B.; Sumpter, R.; Wang, C.; Ware, F.; Sodora, D.L.; Gale, M. Regulation of PKR and IRF-1 during hepatitis C virus RNA replication. *Proc. Natl. Acad. Sci.* **2002**, *99*, 4650–4655, doi:10.1073/pnas.062055699.

82. Ciccaglione, A.R.; Stellacci, E.; Marcantonio, C.; Muto, V.; Equestre, M.; Marsili, G.; Rapicetta, M.; Battistini, A. Repression of Interferon Regulatory Factor 1 by Hepatitis C Virus Core Protein Results in Inhibition of Antiviral and Immunomodulatory Genes. *J. Virol.* **2007**, *81*, 202–214, doi:10.1128/JVI.01011-06.

83. Stone, A.E.L.; Mitchell, A.; Brownell, J.; Miklin, D.J.; Golden-Mason, L.; Polyak, S.J.; Gale, M.J.; Rosen, H.R. Hepatitis C Virus Core Protein Inhibits Interferon Production by a Human Plasmacytoid Dendritic Cell Line and Dysregulates Interferon Regulatory Factor-7 and Signal Transducer and Activator of Transcription (STAT) 1 Protein Expression. *PLoS One* **2014**, *9*, e95627, doi:10.1371/journal.pone.0095627.

84. Lau, D.T.Y.; Fish, P.M.; Sinha, M.; Owen, D.M.; Lemon, S.M.; Gale, M. Interferon regulatory factor-3 activation, hepatic interferon-stimulated gene expression, and immune cell infiltration in hepatitis C virus patients. *Hepatology* **2008**, *47*, 799–809, doi:10.1002/hep.22076.

85. Binder, M.; Kochs, G.; Bartenschlager, R.; Lohmann, V. Hepatitis C virus escape from the interferon regulatory factor 3 pathway by a passive and active evasion strategy. *Hepatology* **2007**, *46*, 1365–1374, doi:10.1002/hep.21829.

86. Inoue, K.; Tsukiyama-Kohara, K.; Matsuda, C.; Yoneyama, M.; Fujita, T.; Kuge, S.; Yoshiba, M.; Kohara, M. Impairment of interferon regulatory factor-3 activation by hepatitis C virus core protein basic amino acid region 1. *Biochem. Biophys. Res. Commun.* **2012**, *428*, 494–499, doi:10.1016/j.bbrc.2012.10.079.

87. Takaoka, A.; Yanai, H.; Kondo, S.; Duncan, G.; Negishi, H.; Mizutani, T.; Kano, S.; Honda,

K.; Ohba, Y.; Mak, T.W.; et al. Integral role of IRF-5 in the gene induction programme activated by Toll-like receptors. *Nature* **2005**, *434*, 243–249, doi:10.1038/nature03308.

88. Cevik, O.; Li, D.; Baljinnyam, E.; Manvar, D.; Pimenta, E.M.; Waris, G.; Barnes, B.J.; Kaushik-Basu, N. Interferon regulatory factor 5 (IRF5) suppresses hepatitis C virus (HCV) replication and HCV-associated hepatocellular carcinoma. *J. Biol. Chem.* **2017**, *292*, 21676–21689, doi:10.1074/jbc.M117.792721.
89. Lee, H.-C.; Narayanan, S.; Park, S.-J.; Seong, S.-Y.; Hahn, Y.S. Transcriptional Regulation of IFN-λ Genes in Hepatitis C Virus-infected Hepatocytes via IRF-3·IRF-7·NF-κB Complex. *J. Biol. Chem.* **2014**, *289*, 5310–5319, doi:10.1074/jbc.M113.536102.
90. Lazear, H.M.; Lancaster, A.; Wilkins, C.; Suthar, M.S.; Huang, A.; Vick, S.C.; Clepper, L.; Thackray, L.; Brassil, M.M.; Virgin, H.W.; et al. IRF-3, IRF-5, and IRF-7 Coordinately Regulate the Type I IFN Response in Myeloid Dendritic Cells Downstream of MAVS Signaling. *PLoS Pathog.* **2013**, *9*, e1003118, doi:10.1371/journal.ppat.1003118.
91. Zhang, T.; Lin, R.-T.; Li, Y.; Douglas, S.D.; Maxcey, C.; Ho, C.; Lai, J.-P.; Wang, Y.-J.; Wan, Q.; Ho, W.-Z. Hepatitis C virus inhibits intracellular interferon alpha expression in human hepatic cell lines. *Hepatology* **2005**, *42*, 819–827, doi:10.1002/hep.20854.
92. Raychoudhuri, A.; Shrivastava, S.; Steele, R.; Dash, S.; Kanda, T.; Ray, R.; Ray, R.B. Hepatitis C Virus Infection Impairs IRF-7 Translocation and Alpha Interferon Synthesis in Immortalized Human Hepatocytes. *J. Virol.* **2010**, *84*, 10991–10998, doi:10.1128/JVI.00900-10.
93. Heim, M.H.; Thimme, R. Innate and adaptive immune responses in HCV infections. *J. Hepatol.* **2014**, *61*, S14–S25, doi:10.1016/j.jhep.2014.06.035.
94. Sadler, A.J.; Williams, B.R.G. Interferon-inducible antiviral effectors. *Nat. Rev. Immunol.* **2008**, *8*, 559–568, doi:10.1038/nri2314.
95. Levy, D.E.; Marié, I.J.; Durbin, J.E. Induction and function of type I and III interferon in response to viral infection. *Curr. Opin. Virol.* **2011**, *1*, 476–486, doi:10.1016/j.coviro.2011.11.001.
96. Bode, J.G.; Ludwig, S.; Ehrhardt, C.; Erhardt, A.; Albrecht, U.; Schaper, F.; Heinrich, P.C.; Häussinger, D. IFN-α antagonistic activity of HCV core protein involves induction of suppressor of cytokine signaling-3. *FASEB J.* **2003**, *17*, 1–16, doi:10.1096/fj.02-0664fje.
97. Polyak, S.J.; Khabar, K.S.A.; Rezeiq, M.; Gretch, D.R. Elevated Levels of Interleukin-8 in Serum Are Associated with Hepatitis C Virus Infection and Resistance to Interferon Therapy. *J. Virol.* **2001**, *75*, 6209–6211, doi:10.1128/JVI.75.13.6209-6211.2001.
98. Randall, G.; Chen, L.; Panis, M.; Fischer, A.K.; Lindenbach, B.D.; Sun, J.; Heathcote, J.; Rice, C.M.; Edwards, A.M.; McGilvray, I.D. Silencing of USP18 Potentiates the Antiviral Activity

of Interferon Against Hepatitis C Virus Infection. *Gastroenterology* **2006**, *131*, 1584–1591, doi:10.1053/j.gastro.2006.08.043.

99. Ortega-Prieto, A.M.; Dorner, M. Immune Evasion Strategies during Chronic Hepatitis B and C Virus Infection. *Vaccines* **2017**, *5*, 24, doi:10.3390/vaccines5030024.
100. Metz, P.; Reuter, A.; Bender, S.; Bartenschlager, R. Interferon-stimulated genes and their role in controlling hepatitis C virus. *J. Hepatol.* **2013**, *59*, 1331–1341, doi:10.1016/j.jhep.2013.07.033.
101. Kietzmann, T. Metabolic zonation of the liver: The oxygen gradient revisited. *Redox Biol.* **2017**, *11*, 622–630, doi:10.1016/j.redox.2017.01.012.
102. Ben-Moshe, S.; Itzkovitz, S. Spatial heterogeneity in the mammalian liver. *Nat. Rev. Gastroenterol. Hepatol.* **2019**, *16*, 395–410, doi:10.1038/s41575-019-0134-x.
103. Löfstedt, T.; Fredlund, E.; Holmquist-Mengelbier, L.; Pietras, A.; Ovenberger, M.; Poellinger, L.; Påhlman, S. Hypoxia Inducible Factor-2α in Cancer. *Cell Cycle* **2007**, *6*, 919–926, doi:10.4161/cc.6.8.4133.
104. Mahon, P.C. FIH-1: a novel protein that interacts with HIF-1alpha and VHL to mediate repression of HIF-1 transcriptional activity. *Genes Dev.* **2001**, *15*, 2675–2686, doi:10.1101/gad.924501.
105. Wilson, G.K.; Tennant, D.A.; McKeating, J.A. Hypoxia inducible factors in liver disease and hepatocellular carcinoma: Current understanding and future directions. *J. Hepatol.* **2014**, *61*, 1397–1406, doi:10.1016/j.jhep.2014.08.025.
106. van Uden, P.; Kenneth, N.S.; Rocha, S. Regulation of hypoxia-inducible factor-1α by NF-κB. *Biochem. J.* **2008**, *412*, 477–484, doi:10.1042/BJ20080476.
107. Jung, Y.; Isaacs, J.S.; Lee, S.; Trepel, J.; Liu, Z.-G.; Neckers, L. Hypoxia-inducible factor induction by tumour necrosis factor in normoxic cells requires receptor-interacting protein-dependent nuclear factor kappa B activation. *Biochem. J.* **2003**, *370*, 1011–7, doi:10.1042/BJ20021279.
108. Jung, Y.-J.; Isaacs, J.S.; Lee, S.; Trepel, J.; Neckers, L. IL-1β mediated up-regulation of HIF-lα via an NFkB/COX-2 pathway identifies HIF-1 as a critical link between inflammation and oncogenesis. *FASEB J.* **2003**, *17*, 1–22, doi:10.1096/fj.03-0329fje.
109. El Guerrab, A.; Cayre, A.; Kwiatkowski, F.; Privat, M.; Rossignol, J.-M.; Rossignol, F.; Penault-Llorca, F.; Bignon, Y.-J. Quantification of hypoxia-related gene expression as a potential approach for clinical outcome prediction in breast cancer. *PLoS One* **2017**, *12*, e0175960, doi:10.1371/journal.pone.0175960.
110. van den Beucken, T.; Koritzinsky, M.; Niessen, H.; Dubois, L.; Savelkouls, K.; Mujcic, H.;

Jutten, B.; Kopacek, J.; Pastorekova, S.; van der Kogel, A.J.; et al. Hypoxia-induced Expression of Carbonic Anhydrase 9 Is Dependent on the Unfolded Protein Response. *J. Biol. Chem.* **2009**, *284*, 24204–24212, doi:10.1074/jbc.M109.006510.

111. Ayabe, H.; Anada, T.; Kamoya, T.; Sato, T.; Kimura, M.; Yoshizawa, E.; Kikuchi, S.; Ueno, Y.; Sekine, K.; Camp, J.G.; et al. Optimal Hypoxia Regulates Human iPSC-Derived Liver Bud Differentiation through Intercellular TGFB Signaling. *Stem Cell Reports* **2018**, *11*, 306–316, doi:10.1016/j.stemcr.2018.06.015.
112. Nelson, B.S.; Kremer, D.M.; Lyssiotis, C.A. New tricks for an old drug. *Nat. Chem. Biol.* **2018**, *14*, 990–991, doi:10.1038/s41589-018-0137-x.
113. Wu, D.; Yotnda, P. Induction and testing of hypoxia in cell culture. *J. Vis. Exp.* **2011**, 2899, doi:10.3791/2899.
114. Ujino, S.; Nishitsuji, H.; Hishiki, T.; Sugiyama, K.; Takaku, H.; Shimotohno, K. Hepatitis C virus utilizes VLDLR as a novel entry pathway. *Proc. Natl. Acad. Sci.* **2016**, *113*, 188–193, doi:10.1073/pnas.1506524113.
115. Vassilaki, N.; Kalliampakou, K.I.; Kotta-Loizou, I.; Befani, C.; Liakos, P.; Simos, G.; Mentis, A.F.; Kalliaropoulos, A.; Doumba, P.P.; Smirlis, D.; et al. Low Oxygen Tension Enhances Hepatitis C Virus Replication. *J. Virol.* **2013**, *87*, 2935–2948, doi:10.1128/JVI.02534-12.
116. Ripoli, M.; D'Aprile, A.; Quarato, G.; Sarasin-Filipowicz, M.; Gouttenoire, J.; Scrima, R.; Cela, O.; Boffoli, D.; Heim, M.H.; Moradpour, D.; et al. Hepatitis C Virus-Linked Mitochondrial Dysfunction Promotes Hypoxia-Inducible Factor 1α-Mediated Glycolytic Adaptation. *J. Virol.* **2010**, *84*, 647–660, doi:10.1128/JVI.00769-09.
117. ZHU, C.; LIU, X.; WANG, S.; YAN, X.; TANG, Z.; WU, K.; LI, Y.; LIU, F. Hepatitis C virus core protein induces hypoxia-inducible factor 1α-mediated vascular endothelial growth factor expression in Huh7.5.1 cells. *Mol. Med. Rep.* **2014**, *9*, 2010–2014, doi:10.3892/mmr.2014.2039.
118. Wilson, G.K.; Brimacombe, C.L.; Rowe, I.A.; Reynolds, G.M.; Fletcher, N.F.; Stamataki, Z.; Bhogal, R.H.; Simões, M.L.; Ashcroft, M.; Afford, S.C.; et al. A dual role for hypoxia inducible factor-1α in the hepatitis C virus lifecycle and hepatoma migration. *J. Hepatol.* **2012**, *56*, 803–809, doi:10.1016/j.jhep.2011.11.018.
119. Mee, C.J.; Farquhar, M.J.; Harris, H.J.; Hu, K.; Ramma, W.; Ahmed, A.; Maurel, P.; Bicknell, R.; Balfe, P.; McKeating, J.A. Hepatitis C Virus Infection Reduces Hepatocellular Polarity in a Vascular Endothelial Growth Factor–Dependent Manner. *Gastroenterology* **2010**, *138*, 1134–1142, doi:10.1053/j.gastro.2009.11.047.
120. Gower, E.; Estes, C.; Blach, S.; Razavi-Shearer, K.; Razavi, H. Global epidemiology and

genotype distribution of the hepatitis C virus infection. *J. Hepatol.* **2014**, *61*, S45–S57, doi:10.1016/j.jhep.2014.07.027.

121. Lee, M.-H.; Yang, H.-I.; Yuan, Y.; L'Italien, G.; Chen, C.-J. Epidemiology and natural history of hepatitis C virus infection. *World J. Gastroenterol.* **2014**, *20*, 9270–80, doi:10.3748/wjg.v20.i28.9270.
122. Memon, M.I.; Memon, M.A. Hepatitis C: An epidemiological review. *J. Viral Hepat.* 2002.
123. Chan, D.P.C.; Sun, H.-Y.; Wong, H.T.H.; Lee, S.-S.; Hung, C.-C. Sexually acquired hepatitis C virus infection: a review. *Int. J. Infect. Dis.* **2016**, *49*, 47–58, doi:10.1016/j.ijid.2016.05.030.
124. Scaraggi, F.; Lomuscio, S.; Perricci, A.; De Mitrio, V.; Napoli, N.; Schíraldi, O. Intrafamilial and sexual transmission of hepatitis C virus. *Lancet* **1993**, *342*, 1300–1301, doi:10.1016/0140-6736(93)92391-6.
125. Heim, M.H. 25 years of interferon-based treatment of chronic hepatitis C: an epoch coming to an end. *Nat. Rev. Immunol.* **2013**, *13*, 535–542, doi:10.1038/nri3463.
126. Lee, J.; Tian, Y.; Chan, S.T.; Kim, J.Y.; Cho, C.; Ou, J.J. TNF-α Induced by Hepatitis C Virus via TLR7 and TLR8 in Hepatocytes Supports Interferon Signaling via an Autocrine Mechanism. *PLOS Pathog.* **2015**, *11*, e1004937, doi:10.1371/journal.ppat.1004937.
127. Wang, W.; Xu, L.; Brandsma, J.H.; Wang, Y.; Hakim, M.S.; Zhou, X.; Yin, Y.; Fuhler, G.M.; van der Laan, L.J.W.; van der Woude, C.J.; et al. Convergent Transcription of Interferon-stimulated Genes by TNF-α and IFN-α Augments Antiviral Activity against HCV and HEV. *Sci. Rep.* **2016**, *6*, 25482, doi:10.1038/srep25482.
128. Laidlaw, S.M.; Marukian, S.; Gilmore, R.H.; Cashman, S.B.; Nechyporuk-Zloy, V.; Rice, C.M.; Dustin, L.B. Tumor Necrosis Factor Inhibits Spread of Hepatitis C Virus Among Liver Cells, Independent From Interferons. *Gastroenterology* **2017**, *153*, 566-578.e5, doi:10.1053/j.gastro.2017.04.021.
129. Chen, S.L.; Morgan, T.R. The Natural History of Hepatitis C Virus (HCV) Infection. *Int. J. Med. Sci.* **2006**, 47–52, doi:10.7150/ijms.3.47.
130. Westbrook, R.H.; Dusheiko, G. Natural history of hepatitis C. *J. Hepatol.* **2014**, *61*, S58–S68, doi:10.1016/j.jhep.2014.07.012.
131. Capone, F.; Guerriero, E.; Colonna, G.; Maio, P.; Mangia, A.; Castello, G.; Costantini, S. Cytokinome profile evaluation in patients with hepatitis C virus infection. *World J. Gastroenterol.* **2014**, *20*, 9261–9, doi:10.3748/wjg.v20.i28.9261.
132. Asselah, T.; Bièche, I.; Laurendeau, I.; Paradis, V.; Vidaud, D.; Degott, C.; Martinot, M.; Bedossa, P.; Valla, D.; Vidaud, M.; et al. Liver Gene Expression Signature of Mild Fibrosis in Patients With Chronic Hepatitis C. *Gastroenterology* **2005**, *129*, 2064–2075,

doi:10.1053/j.gastro.2005.09.010.

133. Schulze-Krebs, A.; Preimel, D.; Popov, Y.; Bartenschlager, R.; Lohmann, V.; Pinzani, M.; Schuppan, D. Hepatitis C Virus-Replicating Hepatocytes Induce Fibrogenic Activation of Hepatic Stellate Cells. *Gastroenterology* **2005**, *129*, 246–258, doi:10.1053/j.gastro.2005.03.089.

134. Zhang, C.-Y.; Yuan, W.-G.; He, P.; Lei, J.-H.; Wang, C.-X. Liver fibrosis and hepatic stellate cells: Etiology, pathological hallmarks and therapeutic targets. *World J. Gastroenterol.* **2016**, *22*, 10512, doi:10.3748/wjg.v22.i48.10512.

135. Sasaki, R.; Devhare, P.B.; Steele, R.; Ray, R.; Ray, R.B. Hepatitis C virus-induced CCL5 secretion from macrophages activates hepatic stellate cells. *Hepatology* **2017**, *66*, 746–757, doi:10.1002/hep.29170.

136. Chan, A.; Patel, K.; Naggie, S. Genotype 3 Infection: The Last Stand of Hepatitis C Virus. *Drugs* **2017**, *77*, 131–144, doi:10.1007/s40265-016-0685-x.

137. d'Avigdor, W.M.H.; Budzinska, M.A.; Lee, M.; Lam, R.; Kench, J.; Stapelberg, M.; McLennan, S. V.; Farrell, G.; George, J.; McCaughan, G.W.; et al. Virus Genotype-Dependent Transcriptional Alterations in Lipid Metabolism and Inflammation Pathways in the Hepatitis C Virus-infected Liver. *Sci. Rep.* **2019**, *9*, 10596, doi:10.1038/s41598-019-46664-0.

138. Thomas, D.L.; Thio, C.L.; Martin, M.P.; Qi, Y.; Ge, D.; O'hUigin, C.; Kidd, J.; Kidd, K.; Khakoo, S.I.; Alexander, G.; et al. Genetic variation in IL28B and spontaneous clearance of hepatitis C virus. *Nature* **2009**, *461*, 798–801, doi:10.1038/nature08463.

139. Shi, X.; Pan, Y.; Wang, M.; Wang, D.; Li, W.; Jiang, T.; Zhang, P.; Chi, X.; Jiang, Y.; Gao, Y.; et al. IL28B Genetic Variation Is Associated with Spontaneous Clearance of Hepatitis C Virus, Treatment Response, Serum IL-28B Levels in Chinese Population. *PLoS One* **2012**, *7*, e37054, doi:10.1371/journal.pone.0037054.

140. Trépo, E.; Romeo, S.; Zucman-Rossi, J.; Nahon, P. PNPLA3 gene in liver diseases. *J. Hepatol.* **2016**, *65*, 399–412, doi:10.1016/j.jhep.2016.03.011.

141. Singal, A.G.; Manjunath, H.; Yopp, A.C.; Beg, M.S.; Marrero, J.A.; Gopal, P.; Waljee, A.K. The Effect of PNPLA3 on Fibrosis Progression and Development of Hepatocellular Carcinoma: A Meta-analysis. *Am. J. Gastroenterol.* **2014**, *109*, 325–334, doi:10.1038/ajg.2013.476.

142. Bruschi, F. V.; Tardelli, M.; Herac, M.; Claudel, T.; Trauner, M. Metabolic regulation of hepatic PNPLA3 expression and severity of liver fibrosis in patients with NASH. *Liver Int.* **2020**, *40*, 1098–1110, doi:10.1111/liv.14402.

143. Abul-Husn, N.S.; Cheng, X.; Li, A.H.; Xin, Y.; Schurmann, C.; Stevis, P.; Liu, Y.; Kozlitina,

J.; Stender, S.; Wood, G.C.; et al. A Protein-Truncating HSD17B13 Variant and Protection from Chronic Liver Disease. *N. Engl. J. Med.* **2018**, *378*, 1096–1106, doi:10.1056/NEJMoa1712191.

144. Trépo, E.; Valenti, L. Update on NAFLD genetics: From new variants to the clinic. *J. Hepatol.* **2020**, *72*, 1196–1209, doi:10.1016/j.jhep.2020.02.020.
145. Mahdessian, H.; Taxiarchis, A.; Popov, S.; Silveira, A.; Franco-Cereceda, A.; Hamsten, A.; Eriksson, P.; van't Hooft, F. TM6SF2 is a regulator of liver fat metabolism influencing triglyceride secretion and hepatic lipid droplet content. *Proc. Natl. Acad. Sci.* **2014**, *111*, 8913–8918, doi:10.1073/pnas.1323785111.
146. Liu, S.; Murakami, E.; Nakahara, T.; Ohya, K.; Teraoka, Y.; Makokha, G.; Uchida, T.; Morio, K.; Fujino, H.; Ono, A.; et al. In vitro analysis of hepatic stellate cell activation influenced by transmembrane 6 superfamily 2 polymorphism. *Mol. Med. Rep.* **2020**, *23*, 16, doi:10.3892/mmr.2020.11654.
147. Thabet, K.; Asimakopoulos, A.; Shojaei, M.; Romero-Gomez, M.; Mangia, A.; Irving, W.L.; Berg, T.; Dore, G.J.; Grønbæk, H.; Sheridan, D.; et al. MBOAT7 rs641738 increases risk of liver inflammation and transition to fibrosis in chronic hepatitis C. *Nat. Commun.* **2016**, *7*, 12757, doi:10.1038/ncomms12757.
148. Mancina, R.M.; Dongiovanni, P.; Petta, S.; Pingitore, P.; Meroni, M.; Rametta, R.; Borén, J.; Montalcini, T.; Pujia, A.; Wiklund, O.; et al. The MBOAT7-TMC4 Variant rs641738 Increases Risk of Nonalcoholic Fatty Liver Disease in Individuals of European Descent. *Gastroenterology* **2016**, *150*, 1219-1230.e6, doi:10.1053/j.gastro.2016.01.032.
149. Luukkonen, P.K.; Zhou, Y.; Hyötyläinen, T.; Leivonen, M.; Arola, J.; Orho-Melander, M.; Orešič, M.; Yki-Järvinen, H. The MBOAT7 variant rs641738 alters hepatic phosphatidylinositols and increases severity of non-alcoholic fatty liver disease in humans. *J. Hepatol.* **2016**, *65*, 1263–1265, doi:10.1016/j.jhep.2016.07.045.
150. Mui, U.; Haley, C.; Tyring, S. Viral Oncology: Molecular Biology and Pathogenesis. *J. Clin. Med.* **2017**, *6*, 111, doi:10.3390/jcm6120111.
151. Wilkins, T.; Malcolm, J.K.; Raina, D.; Schade, R.R. Hepatitis C: diagnosis and treatment. *Am. Fam. Physician* **2010**, *81*, 1351–7.
152. Fried, M.W. Side effects of therapy of hepatitis C and their management. *Hepatology* **2002**, *36*, s237–s244, doi:10.1053/jhep.2002.36810.
153. Vieyres, G.; Pietschmann, T. Entry and replication of recombinant hepatitis C viruses in cell culture. *Methods* **2013**, *59*, 233–248, doi:10.1016/j.ymeth.2012.09.005.
154. Pockros, P.J. Nucleoside/Nucleotide Analogue Polymerase Inhibitors in Development. *Clin.*

Liver Dis. **2013**, *17*, 105–110, doi:10.1016/j.cld.2012.09.007.

155. Tamori, A.; Enomoto, M.; Kawada, N. Recent Advances in Antiviral Therapy for Chronic Hepatitis C. *Mediators Inflamm.* **2016**, *2016*, 1–11, doi:10.1155/2016/6841628.
156. Feeney, E.R.; Chung, R.T. Antiviral treatment of hepatitis C. *BMJ* **2014**, *349*, g3308–g3308, doi:10.1136/bmj.g3308.
157. Sarrazin, C. Treatment failure with DAA therapy: Importance of resistance. *J. Hepatol.* **2021**, *74*, 1472–1482, doi:10.1016/j.jhep.2021.03.004.
158. Wu, X.; Roberto, J.B.; Knupp, A.; Greninger, A.L.; Truong, C.D.; Hollingshead, N.; Kenerson, H.L.; Tuefferd, M.; Chen, A.; Horton, H.; et al. Liver immune abnormalities persist after cure of hepatitis C Virus by anti-viral therapy. *medRxiv* 2020.
159. Hamdane, N.; Jühling, F.; Crouchet, E.; El Saghire, H.; Thumann, C.; Oudot, M.A.; Bandiera, S.; Saviano, A.; Ponsolles, C.; Roca Suarez, A.A.; et al. HCV-Induced Epigenetic Changes Associated With Liver Cancer Risk Persist After Sustained Virologic Response. *Gastroenterology* **2019**, *156*, 2313-2329.e7, doi:10.1053/j.gastro.2019.02.038.
160. Polyak, S.J.; Crispe, I.N.; Baumert, T.F. Liver Abnormalities after Elimination of HCV Infection: Persistent Epigenetic and Immunological Perturbations Post-Cure. *Pathogens* **2021**, *10*, 44, doi:10.3390/pathogens10010044.
161. Micallef, J.M.; Kaldor, J.M.; Dore, G.J. Spontaneous viral clearance following acute hepatitis C infection: a systematic review of longitudinal studies. *J. Viral Hepat.* **2006**, *13*, 34–41, doi:10.1111/j.1365-2893.2005.00651.x.
162. Grebely, J.; Page, K.; Sacks-Davis, R.; van der Loeff, M.S.; Rice, T.M.; Bruneau, J.; Morris, M.D.; Hajarizadeh, B.; Amin, J.; Cox, A.L.; et al. The effects of female sex, viral genotype, and IL28B genotype on spontaneous clearance of acute hepatitis C virus infection. *Hepatology* **2014**, *59*, 109–120, doi:10.1002/hep.26639.
163. Deuffic-Burban, S.; Poynard, T.; Valleron, A.-J. Quantification of fibrosis progression in patients with chronic hepatitis C using a Markov model. *J. Viral Hepat.* **2002**, *9*, 114–122, doi:10.1046/j.1365-2893.2002.00340.x.
164. Di Martino, V.; Lebray, P.; Myers, R.P.; Pannier, E.; Paradis, V.; Charlotte, F.; Moussalli, J.; Thabut, D.; Buffet, C.; Poynard, T. Progression of liver fibrosis in women infected with hepatitis C: Long-term benefit of estrogen exposure. *Hepatology* **2004**, *40*, 1426–1433, doi:10.1002/hep.20463.
165. Villa, E.; Vukotic, R.; Cammà, C.; Petta, S.; Di Leo, A.; Gitto, S.; Turola, E.; Karampatou, A.; Losi, L.; Bernabucci, V.; et al. Reproductive Status Is Associated with the Severity of Fibrosis in Women with Hepatitis C. *PLoS One* **2012**, *7*, e44624, doi:10.1371/journal.pone.0044624.

166. Bernabucci, V.; Villa, E. The role played by gender in viral hepatitis. *Scand. J. Clin. Lab. Invest.* **2014**, *74*, 90–94, doi:10.3109/00365513.2014.936695.
167. Akram, M.; Idrees, M.; Zafar, S.; Hussain, A.; Butt, S.; Afzal, S.; Rehman, I.; Liaqat, A.; Saleem, S.; Ali, M.; et al. Effects of Host and virus related factors on Interferon-α+ribavirin and Pegylated-interferon+ribavirin treatment outcomes in Chronic Hepatitis C patients. *Virol. J.* **2011**, *8*, 234, doi:10.1186/1743-422X-8-234.
168. Akuta, N.; Suzuki, F.; Kawamura, Y.; Yatsuji, H.; Sezaki, H.; Suzuki, Y.; Hosaka, T.; Kobayashi, M.; Kobayashi, M.; Arase, Y.; et al. Predictive factors of early and sustained responses to peginterferon plus ribavirin combination therapy in Japanese patients infected with hepatitis C virus genotype 1b: Amino acid substitutions in the core region and low-density lipoprotein cholesterol l. *J. Hepatol.* **2007**, *46*, 403–410, doi:10.1016/j.jhep.2006.09.019.
169. Narciso-Schiavon, J.L.; Schiavon, L. de L.; Carvalho-Filho, R.J.; Sampaio, J.P.; Batah, P.N. El; Barbosa, D.V.; Ferraz, M.L.G.; Silva, A.E.B. Gender influence on treatment of chronic hepatitis C genotype 1. *Rev. Soc. Bras. Med. Trop.* **2010**, *43*, 217–223, doi:10.1590/S0037-86822010000300001.
170. Lanini, S.; Scognamiglio, P.; Mecozzi, A.; Lombardozzi, L.; Vullo, V.; Angelico, M.; Gasbarrini, A.; Taliani, G.; Attili, A.F.; Perno, C.F.; et al. Impact of new DAA therapy on real clinical practice: a multicenter region-wide cohort study. *BMC Infect. Dis.* **2018**, *18*, 223, doi:10.1186/s12879-018-3125-6.
171. Di Marco, V.; Covolo, L.; Calvaruso, V.; Levrero, M.; Puoti, M.; Suter, F.; Gaeta, G.B.; Ferrari, C.; Raimondo, G.; Fattovich, G.; et al. Who is more likely to respond to dual treatment with pegylated-interferon and ribavirin for chronic hepatitis C? A gender-oriented analysis. *J. Viral Hepat.* **2013**, *20*, 790–800, doi:10.1111/jvh.12106.
172. Codes, L.; Asselah, T.; Cazals-Hatem, D.; Tubach, F.; Vidaud, D.; Paraná, R.; Bedossa, P.; Valla, D.; Marcellin, P. Liver fibrosis in women with chronic hepatitis C: Evidence for the negative role of the menopause and steatosis and the potential benefit of hormone replacement therapy. *Gut* **2007**, *56*, 390–395, doi:10.1136/gut.2006.101931.
173. Corsi, D.J.; Karges, W.; Thavorn, K.; Crawley, A.M.; Cooper, C.L. Influence of female sex on hepatitis C virus infection progression and treatment outcomes. *Eur. J. Gastroenterol. Hepatol.* **2016**, *28*, 405–11, doi:10.1097/MEG.0000000000000567.
174. Burlone, M.E.; Pedrinelli, A.R.; Giarda, P.; Minisini, R.; Pirisi, M. Influence of age on sex-related differences among patients with hepatitis C. *Eur. J. Gastroenterol. Hepatol.* **2016**, *28*, 1100–1101, doi:10.1097/MEG.0000000000000668.
175. Hourigan, L.F.; Macdonald, G.A.; Purdie, D.; Whitehall, V.H.; Shorthouse, C.; Clouston, A.;

Powell, E.E. Fibrosis in chronic hepatitis C correlates significantly with body mass index and steatosis. *Hepatology* **1999**, *29*, 1215–1219, doi:10.1002/hep.510290401.

176. Langer, C.; Gansz, B.; Goepfert, C.; Engel, T.; Uehara, Y.; von Dehn, G.; Jansen, H.; Assmann, G.; von Eckardstein, A. Testosterone up-regulates scavenger receptor BI and stimulates cholesterol efflux from macrophages. *Biochem. Biophys. Res. Commun.* **2002**, *296*, 1051–1057, doi:10.1016/S0006-291X(02)02038-7.
177. Meng, J.; Mostaghel, E.A.; Vakar-Lopez, F.; Montgomery, B.; True, L.; Nelson, P.S. Testosterone Regulates Tight Junction Proteins and Influences Prostatic Autoimmune Responses. *Horm. Cancer* **2011**, *2*, 145–156, doi:10.1007/s12672-010-0063-1.
178. Srivastava, R.A.K. Scavenger receptor class B type I expression in murine brain and regulation by estrogen and dietary cholesterol. *J. Neurol. Sci.* **2003**, *210*, 11–18, doi:10.1016/S0022-510X(03)00006-6.
179. Mekky, R.Y.; Hamdi, N.; El-Akel, W.; Esmat, G.; Abdelaziz, A.I. Estrogen-related MxA transcriptional variation in hepatitis C virus-infected patients. *Transl. Res.* **2012**, *159*, 190–196, doi:10.1016/j.trsl.2011.08.002.
180. Fawzy, I.O.; Negm, M.; Ahmed, R.; Esmat, G.; Hamdi, N.; Abdelaziz, A.I. Tamoxifen downregulates MxA expression by suppressing TLR7 expression in PBMCs of males infected with HCV. *J. Med. Virol.* **2014**, *86*, 1113–1119, doi:10.1002/jmv.23928.
181. Krämer, B.; Körner, C.; Kebschull, M.; Glässner, A.; Eisenhardt, M.; Nischalke, H.-D.; Alexander, M.; Sauerbruch, T.; Spengler, U.; Nattermann, J. Natural killer p46 High expression defines a natural killer cell subset that is potentially involved in control of hepatitis C virus replication and modulation of liver fibrosis. *Hepatology* **2012**, *56*, 1201–1213, doi:10.1002/hep.25804.
182. Golden-Mason, L.; Stone, A.E.L.; Bambha, K.M.; Cheng, L.; Rosen, H.R. Race- and gender-related variation in natural killer p46 expression associated with differential anti-hepatitis c virus immunity. *Hepatology* **2012**, *56*, 1214–1222, doi:10.1002/hep.25771.
183. Fakhir, F.-Z.; Lkhider, M.; Badre, W.; Alaoui, R.; Meurs, E.F.; Pineau, P.; Ezzikouri, S.; Benjelloun, S. Genetic variations in toll-like receptors 7 and 8 modulate natural hepatitis C outcomes and liver disease progression. *Liver Int.* **2018**, *38*, 432–442, doi:10.1111/liv.13533.
184. Yue, M.; Feng, L.; Tang, S.; Wang, J.; Xue, X.; Ding, W.; Zhang, Y.; Deng, X. Sex-specific association between X-linked Toll-like receptor 7 with the outcomes of hepatitis C virus infection. *Gene* **2014**, *548*, 244–50, doi:10.1016/j.gene.2014.07.040.
185. Fischer, J.; Weber, A.N.R.; Böhm, S.; Dickhöfer, S.; El Maadidi, S.; Deichsel, D.; Knop, V.; Klinker, H.; Möller, B.; Rasenack, J.; et al. Sex-specific effects of TLR9 promoter variants on

spontaneous clearance of HCV infection. *Gut* **2017**, *66*, 1829–1837, doi:10.1136/gutjnl-2015-310239.

186. van den Berg, C.H.B.S.; Grady, B.P.X.; Schinkel, J.; van de Laar, T.; Molenkamp, R.; van Houdt, R.; Coutinho, R.A.; van Baarle, D.; Prins, M. Female Sex and IL28B, a Synergism for Spontaneous Viral Clearance in Hepatitis C Virus (HCV) Seroconverters from a Community-Based Cohort. *PLoS One* **2011**, *6*, e27555, doi:10.1371/journal.pone.0027555.
187. Griesbeck, M.; Ziegler, S.; Laffont, S.; Smith, N.; Chauveau, L.; Tomezsko, P.; Sharei, A.; Kourjian, G.; Porichis, F.; Hart, M.; et al. Sex Differences in Plasmacytoid Dendritic Cell Levels of IRF5 Drive Higher IFN- Production in Women. *J. Immunol.* **2015**, *195*, 5327–5336, doi:10.4049/jimmunol.1501684.
188. Berghöfer, B.; Frommer, T.; Haley, G.; Fink, L.; Bein, G.; Hackstein, H. TLR7 Ligands Induce Higher IFN-α Production in Females. *J. Immunol.* **2006**, *177*, 2088–2096, doi:10.4049/jimmunol.177.4.2088.
189. Cengiz, M.; Ozenirler, S.; Yılmaz, G. Estrogen Receptor Alpha Expression and Liver Fibrosis in Chronic Hepatitis C Virus Genotype 1b: A Clinicopathological Study. *Hepat. Mon.* **2014**, *14*, 0–5, doi:10.5812/hepatmon.21885.
190. Iyer, J.K.; Kalra, M.; Kaul, A.; Payton, M.E.; Kaul, R. Estrogen receptor expression in chronic hepatitis C and hepatocellular carcinoma pathogenesis. *World J. Gastroenterol.* **2017**, *23*, 6802–6816, doi:10.3748/wjg.v23.i37.6802.
191. Lu, G.; Shimizu, I.; Cui, X.; Itonaga, M.; Tamaki, K.; Fukuno, H.; Inoue, H.; Honda, H.; Ito, S. Antioxidant and antiapoptotic activities of idoxifene and estradiol in hepatic fibrosis in rats. *Life Sci.* **2004**, *74*, 897–907, doi:10.1016/j.lfs.2003.08.004.
192. Lacort, M.; Leal, A.M.; Liza, M.; Martín, C.; Martínez, R.; Ruiz-Larrea, M.B. Protective effect of estrogens and catecholestrogens against peroxidative membrane damagein vitro. *Lipids* **1995**, *30*, 141–146, doi:10.1007/BF02538267.
193. Naugler, W.E.; Sakurai, T.; Kim, S.; Maeda, S.; Kim, K.H.; Elsharkawy, A.M.; Karin, M. Gender disparity in liver cancer due to sex differences in MyD88-dependent IL-6 production. *Science (80-.).* **2007**, *317*, 121–124, doi:10.1126/science.1140485.
194. Nakagawa, H.; Maeda, S.; Yoshida, H.; Tateishi, R.; Masuzaki, R.; Ohki, T.; Hayakawa, Y.; Kinoshita, H.; Yamakado, M.; Kato, N.; et al. Serum IL-6 levels and the risk for hepatocarcinogenesis in chronic hepatitis C patients: An analysis based on gender differences. *Int. J. Cancer* **2009**, *125*, 2264–2269, doi:10.1002/ijc.24720.
195. Vescovo, T.; Refolo, G.; Vitagliano, G.; Fimia, G.M.; Piacentini, M. Molecular mechanisms of hepatitis C virus–induced hepatocellular carcinoma. *Clin. Microbiol. Infect.* **2016**, *22*, 853–

861, doi:10.1016/j.cmi.2016.07.019.

196. Kilbourne, E.; Scicchitano, M. The Activation of Plasminogen Activator Inhibitor-1 Expression by IL-1β Is Attenuated by Estrogen in Hepatoblastoma HepG2 Cells Expressing Estrogen Receptor α. *Thromb. Haemost.* **1999**, *81*, 423–427, doi:10.1055/s-0037-1614489.
197. Özveri, E.S.; Bozkurt, A.; Haklar, G.; Çetinel, Ş.; Arbak, S.; Yeğen, C.; Yeğen, B.Ç. Estrogens ameliorate remote organ inflammation induced by burn injury in rats. *Inflamm. Res.* **2001**, *50*, 585–591, doi:10.1007/PL00000238.
198. Shimizu, I.; Mizobuchi, Y.; Yasuda, M.; Shiba, M.; Ma, Y.-R.; Horie, T.; Liu, F.; Ito, S. Inhibitory effect of oestradiol on activation of rat hepatic stellate cells in vivo and in vitro. *Gut* **1999**, *44*, 127–136, doi:10.1136/gut.44.1.127.
199. Ilyas, S.Z.; Tabassum, R.; Hamed, H.; Rehman, S.U.; Qadri, I. Hepatitis C Virus-Associated Extrahepatic Manifestations in Lung and Heart and Antiviral Therapy-Related Cardiopulmonary Toxicity. *Viral Immunol.* **2017**, *30*, 633–641, doi:10.1089/vim.2017.0009.
200. Surico, D.; Ercoli, A.; Farruggio, S.; Raina, G.; Filippini, D.; Mary, D.; Minisini, R.; Surico, N.; Pirisi, M.; Grossini, E. Modulation of Oxidative Stress by 17 β-Estradiol and Genistein in Human Hepatic Cell Lines In Vitro. *Cell. Physiol. Biochem.* **2017**, *42*, 1051–1062, doi:10.1159/000478752.
201. Watashi, K.; Inoue, D.; Hijikata, M.; Goto, K.; Aly, H.H.; Shimotohno, K. Anti-hepatitis C virus activity of tamoxifen reveals the functional association of estrogen receptor with viral RNA polymerase NS5B. *J. Biol. Chem.* **2007**, *282*, 32765–32772, doi:10.1074/jbc.M704418200.
202. Hillung, J.; Ruiz-López, E.; Bellón-Echeverría, I.; Clemente-Casares, P.; Mas, A. Characterization of the interaction between hepatitis C virus NS5B and the human oestrogen receptor alpha. *J. Gen. Virol.* **2012**, *93*, 780–785, doi:10.1099/vir.0.039396-0.
203. Hayashida, K.; Shoji, I.; Deng, L.; Jiang, D.P.; Ide, Y.H.; Hotta, H. 17β-estradiol inhibits the production of infectious particles of hepatitis C virus. *Microbiol. Immunol.* **2010**, *54*, 684–690, doi:10.1111/j.1348-0421.2010.00268.x.
204. Ulitzky, L.; Lafer, M.M.; KuKuruga, M.A.; Silberstein, E.; Cehan, N.; Taylor, D.R. A New Signaling Pathway for HCV Inhibition by Estrogen: GPR30 Activation Leads to Cleavage of Occludin by MMP-9. *PLoS One* **2016**, *11*, e0145212, doi:10.1371/journal.pone.0145212.
205. Andrea Magri, Matteo N. Barbaglia, Chiara Z. Foglia, Elisa Boccato, Michela E. Burlone, Sarah Cole, Paola Giarda, Elena Grossini, Arvind H. Patel, Rosalba Minisini, M.P. 17,β-estradiol inhibits hepatitis C virus mainly by interference with the release phase of its life cycle. *Liver Int.* **2016**, *37*, doi:10.1111/liv.13303.

206. Olivo-Marston, S.E.; Mechanic, L.E.; Mollerup, S.; Bowman, E.D.; Remaley, A.T.; Forman, M.R.; Skaug, V.; Zheng, Y.-L.; Haugen, A.; Harris, C.C. Serum estrogen and tumor-positive estrogen receptor-alpha are strong prognostic classifiers of non-small-cell lung cancer survival in both men and women. *Carcinogenesis* **2010**, *31*, 1778–1786, doi:10.1093/carcin/bgq156.
207. Cui, J.; Shen, Y.; Li, R. Estrogen synthesis and signaling pathways during aging: from periphery to brain. *Trends Mol. Med.* **2013**, *19*, 197–209, doi:10.1016/j.molmed.2012.12.007.
208. Lombardi, G.; Zarrilli, S.; Colao, A.; Paesano, L.; Di Somma, C.; Rossi, F.; De Rosa, M. Estrogens and health in males. *Mol. Cell. Endocrinol.* **2001**, *178*, 51–55, doi:10.1016/S0303-7207(01)00420-8.
209. Kasper, C. par D.L.; Braunwald, E.; Fauci, A.S.; Hauser, S.L.; Longo, D.L.; Jameson, J.L. Harrison - Principes de Médecine Interne (16e éd.). *NPG Neurol. - Psychiatr. - Gériatrie* **2006**, *6*, 52, doi:10.1016/S1627-4830(06)75276-X.
210. Paterni, I.; Granchi, C.; Katzenellenbogen, J.A.; Minutolo, F. Estrogen receptors alpha (ERα) and beta (ERβ): Subtype-selective ligands and clinical potential. *Steroids* **2014**, *90*, 13–29, doi:10.1016/j.steroids.2014.06.012.
211. Khan, D.; Cowan, C.; Ahmed, S.A. Estrogen and signaling in the cells of immune system. *Adv. Neuroimmune Biol.* **2012**, *3*, 73–93, doi:10.3233/NIB-2012-012039.
212. Ikeda, K.; Horie-Inoue, K.; Inoue, S. Identification of estrogen-responsive genes based on the DNA binding properties of estrogen receptors using high-throughput sequencing technology. *Acta Pharmacol. Sin.* **2015**, *36*, 24–31, doi:10.1038/aps.2014.123.
213. Kovats, S. Estrogen receptors regulate innate immune cells and signaling pathways. *Cell. Immunol.* **2015**, *294*, 63–69, doi:10.1016/j.cellimm.2015.01.018.
214. Martin, H.L.; Smith, L.; Tomlinson, D.C. Multidrug-resistant breast cancer: current perspectives. *Breast cancer (Dove Med. Press.* **2014**, *6*, 1–13, doi:10.2147/BCTT.S37638.
215. Xu, S.; Yu, S.; Dong, D.; Lee, L.T.O. G Protein-Coupled Estrogen Receptor: A Potential Therapeutic Target in Cancer. *Front. Endocrinol. (Lausanne).* **2019**, *10*, 725, doi:10.3389/fendo.2019.00725.
216. Pietras, R.J.; Márquez-Garbán, D.C. Membrane-Associated Estrogen Receptor Signaling Pathways in Human Cancers: Fig. 1. *Clin. Cancer Res.* **2007**, *13*, 4672–4676, doi:10.1158/1078-0432.CCR-07-1373.
217. Trenti, A.; Tedesco, S.; Boscaro, C.; Trevisi, L.; Bolego, C.; Cignarella, A. Estrogen, Angiogenesis, Immunity and Cell Metabolism: Solving the Puzzle. *Int. J. Mol. Sci.* **2018**, *19*, 859, doi:10.3390/ijms19030859.
218. Stoner, M.; Wormke, M.; Saville, B.; Samudio, I.; Qin, C.; Abdelrahim, M.; Safe, S. Estrogen

regulation of vascular endothelial growth factor gene expression in ZR-75 breast cancer cells through interaction of estrogen receptor α and SP proteins. *Oncogene* **2004**, *23*, 1052–1063, doi:10.1038/sj.onc.1207201.

219. Krock, B.L.; Skuli, N.; Simon, M.C. Hypoxia-Induced Angiogenesis: Good and Evil. *Genes Cancer* **2011**, *2*, 1117–1133, doi:10.1177/1947601911423654.
220. Straub, R.H. The Complex Role of Estrogens in Inflammation. *Endocr. Rev.* **2007**, *28*, 521–574, doi:10.1210/er.2007-0001.
221. Stoner, M.; Saville, B.; Wormke, M.; Dean, D.; Burghardt, R.; Safe, S. Hypoxia Induces Proteasome-Dependent Degradation of Estrogen Receptor α in ZR-75 Breast Cancer Cells. *Mol. Endocrinol.* **2002**, *16*, 2231–2242, doi:10.1210/me.2001-0347.
222. Tamir, S.; Izrael, S.; Vaya, J. The effect of oxidative stress on ERα and ERβ expression. *J. Steroid Biochem. Mol. Biol.* **2002**, *81*, 327–332, doi:10.1016/S0960-0760(02)00115-2.
223. Karas, R.H.; Gauer, E.A.; Bieber, H.E.; Baur, W.E.; Mendelsohn, M.E. Growth factor activation of the estrogen receptor in vascular cells occurs via a mitogen-activated protein kinase-independent pathway. *J. Clin. Invest.* **1998**, *101*, 2851–2861, doi:10.1172/JCI1416.
224. Forsythe, J.A.; Jiang, B.H.; Iyer, N. V; Agani, F.; Leung, S.W.; Koos, R.D.; Semenza, G.L. Activation of vascular endothelial growth factor gene transcription by hypoxia-inducible factor 1. *Mol. Cell. Biol.* **1996**, *16*, 4604–4613, doi:10.1128/MCB.16.9.4604.
225. DeMorrow, S. Cholangiocarcinoma: Estrogen-induced autocrine effects of VEGF on cell proliferation. *Dig. Liver Dis.* **2009**, *41*, 164–165, doi:10.1016/j.dld.2008.11.005.
226. Yang, J.; Jubb, A.M.; Pike, L.; Buffa, F.M.; Turley, H.; Baban, D.; Leek, R.; Gatter, K.C.; Ragoussis, J.; Harris, A.L. The Histone Demethylase JMJD2B Is Regulated by Estrogen Receptor α and Hypoxia, and Is a Key Mediator of Estrogen Induced Growth. *Cancer Res.* **2010**, *70*, 6456–6466, doi:10.1158/0008-5472.CAN-10-0413.
227. Yang, J.; Harris, A.; Davidoff, A. Hypoxia and Hormone-Mediated Pathways Converge at the Histone Demethylase KDM4B in Cancer. *Int. J. Mol. Sci.* **2018**, *19*, 240, doi:10.3390/ijms19010240.
228. De Francesco, E.M.; Pellegrino, M.; Santolla, M.F.; Lappano, R.; Ricchio, E.; Abonante, S.; Maggiolini, M. GPER Mediates Activation of HIF1α/VEGF Signaling by Estrogens. *Cancer Res.* **2014**, *74*, 4053–4064, doi:10.1158/0008-5472.CAN-13-3590.
229. Yi, J.M.; Kwon, H.Y.; Cho, J.Y.; Lee, Y.J. Estrogen and hypoxia regulate estrogen receptor alpha in a synergistic manner. *Biochem. Biophys. Res. Commun.* **2009**, *378*, 842–846, doi:10.1016/j.bbrc.2008.11.142.
230. Lim, W.; Cho, J.; Kwon, H.; Park, Y.; Rhyu, M.-R.; Lee, Y. Hypoxia-inducible factor 1α

activates and is inhibited by unoccupied estrogen receptor β. *FEBS Lett.* **2009**, *583*, 1314–1318, doi:10.1016/j.febslet.2009.03.028.

231. Mukundan, H.; Kanagy, N.L.; Resta, T.C. 17-β Estradiol Attenuates Hypoxic Induction of HIF-1α and Erythropoietin in Hep3B Cells. *J. Cardiovasc. Pharmacol.* **2004**, *44*, 93–100, doi:10.1097/00005344-200407000-00013.
232. Kim, M.; Neinast, M.D.; Frank, A.P.; Sun, K.; Park, J.; Zehr, J.A.; Vishvanath, L.; Morselli, E.; Amelotte, M.; Palmer, B.F.; et al. ERα upregulates Phd3 to ameliorate HIF-1 induced fibrosis and inflammation in adipose tissue. *Mol. Metab.* **2014**, *3*, 642–651, doi:10.1016/j.molmet.2014.05.007.
233. Dey, P.; Velazquez-Villegas, L.A.; Faria, M.; Turner, A.; Jonsson, P.; Webb, P.; Williams, C.; Gustafsson, J.-Å.; Ström, A.M. Estrogen Receptor β2 Induces Hypoxia Signature of Gene Expression by Stabilizing HIF-1α in Prostate Cancer. *PLoS One* **2015**, *10*, e0128239, doi:10.1371/journal.pone.0128239.
234. Rasmussen, N.S.; Nielsen, C.T.; Jacobsen, S.; Nielsen, C.H. Stimulation of Mononuclear Cells Through Toll-Like Receptor 9 Induces Release of Microvesicles Expressing Double-Stranded DNA and Galectin 3-Binding Protein in an Interferon-α-Dependent Manner. *Front. Immunol.* **2019**, *10*, 2391, doi:10.3389/fimmu.2019.02391.
235. Geppert, T.; Bauer, S.; Hiss, J.A.; Conrad, E.; Reutlinger, M.; Schneider, P.; Weisel, M.; Pfeiffer, B.; Altmann, K.H.; Waibler, Z.; et al. Immunosuppressive small molecule discovered by structure-based virtual screening for inhibitors of protein-protein interactions. *Angew. Chemie - Int. Ed.* **2012**, *51*, 258–261, doi:10.1002/anie.201105901.
236. Mohd Hanafiah, K.; Groeger, J.; Flaxman, A.D.; Wiersma, S.T. Global epidemiology of hepatitis C virus infection: New estimates of age-specific antibody to HCV seroprevalence. *Hepatology* **2013**, *57*, 1333–1342, doi:10.1002/hep.26141.
237. Marianne Martinello*, Behzad Hajarizadeh , Jason Grebely, G.J.D.; Matthews, and G. V.; Martinello, M.; Hajarizadeh, B.; Grebely, J.; Dore, G.J.; Matthews, G. V. Management of acute HCV infection in the era of direct-acting antiviral therapy. *Nat. Rev. Gastroenterol. Hepatol.* **2018**, *15*, 412–424, doi:10.1038/s41575-018-0026-5.
238. Baden, R.; Rockstroh, J.K.; Buti, M. Natural History and Management of Hepatitis C: Does Sex Play a Role? *J. Infect. Dis.* **2014**, *209*, S81–S85, doi:10.1093/infdis/jiu057.
239. Bakr, I. Higher clearance of hepatitis C virus infection in females compared with males. *Gut* **2005**, *55*, 1183–1187, doi:10.1136/gut.2005.078147.
240. Page, K.; Hahn, J.A.; Evans, J.; Shiboski, S.; Lum, P.; Delwart, E.; Tobler, L.; Andrews, W.; Avanesyan, L.; Cooper, S.; et al. Acute Hepatitis C Virus Infection in Young Adult Injection

Drug Users: A Prospective Study of Incident Infection, Resolution, and Reinfection. *J. Infect. Dis.* **2009**, *200*, 1216–1226, doi:10.1086/605947.

241. Tasker, C.; Ding, J.; Schmolke, M.; Rivera-Medina, A.; García-Sastre, A.; Chang, T.L. 17β-Estradiol Protects Primary Macrophages Against HIV Infection Through Induction of Interferon-Alpha. *Viral Immunol.* **2014**, *27*, 140–150, doi:10.1089/vim.2013.0120.
242. Kadel, S.; Kovats, S. Sex hormones regulate innate immune cells and promote sex differences in respiratory virus infection. *Front. Immunol.* **2018**, *9*, 1–15, doi:10.3389/fimmu.2018.01653.
243. Fuentes, N.; Silveyra, P. Estrogen receptor signaling mechanisms. In *Advances in Protein Chemistry and Structural Biology*; 2019; pp. 135–170 ISBN 9780128155615.
244. Schöbel, A.; Rösch, K.; Herker, E. Functional innate immunity restricts Hepatitis C Virus infection in induced pluripotent stem cell–derived hepatocytes. *Sci. Rep.* **2018**, *8*, 3893, doi:10.1038/s41598-018-22243-7.
245. Wang, Y.; Li, J.; Wang, X.; Ye, L.; Zhou, Y.; Thomas, R.M.; Ho, W. Hepatitis C virus impairs TLR3 signaling and inhibits IFN-λ 1 expression in human hepatoma cell line. *Innate Immun.* **2014**, *20*, 3–11, doi:10.1177/1753425913478991.
246. Sinigaglia, L.; Gracias, S.; Décembre, E.; Fritz, M.; Bruni, D.; Smith, N.; Herbeuval, J.-P.; Martin, A.; Dreux, M.; Tangy, F.; et al. Immature particles and capsid-free viral RNA produced by Yellow fever virus-infected cells stimulate plasmacytoid dendritic cells to secrete interferons. *Sci. Rep.* **2018**, *8*, 10889, doi:10.1038/s41598-018-29235-7.
247. Dong, G.; Fan, H.; Yang, Y.; Zhao, G.; You, M.; Wang, T.; Hou, Y. 17β-Estradiol enhances the activation of IFN-α signaling in B cells by down-regulating the expression of let-7e-5p, miR-98-5p and miR-145a-5p that target IKKε. *Biochim. Biophys. Acta - Mol. Basis Dis.* **2015**, *1852*, 1585–1598, doi:10.1016/j.bbadis.2015.04.019.
248. Smith, S.; Ní Gabhann, J.; McCarthy, E.; Coffey, B.; Mahony, R.; Byrne, J.C.; Stacey, K.; Ball, E.; Bell, A.; Cunnane, G.; et al. Estrogen Receptor α Regulates Tripartite Motif-Containing Protein 21 Expression, Contributing to Dysregulated Cytokine Production in Systemic Lupus Erythematosus. *Arthritis Rheumatol.* **2014**, *66*, 163–172, doi:10.1002/art.38187.
249. Perng, Y.C.; Lenschow, D.J. ISG15 in antiviral immunity and beyond. *Nat. Rev. Microbiol.* **2018**, *16*, 423–439, doi:10.1038/s41579-018-0020-5.
250. Chen, L.; Li, S.; McGilvray, I. The ISG15/USP18 ubiquitin-like pathway (ISGylation system) in Hepatitis C Virus infection and resistance to interferon therapy. *Int. J. Biochem. Cell Biol.* **2011**, *43*, 1427–1431, doi:10.1016/j.biocel.2011.06.006.
251. Swaim, C.D.; Canadeo, L.A.; Monte, K.J.; Khanna, S.; Lenschow, D.J.; Huibregtse, J.M.

Modulation of Extracellular ISG15 Signaling by Pathogens and Viral Effector Proteins. *Cell Rep.* **2020**, *31*, 107772, doi:10.1016/j.celrep.2020.107772.

252. Wagoner, J.; Austin, M.; Green, J.; Imaizumi, T.; Casola, A.; Brasier, A.; Khabar, K.S.A.; Wakita, T.; Gale, M.; Polyak, S.J. Regulation of CXCL-8 (Interleukin-8) Induction by Double-Stranded RNA Signaling Pathways during Hepatitis C Virus Infection. *J. Virol.* **2007**, *81*, 309–318, doi:10.1128/JVI.01411-06.
253. Koo, B.C.A.; McPoland, P.; Wagoner, J.P.; Kane, O.J.; Lohmann, V.; Polyak, S.J. Relationships between Hepatitis C Virus Replication and CXCL-8 Production In Vitro. *J. Virol.* **2006**, *80*, 7885–7893, doi:10.1128/JVI.00519-06.
254. Boltjes, A.; Movita, D.; Boonstra, A.; Woltman, A.M. The role of Kupffer cells in hepatitis B and hepatitis C virus infections. *J. Hepatol.* **2014**, *61*, 660–671, doi:10.1016/j.jhep.2014.04.026.
255. Zhdanov, A. V.; Okkelman, I.A.; Collins, F.W.J.; Melgar, S.; Papkovsky, D.B. A novel effect of DMOG on cell metabolism: direct inhibition of mitochondrial function precedes HIF target gene expression. *Biochim. Biophys. Acta - Bioenerg.* **2015**, *1847*, 1254–1266, doi:10.1016/j.bbabio.2015.06.016.
256. Volke, M.; Gale, D.P.; Maegdefrau, U.; Schley, G.; Klanke, B.; Bosserhoff, A.-K.; Maxwell, P.H.; Eckardt, K.-U.; Warnecke, C. Evidence for a lack of a direct transcriptional suppression of the iron regulatory peptide hepcidin by hypoxia-inducible factors. *PLoS One* **2009**, *4*, e7875, doi:10.1371/journal.pone.0007875.
257. Menon, A.; Creo, P.; Piccoli, M.; Bergante, S.; Conforti, E.; Banfi, G.; Randelli, P.; Anastasia, L. Chemical Activation of the Hypoxia-Inducible Factor Reversibly Reduces Tendon Stem Cell Proliferation, Inhibits Their Differentiation, and Maintains Cell Undifferentiation. *Stem Cells Int.* **2018**, *2018*, 1–13, doi:10.1155/2018/9468085.
258. Zhang, L.; Jiang, G.; Zhao, X.; Gong, Y. Dimethyloxalylglycine Promotes Bone Marrow Mesenchymal Stem Cell Osteogenesis via Rho/ROCK Signaling. *Cell. Physiol. Biochem.* **2016**, *39*, 1391–1403, doi:10.1159/000447843.
259. Singh, A.; Wilson, J.W.; Schofield, C.J.; Chen, R. Author Correction: Hypoxia-inducible factor (HIF) prolyl hydroxylase inhibitors induce autophagy and have a protective effect in an in-vitro ischaemia model. *Sci. Rep.* **2020**, *10*, 6041, doi:10.1038/s41598-020-63108-2.
260. Ujino, S.; Nishitsuji, H.; Hishiki, T.; Sugiyama, K.; Takaku, H.; Shimotohno, K. Hepatitis C virus utilizes VLDLR as a novel entry pathway. *Proc. Natl. Acad. Sci.* **2016**, *113*, 188–193, doi:10.1073/pnas.1506524113.
261. Andrea Magri, Michelle Hill, Alvina Lai, Nicole Zitzmann, Andrew Davidosn, A.K. and J.M.

Oxygen-dependent hydroxylases regulate HCV and related flavivirus replication.; 25th International Symposium on Hepatitis C Virus and Related Viruses, 2018.

262. Coffey, K.; Rogerson, L.; Ryan-Munden, C.; Alkharaif, D.; Stockley, J.; Heer, R.; Sahadevan, K.; O'Neill, D.; Jones, D.; Darby, S.; et al. The lysine demethylase, KDM4B, is a key molecule in androgen receptor signalling and turnover. *Nucleic Acids Res.* **2013**, *41*, 4433–4446, doi:10.1093/nar/gkt106.
263. Angst, E.; Sibold, S.; Tiffon, C.; Weimann, R.; Gloor, B.; Candinas, D.; Stroka, D. Cellular differentiation determines the expression of the hypoxia-inducible protein NDRG1 in pancreatic cancer. *Br. J. Cancer* **2006**, *95*, 307–313, doi:10.1038/sj.bjc.6603256.
264. Sibold, S.; Roh, V.; Keogh, A.; Studer, P.; Tiffon, C.; Angst, E.; Vorburger, S.A.; Weimann, R.; Candinas, D.; Stroka, D. Hypoxia increases cytoplasmic expression of NDRG1, but is insufficient for its membrane localization in human hepatocellular carcinoma. *FEBS Lett.* **2007**, *581*, 989–994, doi:10.1016/j.febslet.2007.01.080.
265. Schweitzer, C.J.; Zhang, F.; Boyer, A.; Valdez, K.; Cam, M.; Liang, T.J. N-Myc Downstream-Regulated Gene 1 Restricts Hepatitis C Virus Propagation by Regulating Lipid Droplet Biogenesis and Viral Assembly. *J. Virol.* **2018**, *92*, e01166-17, doi:10.1128/JVI.01166-17.
266. Yang, J.; AlTahan, A.; Jones, D.T.; Buffa, F.M.; Bridges, E.; Interiano, R.B.; Qu, C.; Vogt, N.; Li, J.-L.; Baban, D.; et al. Estrogen receptor-α directly regulates the hypoxia-inducible factor 1 pathway associated with antiestrogen response in breast cancer. *Proc. Natl. Acad. Sci.* **2015**, *112*, 15172–15177, doi:10.1073/pnas.1422015112.
267. Bellan, M.; Colletta, C.; Barbaglia, M.N.; Salmi, L.; Clerici, R.; Mallela, V.R.; Castello, L.M.; Saglietti, G.; Carnevale Schianca, G.P.; Minisini, R.; et al. Severity of nonalcoholic fatty liver disease in type 2 diabetes mellitus: Relationship between nongenetic factors and PNPLA3/HSD17B13 polymorphisms. *Diabetes Metab. J.* **2019**, *43*, 700–710, doi:10.4093/dmj.2018.0201.
268. Smirne, C.; Mulas, V.; Barbaglia, M.N.; Mallela, V.R.; Minisini, R.; Barizzone, N.; Burlone, M.E.; Pirisi, M.; Grossini, E. Periostin Circulating Levels and Genetic Variants in Patients with Non-Alcoholic Fatty Liver Disease. *Diagnostics* **2020**, *10*, 1003, doi:10.3390/diagnostics10121003.
269. De Benedittis, C.; Bellan, M.; Crevola, M.; Boin, E.; Barbaglia, M.N.; Mallela, V.R.; Ravanini, P.; Ceriani, E.; Fangazio, S.; Sainaghi, P.P.; et al. Interplay of PNPLA3 and HSD17B13 Variants in Modulating the Risk of Hepatocellular Carcinoma among Hepatitis C Patients. *Gastroenterol. Res. Pract.* **2020**, *2020*, 1–8, doi:10.1155/2020/4216451.
270. Simone Famularo, Matteo Nazzareno Barbaglia, Livia Salmi, Cristina Ciulli, Francesca

Carissimi, Linda Roccamatisi, Giuseppe Cordaro, Venkata Ramana Mallela, Luciano De Carlis, Andrea Lauterio, Rosalba Minisini, Biagio Eugenio Leone, Fabrizio Romano, M.P. Association between postoperative early recurrence of hepatocellular carcinoma and the expression pattern of circulating tumor cells in peripheral blood sample: a preliminary study.; EASL - Digital Liver Cancer Summit, 5-6 February 2021, 2021; p. 28.